2014-04-01

Engineering Cell-Free Systems for Vaccine Development, Self-Assembling Nanoparticles and Codon Reassignment Applications

Mark T. Smith
Brigham Young University - Provo

Engineering Cell-Free Systems for Vaccine Development, Self-Assembling Nanoparticles and Codon Reassignment Applications

Mark Thomas Smith

A dissertation submitted to the faculty of
Brigham Young University
in partial fulfillment of the requirements for the degree of

Doctor of Philosophy

Bradley C. Bundy, Chair
Bradford K. Berges
Randy S. Lewis
Larry L. Baxter
Greg Nordin

Department of Chemical Engineering

Brigham Young University

April 2014

ABSTRACT

Engineering Cell-Free Systems for Vaccine Development,
Self-Assembling Nanoparticles and
Codon Reassignment Applications

Mark Thomas Smith
Department of Chemical Engineering, BYU
Doctor of Philosophy

This dissertation reports on the technology of cell-free protein synthesis (CFPS) including 1) stabilized lyophilized cell-free systems and 2) enhanced heterogeneous cell extracts. This work further considers applications of CFPS systems in 1) rapid vaccine development, 2) functional virus-based nanoparticles, 3) site-specific protein immobilization, and 4) expanding the language of biology using unnatural amino acids.

CFPS technology is a versatile protein production platform that has many features unavailable in *in vivo* expression systems. The primary benefit cell-free systems provide is the direct access to the reaction environment, which is no longer hindered by the presence of a cell-wall. The "openness" of the system makes it a compelling candidate for many technologies. One limitation of CFPS is the necessity of freezing for long-term viable storage. We demonstrate that a lyophilized CFPS system is more stable against nonideal storage than traditional CFPS reagents. The *Escherichia coli*-based CFPS system in this work is limited by the biocatalytic machinery found natively in *E. coli*. To combat these limitations, exogenous biocatalysts can be expressed during fermentation of cells prepared into extract. We demonstrate that simple adjustments in the fermentation conditions can significantly increase the activity of the heterogeneous extract.

Towards virus-based particles and vaccines, we demonstrate that the open nature of CFPS can be utilized for coexpression of virus proteins and self-assembly of virus particles. This technique allows for the rapid production of potential vaccines and novel functional virus-based nanoparticles.

Unnatural amino acids expand the effective language of protein biology. Utilizing CFPS as an expression system, we demonstrated that the incorporation of a single specific unnatural amino acid allows for site-specific immobilization, thus stabilizing the protein against elevated temperatures and chemical denaturants. Current unnatural amino acid incorporation technologies are limited to one or few simultaneous incorporations and suffer from low efficiency. This work proposes a system that could potentially allow for upwards of 40 unnatural amino acids to be simultaneously incorporated, effectively tripling the protein code.

These projects demonstrate the power and versatility of CFPS technologies while laying the foundation for promising technologies in the field of biotechnology.

Keywords: Mark Smith, cell-free protein synthesis, virus-based particles, Foot-and-mouth disease virus, unnatural amino acids, codon reassignment

ACKNOWLEDGEMENTS

I would like to thank the Department of Chemical Engineering, Brigham Young University for the opportunities, facilities, and experiences provided me during my studies. Special thanks to Dr. Bundy for his guidance and support on my path towards becoming a successful independent researcher.

I thank my committee members Dr. Berges, Dr. Nordin, Dr. Lewis, and Dr. Baxter for their examples, time, and willingness to mentor me. I would especially thank them for their time invested in my work from the prospectus through this work. Also, I thank Dr. David Belnap, who originally participated on my committee, for his support, advice, and example. I thank Michael Beliveau for his support and advice. I acknowledge my funding sources: DARPA YFA #D13AP0037, NSF CAREER #1254148, NSF EAGER #1115229, National Pork Board #13-104, and NASA Utah Space Grant #NNX09AO73A.

I thank the many Bundy lab researchers who contributed to my research success including Chad Varner, Prashanta Shrestha, Anna Katz Hawes, Chris Werner, Amin Salehi, Matt Schinn, Andrew Broadbent, Jeffrey Wu, Derek Bush, Jay Rainsdon, Scott Berkheimer, Jeremy Hunt, Anthony Bennett, Troy Holland, Mark Matthews, Jon Terry, Matthew Burnham, Julie Swenson, and the many other researchers who have supported the Bundy Lab. I especially thank Chad for all his dedicated work, guidance and friendship at the beginning of my graduate tenure, which gave me a strong and sound foundation on which to build.

Finally, I thank my family and friends for their love, support and sacrifice. In particular, I would like to thank my wife for putting up with long hours and nerdy conversations.

TABLE OF CONTENTS

LIST OF TABLES

LIST OF FIGURES

1 INTRODUCTION

In vitro or cell-free systems are biologically-based reaction systems that harness the power of cells without many of the inconveniences of such. These systems are produced by extracting and/or purifying cellular machinery and placing the machinery into an environment sufficiently mimicking intracellular conditions to undertake biological reactions. There are myriad powerful tools in the subset of cell-free systems, such as cell-free protein synthesis (CFPS), cell-free transcription (CFT) and polymerase chain reaction (PCR). This work has employed all of these techniques with the primary focus on CFPS. The diverse and powerful potential of cell-free systems make them compelling tools in the belt of the chemical engineer.

The dominant advantage of CFPS over *in vivo* protein production systems is the open, unhampered access to the reaction environment. By extracting the cellular machinery, the cell membrane no longer presents a barrier to the reaction. The access allows for facile manipulation and monitoring of the reaction environment. Aspects of the reaction such as pH, salt content, and redox potential are readily controlled (1-4). Reaction content can be controlled such as genetic material (5-7), catalytic enzymes (8-11), chaperones (2,12), energy sources (13-16), and cofactors.

Cell-free systems have many other propitious features. CFPS reactions harness the entire reaction volume for synthesis, unlike production in cell fermentation, where only 5-20% of the fermentation volume (intracellular space) is actively participating in synthesis (17). CFPS is also instantly scalable, in other words, the reactions do not need serial fermentations to get to a final fermentation volume, rather they can be immediately initiated at scale (18-20). Reaction volumes

are broadly scalable, from 15 microliters up to 100 liters (18). Also, cell-free systems have high specific yields and very low levels of byproducts (21). This specificity eases the burden of production, purification, and analysis. Cell-free systems can also be assembled in high-throughput formats that rely on direct expression from PCR products known as linear expression templates (LETs) (7,22,23).

The many favorable features of CFPS make it a compelling tool for a broad range of applications, such as protein engineering, high throughput screening, and microarrays (6,24-26). Many therapeutic and diagnostic oriented applications have been pursued such as functional antibodies (27), therapeutic proteins (28), and functional genomics (29,30). CFPS allows for applications that would otherwise be difficult or impossible *in vivo* such as targeted NMR-based structural analysis (31), incorporation of unnatural amino acids (8,20), and production of toxic proteins (19,32).

1.1 **Scope of the Projects**

Although there are many CFPS applications and systems reported, there remains many promising yet unexplored CFPS technologies and applications. In this work, we aimed to improve and demonstrate the utility of CFPS systems for some of these applications. We consider these projects in 2 primary divisions: 1) enhancement of CFPS technology and 2) application of CFPS technology. Detailed background information for each research project is found within each chapter.

In summary, the objectives of this work are:

1. To produce more stable and accessible reagents for CFPS.
2. To enhance preparation methods of extracts containing exogenous catalysts that aid in protein synthesis.

3. To develop a rapid vaccine production platform based on CFPS.
4. To produce novel functionalized virus-bases nanoparticles.
5. To enhance protein stability through site-specific immobilization.
6. To expand the language of biology through native codon reassignment.

1.1.1 Enhancing CFPS technology: Lyophilization, Alternative Fermentation

Lyophilized CFPS: CFPS systems have many compelling features not found *in vivo*. However, one shared trait is the necessity to store the samples long term below freezing for stability. The storage requirements restrict applications that require long-term transport or non-ideal storage, such as pharmacy-on-a-chip or onsite vaccine production. In efforts towards a more robust system, we produced a lyophilized CFPS system. This system maintained more long-term synthesis viability than standard aqueous systems under non-ideal storage conditions. Furthermore, our lyophilized system demonstrated reduced residual contamination. The development of lyophilized CFPS system reduces the cost of storage, simplifies storage procedure, and expands the viable applications of CFPS technologies.

Alternative Fermentation Conditions: Some CFPS systems require supplemental or exogenous elements to make them functional. For example, expression of the large protein *Candida antartica* Lipase B (CalB) in *Escherichia coli*-based cell extract results in low soluble yields unless excessive exogenous chaperone proteins (GroEL/ES) are introduced. Due to the open nature of CFPS, GroEL/ES can be added directly to the reaction mixture, however, this requires significant preparation in form of cell fermentation, lysis, protein purification, and protein analysis. To avoid these time- and cost-intensive efforts, we produced and optimized an improved system that relies on expressing the supplemental element during extract preparation. This system was based on basic adjustments in the fermentation of cells to be prepared into extract. The resulting

extracts were capable of producing upwards of 5x the amount of soluble CalB compared to the direct addition of GroEL/ES.

1.1.2 Applying CFPS Technology: Vaccines, Nanoparticles, Unnatural Amino Acids

Rapid Vaccine Production: Vaccines typically consist of an immunogenic element that is introduced into the host to induce adaptive immunity. For virus-directed vaccines, these elements are often the virus itself, either in an attenuated form or inactivated. Use of the virus itself raises concerns of potential disease caused by vaccination using viruses that are insufficiently attenuated or inactivated. Recombinant protein technologies allow this issue to be avoided by producing only the proteins necessary for immunogenicity while remaining insufficient for pathogenicity. Using Foot-and-mouth disease virus as a model virus target, we worked towards a rapid vaccine production system that utilizes CFPS as its protein production system. This system would allow for onsite vaccine production and deployment, thus reducing the costs and safety concerns surrounding the production of vaccine for worldwide viral epidemics, such Foot-and-mouth disease.

Novel Functional Virus-based Nanoparticles: The basic principles of recombinant virus protein production found in vaccine production could also produce novel nanoparticles. Viruses typically consist of nucleic acids encased in a nanometric protein-shell, known as a capsid. Capsid proteins typically self-assemble into the full capsid shell using cues from other capsid proteins or short sequences of the nucleic acids. Harnessing these propitious traits, we produced a novel virus-based nanoparticle based on the bacteriophage Qβ. These nanoparticles are thermostable up to 70°C and can form disulfide bonds between capsid proteins. In addition, we demonstrated that the toxic protein A2 can be incorporated in a surface-accessible manner at a level of 1 A2 per 1

nanoparticle. These particles could have applications in imaging techniques or could be similarly engineered for myriad diverse applications.

Stabilized, Site-specifically Immobilized Protein: Immobilizing proteins has long been used for improving the stability of proteins. The most robust protein immobilization techniques are covalent. However, precisely controlling which location on the protein covalently binds to a surface is complicated by the naturally limited pool of only 20 amino acids building blocks. Therefore, covalent immobilization techniques that target residue side-chains often present multiple immobilization possibilities for a single protein. Unnatural amino acids provide a unique functional group that can be designed to react orthogonally to other residues. These unnatural amino acids can be introduced virtually anywhere within a protein, allowing for rational engineering of the recombinant protein with the unnatural amino acid incorporated. Using this technology, we demonstrate that a green fluorescent protein can be site-specifically immobilized. This immobilization enhances the thermostability and robustness of the protein against chemical denaturants. The technology has promising applications in development of robust and reusable biosensors and biocatalysts.

Expanded Language of Biology: The introduction of unnatural amino acids effectively expands the langue of protein biology, allowing for diverse applications such as the above mentioned protein immobilization. Current technologies rely on the stop-codon reassignment or frame-shift codons to incorporate the unnatural amino acid. Stop-codon reassignment is restricted by the existence of only 3 stop codons, one of which must be used to terminate the peptide synthesis. Furthermore, reassigned stop codons will frequently be read as stop, resulting in premature peptide termination. Frame-shift codons suffer from the trouble of competing against the tRNA for the 3-base codon. Due to the inefficiencies, these techniques have only been

successful at incorporating a few different unnatural amino acids simultaneously at low efficiency. We propose the novel method of complete native codon reassignment for unnatural amino acid incorporation. To accomplish this, we remove effectively all of the native tRNA and replace it with a synthetic minimal set of tRNA. This technology could potentially allow up to 40 unnatural amino acids to be incorporated simultaneously, doubling the canonical set of amino acids.

1.2 **Outline**

The bulk of this dissertation constitutes modifications of publications that I lead, developed, and authored, in several cases with significant help from other students as described in more detail in each chapter. These are summarized below.

Chapter 2: Stabilized Cell-free Systems through Lyophilization

This chapter is an adaptation from the article entitled "Lyophilized *Escherichia coli*-based Cell-free Systems for Robust, High-density, Long-term Storage" published in the journal *Biotechniques*, April 2014.

Chapter 3: Alternative Fermentation Conditions for Extract Preparation

This chapter is an adaptation from the article entitled "Alternative Fermentation Conditions for Improved *Escherichia coli*-based Cell-free Protein Synthesis Requiring Supplemental Components for Proper Synthesis" published in the journal *Process Biochemistry*, February 2014.

Chapter 4: Rapid Vaccine Development and Production

This chapter discusses the impetus behind a rapid vaccine development system based on CFPS and the results of the developing technology and is in part an adaptation from a review article entitled "Foot-and-mouth Disease: Technical and Political Challenges to Eradication" submitted to Vaccine Journal, February 2014.

Chapter 5: Novel Virus-based Nanoparticles

This chapter is an adaptation from the article entitled "The Incorporation of A2 Protein to Produce Novel Q[beta] Virus-like Particles using Cell-free Protein Synthesis" published in the journal *Biotechnology Progress*, March 2011.

Chapter 6: Stabilized Protein Through Site-specific Immobilization

This chapter is an adaptation from the article entitled "Enhanced Protein Stability Through Minimally-invasive, Direct, Covalent and Site-specific Immobilization" published in the journal *Biotechnology Progress*, January 2013.

Chapter 7: Expanding the Language of Biology: Sense Codon Reassignment

This chapter discusses the impetus behind expanding the language of biology based on CFPS and the results of the developing technology and is in part an adaption from the article "Cell-free Unnatural Amino Acid Incorporation with Alternative Energy Systems and Linear Expression Templates" published in *New Biotechnology*, January 2014.

Chapter 8: Conclusions and Future Work

This chapter briefly summarizes the novel work performed as part of this dissertation and suggests future impacts and directions for ensuing works.

2 STABILIZED CELL-FREE SYSTEMS THROUGH LYOPHILIZATION

This chapter is an adaptation from the article entitled "Lyophilized *Escherichia coli*-based Cell-free Systems for Robust, High-density, Long-term Storage" accepted to *BioTechniques* for publication in April 2014. This work was developed and lead by myself with the help of Scott Berkheimer and Chris Werner.

2.1 Introduction

Cell-free protein synthesis (CFPS) is a powerful *in vitro* transcription/translation tool for rapid and efficient production of recombinant proteins. Compared to *in vivo* protein production, directly accessible cell-free systems provide superior control over the synthesis environment, higher product selectivity, and faster expression of recombinant genes (7,17,33). These attributes make cell-free technology an excellent platform for high-throughput recombinant expression and synthetic biology technologies (23,33-37). Exploiting the benefits of CFPS, myriad proteins have been produced such as virus-like particles (1,19), proteins containing unnatural amino acids (8,9,38), cytotoxic proteins (19), and a variety of biocatalytic enzymes (12,39).

CFPS has been successfully demonstrated with biochemical machinery extracted from many different organisms and cells types, such as wheat-germ, rabbit reticulocytes, insects, yeast, and HeLa cells (35,40). In this work, we focus on the most prevalent, least expensive, and generally highest yielding cell-free system, which is based upon *Escherichia coli* extract (35).

A common practice in CFPS is to store prepared cellular extracts at -20 ºC or -80 ºC prior to use in efforts to maintain protein synthesis viability (8,41-43). Such practice necessitates fairly significant capital equipment investment in the form of low or ultralow temperature freezers, their maintenance, emergency backup freezers, and emergency backup power. These storage considerations are particularly cumbersome when stockpiling large quantities of extract for applications such as rapid vaccine and/or therapeutic production in response to a pandemic. A further limitation of storing the CFPS extracts below freezing temperatures is the inability to easily transport for mobile use applications.

One possibility to improve CFPS extract storage efficiency and utility is to lyophilize the extracts. Lyophilizing or freeze-drying simple protein solutions is a common process to remove the volatile liquids, leaving behind a protein powder. This technique reduces the storage volume and should slow the rate of protein degradation. We hypothesized that lyophilizing *E. coli* cell extracts would similarly reduce storage volume and potentially allow for longer shelf-life at temperatures above -80ºC. Lyophilized cell-free systems are commercially available and previous studies have reported successful synthesis of various proteins using rehydrated lyophilized extracts (44-48). However, a straightforward method to produce a lyophilized *E. coli*-based cell-free system has yet to be detailed in literature. Furthermore, the impact of lyophilization and storage at non-standard temperatures on protein synthesis performance has yet to be described. Here we report a straightforward method for lyophilizing *E. coli* extract for CFPS using standard machinery. The lyophilized extracts allow for higher density storage and maintain a higher protein synthesis viability at non-standard storage temperatures than aqueous extracts. This simple method provides a viable and convenient alternative to traditional storage strategies by reducing storage costs, protecting extract viability and promoting CFPS accessibility.

2.2 Materials and Methods

2.2.1 Cell Extract Preparation

Cells were grown and extracts prepared as previously described (7,49). All growth stages were performed at 37ºC in LB media at 280 rpm. Briefly, *Escherichia coli* strain BL21-Star™ (DE3) (Life Technologies, New York) was inoculated overnight in 5 mL volumes. Overnight growths were transferred to 500 mL baffled shake flasks containing 100 mL media. The intermediate growths were monitored to an OD_{600} of 2 and transferred to 2.5 L Tunair shake flasks (IBI Scientific, Iowa) containing 1 L of media. Growths were induced with 1 mM IPTG (GoldBio®, Missouri) at OD_{600} of 0.4-0.7 and grown until mid- to late-log phase (OD_{600} of 2.0 in this work). Cells were harvested, washed, homogenized and prepared using the streamlined method described previously (7,50).

2.2.2 Lyophilization of Extracts

Three extract types were lyophilized: 1) standard extract ($xSTD_{lyo}$), 2) extract supplemented with 0.05 gm per mL sucrose as a lyoprotectant ($xSUC_{lyo}$), and 3) a ready-to-use mixture of extract and small molecules necessary for phosphoenolpyruvate-energized CFPS ($[xSTD+ePEP]_{lyo}$). Lyophilization took place in 5 mL volumes as follows. Samples were loaded into 70 mL cylindrical glass vials for shell freezing in a -40 ºC ethanol bath (Just-A-Tilt Shell Freezer Chiller SF-4Az, FTS Systems, New York) and incubated for a minimum of 5 minutes. Vials were transferred to the freeze dryer (Flexi-dry MP, FTS Systems, New York) for 20 minute periods. The operating conditions of the freeze dryer were -60°C and <120 mTorr, with a 19-20 ºC ambient temperature. At the end of each 20 minute drying period, vials were placed in the -40ºC shell freezer for 1 minute and subsequently replaced onto the freeze dryer. Lyophilization

continued in this manner until at least 95% of the estimated water mass was lost (typically 3 cycles), at which time the vials were chilled on shell freezer for 1 minute, then placed back on the freeze dryer for an additional 60 minutes to provide for removal of the more tightly interacting water molecules. Lyophilized product was gently ground using a chemical spatula in a glass vial, aliquoted by mass, and stored in sealed microcentrifuge tubes.

2.2.3 Energy Systems

An aqueous phosphoenolpyruvate-based energy system ($ePEP_{aqu}$) was employed as the primary aqueous energy source for CFPS reactions, as previously described (15). The powdered versions of the $ePEP_{aqu}$ energy system ($ePEP_{pow}$) and a Glucose-based energy system ($eGLU_{pow}$) were used with slightly adapted reagent amounts indicated below (13). $ePEP_{pow}$ contained 0.137gm of phosphoenolpyruvate (PEP), 0.0328gm of ammonium glutamate, 0.711gm of potassium glutamate, 0.0099 gm of potassium oxalate, 0.0044gm of NAD, 0.0041gm of CoA, 0.0136gm of ATP, 0.0091gm of CTP, 0.090gm of GTP, 0.0095gm of UMP, 0.0034gm folinic acid, and 0.0017gm of tRNA. $eGLU_{pow}$ contained 0.1081gm of glucose, 0.0328gm of ammonium glutamate, 0.5284gm of potassium glutamate, 0.0348gm of dibasic potassium phosphate, 0.0044gm of NAD, 0.0040gm of CoA, 0.0094gm of AMP, 0.0063gm of CMP, 0.0070gm of GMP, 0.0063gm of UMP, 0.0007gm of folinic acid, and 0.001706gm of tRNA. A separate solution of amino acids and a separate solution of spermidine and putrescine were prepared. The spermidine and putrescine were kept separate due to their extremely hydrophilic nature. Once all components –excluding amino acid mix and spermidine/putrescine mix - were weighed out, they were combined in a 15mL conical tube and mixed until homogeneous. The powder energy mixes were divided into carefully weighed aliquots ranging from 0.04 to 0.06 g. When suspended in water for CFPS reactions, 4.157 and 5.377 mL water per gram powder were added to the PEP and glucose energy sources,

respectively. The hydration volumes (mL water per gram energy powder) were evaluated such that the final density of powdered components in hydrated powder systems equaled the density of components in prepared aqueous systems (Appendix A Equation 9-4).

2.2.4 Rehydrating Extracts and Cell-Free Protein Synthesis.

DC™ assays (Bio-Rad, Hercules, California) were performed on samples of untreated aqueous extract and rehydrated extract following the manufacturer's specifications with Bovine Serum Albumin as the control protein. Lyophilized extract was rehydrated in water according to optimal ratio determined in DC™ assay (Appendix A).

Cell-free protein synthesis reactions were performed on each extract type as previously described (20). In brief, reactions contained 25% v/v extract, 25% v/v energy source, 12 nM plasmid encoding the GFP reporter protein (pY71-sfGFP), and optimized magnesium glutamate concentration (in this study: 9 mM). Reagents were combined in microcentrifuge tubes and pipetted into a 96-well flat-bottom opaque plate in 20 µL aliquots as droplets in the center of each well. After the wells were sealed, the plate were incubated for 3 hours at 37 ^{o}C. Following the reaction, 45 µL water was added to each well to dilute the reaction over the bottom surface of the well. Resulting GFP fluorescence was measured using a Synergy Mx (BioTek Instruments, Inc., Vermont) and protein yield was determined using a linearly correlated calibration curve, as previously detailed (49).

2.2.5 Bacterial Contamination

To consider potential bacterial contamination of the extracts, liquid extracts or lyophilized extracts rehydrated with sterile ultrapure water were diluted in sterile SOC media and plated on LB Agar Miller plates. Plates were incubated for 24 hours, at which point colonies were counted.

2.3 Results and Discussion

Cell-free protein synthesis (CFPS) affords many benefits over *in vivo* synthesis systems such as open access to the synthesis environment, rapid expression of recombinant PCR-products, and easy application of *in vitro* synthetic biology. An additional beneficial trait of CFPS is that cell extracts can be produced in large batches and stockpiled for future use (18). However, the extract is traditionally stored at -80°C to maintain viability, increasing the storage expense and complicating transport of the extract. Here we demonstrate that straightforward lyophilization of *E. coli*-based CFPS extracts 1) significantly reduces storage volume, 2) stabilizes the extract at less than ideal storage temperatures, and 3) decreases bacterial contamination. We also propose and demonstrate that powdered energy systems may be utilized to create a CFPS system that can be stored at high density and easily transported.

2.3.1 Extract Lyophilization, Rehydration, and CFPS

E. coli cell extracts (Table 2-1) were prepared as reported previously prior to lyophilization (49). Two lyophilized extracts types were prepared: 1) standard extract ($xSTD_{lyo}$) and 2) standard extract with sucrose as a potential lyoprotectant ($xSUC_{lyo}$). By measuring the mass of the lyophilized powered, the total mass loss was measured and percentage water loss approximated based on DC™ assay analysis (Appendix A Equation 9-2), as seen in Figure 2-1A and B, respectively. In all cases, extracts lost more than 97% of their estimated original liquid content. The removal of the majority of liquid content reduced the storage volume over 2 fold and storage mass over 9 fold.

Lyophilized extracts were ground into powders to promote homogeneity, then aliquoted by mass for storage at -80, -20, 4 and 27 °C. Each lyophilized extract had a unique consistency. $xSTD_{lyo}$ had the consistency of well-milled wheat flour and was easily ground into a fine

homogenous powder. The fine powder was easily compressed, allowing for 2-3 times the storage density of liquid extract. $xSUC_{lyo}$ formed sticky heterogeneous granules, making it somewhat difficult to achieve homogeneity and compressed storage.

Table 2-1 – Extracts and Energy Systems

Type		Description
Cell Extracts	$xSTD_{aqu}$	Standard extract, aqueous
	$xSTD_{lyo}$	Standard extract, lyophilized
	$xSUC_{lyo}$	Extract with sucrose, lyophilized
Hybrid	$[xSTD+ePEP]_{lyo}$	1:1 xSTD:ePEP, mixed as solution, lyophilized
Energy Systems	$ePEP_{aqu}$	Phosphoenolpyruvate-based energy system
	$ePEP_{pow}$	Powder mix of ePEP components[1]
	$eGLU_{pow}$	Powder mix of glucose-based energy system[1]

[1] The 19 amino acids, putresine and spermadine were not included in this powdered mix, but added as separate solutions to the eCFPS reactions, as specified in the Supplemental Information.

In preparation for cell-free reactions, extract powders were suspended in sterile ultrapure water. To establish a baseline for rehydration, $xSTD_{lyo}$ was rehydrated at multiple levels and subjected to DC™ assay to approximate what volume-to-mass ratio would provide the equivalent protein density as $xSTD_{aqu}$ (Appendix A Equation 9-1). From this baseline, the rehydration volume:mass ratio was established for $xSTD_{lyo}$ and calculated for $xSUC_{lyo}$ (Appendix A Equation 9-3).

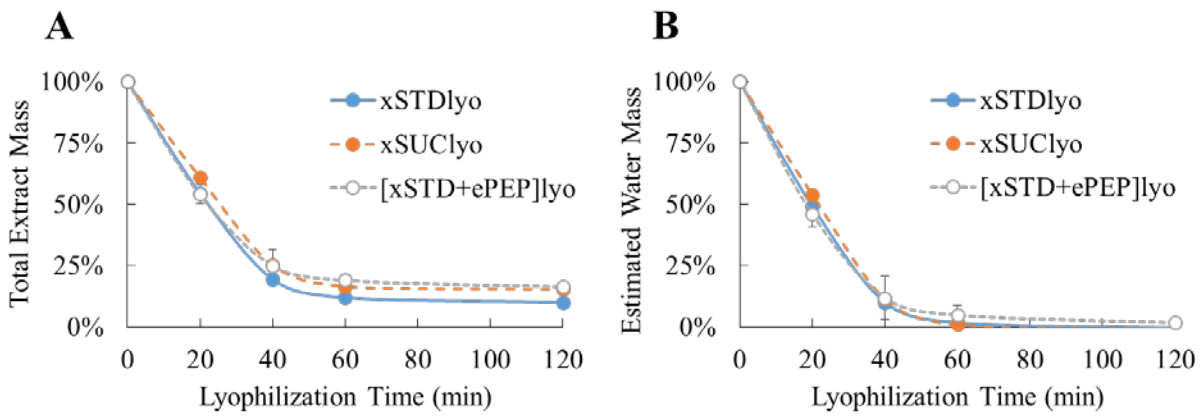

Figure 2-1 – Total Mass and Estimated Water Content during Lyophilization. (A) The total mass of the extract was monitored throughout the lyophilization process. Extracts lost nearly 80% of their total mass in the first 40 minutes of lyophilization. (B) The water content remaining during lyophilization was estimated based on calculated partial densities of water in the extract solution (Appendix A). In all cases, the remaining estimated water content at the end of lyophilization was less than 2%. Error bars represent one standard deviation. n=3 for $xSTD_{lyo}$, n=2 for $[xSTD+ePEP]_{lyo}$, and n=1 for $xSUC_{lyo}$.

Extracts were tested for protein-synthesis viability over extended storage times with the results displayed in Figure 2-2. Notably, $xSTD_{aqu}$ performed equally well at -80 and -20°C over the span of 90 days, suggesting that -80°C storage may not be required for long term storage and viability of CFPS extracts. Indeed, even at 4°C, $xSTD_{aqu}$ maintained effectively all of its activity through 30 days. Under the storage conditions of 27°C, $xSTD_{aqu}$ exhibited exponential decay in synthesis performance with less than 2% activity by day 30 and effectively no activity by day 60.

$xSTD_{lyo}$ and $xSUC_{lyo}$ initially maintained an average 85% of the protein synthesis viability of $xSTD_{aqu}$. Extract viability was retained when stored at -80°C, while increasing storage temperatures corresponded to increasing extract degradation rates. Notably, $xSTD_{lyo}$ and $xSUC_{lyo}$ stored at room temperature maintained about 20% protein synthesis viability at day 90. In contrast, $xSTD_{aqu}$ stored at room temperature retained less than 2% viability by day 30. In short, the lyophilized extracts retained significantly higher protein synthesis viability than the liquid extracts when stored for more than 30 days above freezing.

The addition of sucrose as a lyoprotectant to extracts prior to lyophilization did not appear to be beneficial (Figure 2-2). Sucrose and other protein lyoprotectants theoretically stabilize proteins from becoming denatured during the drying and rehydration process (51). However, lyoprotectants are typically utilized to protect purified proteins in solutions that contain one or few different types of proteins. In the case of extracts, the complex mixture of proteins and other small molecules in solution may contain components that fill the role of stabilizing proteins during drying, making the addition of sucrose unnecessary.

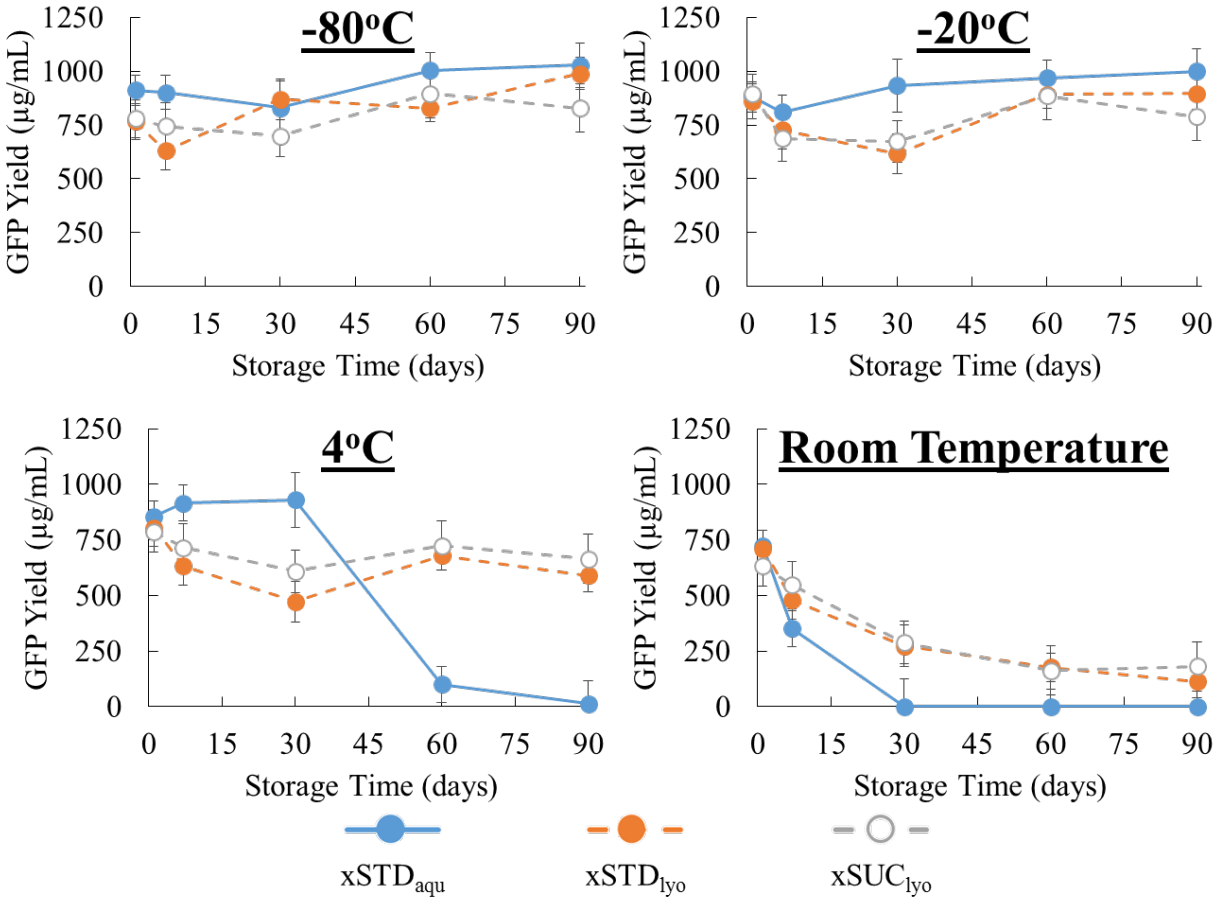

Figure 2-2 – CFPS Yields from Aqueous and Lyophilized Extracts Stored at Various Temperatures. Standard storage for extracts is in an ultralow freezer at -80°C. Here, extracts were stored at -80°C, -20 °C, 4 °C, and room temperature (27 °C±3 °C). The first data point (day 1) correspond to one day after lyophilization. Error bars represent one standard deviation of protein yield and error contributed to rehydrating the extracts. n=3.

To identify potential causes of lost extract viability at higher storage temperatures, we examined bacterial contamination. Lysis efficiency using a high-pressure homogenizer such as that used for this work has been reported to be 99.9996% (49). Prior to lysis, cell concentrations are approximately 600 billion per mL, thus even at 99.9996% prepared extracts can have upwards of 2.4 million cells per mL extract. Bacterial contamination was measured in colonies per μL extract plated (Appendix A Figure 9-2). Regardless of storage conditions, $xSTD_{aqu}$ had the highest amount of contamination, with an effective cell lysis efficiency of 99.99998% for $xSTD_{aqu}$ stored at -80ºC. By 14 days, $xSTD_{aqu}$ stored at room temperature was too contaminated to quantify accurately and total CFPS viability dropped significantly, suggesting that bacterial growth likely played a role in degrading the extract. In contrast, $xSTD_{lyo}$ showed zero colonies after 30 days at room temperature and retained CFPS viability (Supplement Information Figure 9-2).

2.3.2 Powdered Energy Systems

Straightforward lyophilization of extracts lays the foundation for high-density and long-term storage of CFPS systems. However, extracts must be provided with an energy source and essential building blocks to successfully transcribe mRNA and translate protein. Typically, energy sources for CFPS are stored as solutions at -80ºC due to the temperature sensitive nature of high-energy components such as nucleoside triphosphates, nicotinamide adenine dinucleotide, coenzyme A, and phosphoenolpyruvate (PEP). In powdered formats, high density mixtures of energy-rich components are less likely to suffer degradation. We therefore considered powdered energy systems as a possible alternative to aqueous storage.

PEP-based energy systems are some of the highest yielding CFPS energy systems (14,52). We therefore developed two PEP-based powdered energy systems: 1) a mix of extract and a PEP-based energy system subsequently lyophilized into powder ($[xSTD+ePEP]_{lyo}$) and 2) a powder mix

of individual components for a PEP-based energy system ($ePEP_{pow}$) (Table 2-1) (14). To produce $[xSTD+ePEP]_{lyo}$, an 1-to-1 aqueous solution of $xSTD_{aqu}$ to $ePEP_{aqu}$ was lyophilized as described above. The resulting powder exhibited a sticky heterogeneity similar to $xSUC_{lyo}$. $[xSTD+ePEP]_{lyo}$ was maintained at -80 or -20 ^{o}C to mitigate extract degradation effects caused by higher temperature storage, as seen in $eSTD_{lyo}$ and $eSUC_{lyo}$. $ePEP_{pow}$ was stored across all temperatures to check against temperature sensitive degradation specific to the energy system.

The temperature sensitive nature of many $ePEP_{pow}$ components compelled us to propose a more stable powdered energy system. We consulted the previously reported alternative energy systems consisting of components less sensitive to temperature (7,13,15,53) (Appendix A). A powdered glucose-based system ($eGLU_{pow}$) was selected based on the stability of its components to compare with powdered $ePEP_{pow}$. Glucose is significantly cheaper than PEP and glucose-based energy systems have been reported to reduce protein yield expenses compared to PEP-based systems (USD per mg protein) (7). Also, glucose is quite stable in crystal form. To further increase the stability of the glucose-based system, nucleotide triphosphates were replaced with their monophosphate counterparts.

Rehydrating the powdered energy systems in small volumes added a challenge of obtaining a proper pH. The PEP contained in $ePEP_{pow}$ has a low pKa, yet remains primarily insoluble below pH 6. For $[xSTD+ePEP]_{lyo}$, pH is addressed prior to lyophilization and the appropriate pH and buffer ingredients are adjusted prior to lyophilization. However, $ePEP_{pow}$ pH must be considered at the time of hydration. To address this concern, NaOH was added to the hydration mix at an optimized level (Appendix A Figure 9-3).

CFPS using the powdered energy systems initially produced high protein yields, as seen in Figure 2-3. Indeed, pH-optimized $ePEP_{pow}$ outperformed aqueous $ePEP_{aqu}$. Comparisons of these

two systems' reveal that pH-optimized $ePEP_{pow}$ has a lower pH than $ePEP_{aqu}$, suggesting that the $ePEP_{aqu}$ system would benefit from pH-optimization (Appendix A Figure 9-4). Initial yields from $eGLU_{pow}$ were very low, totaling less than 5% of the $ePEP_{aqu,}$ which was not unexpected based on previous work and the longer pathway required to properly metabolize glucose (7).

Over the 60 day storage time, $ePEP_{aqu}$ performed surprising well at elevated storage temperatures, maintaining over 25% viability at room temperatures (Figure 2-3). This result was unexpected due to the purported instability of its components. $eGLU_{pow}$ yields remained low throughout storage, but remained relatively consistent with no observable loss in yields, suggesting it is quite stable. However, the low yields produced with $eGLU_{pow}$ severely limit the utility of such a CFPS system.

The powdered PEP-based energy systems ($[xSTD+ePEP]_{lyo}$ and $ePEP_{pow}$) maintained a minimum of 35% of the viability of the $ePEP_{aqu}$ over 60 days. Although $[xSTD+ePEP]_{lyo}$ displayed upwards of 95% viability compared to $xSTD_{aqu}$ with $ePEP_{aqu}$, the lyophilized system exhibited significant inconsistencies in performance. Inconsistent performance of $[xSTD+ePEP]_{lyo}$ is likely due to the difficulty to homogenize the sticky lyophilized powder. $ePEP_{pow}$ with optimized pH performed well overtime at all storage conditions. Indeed, at 60 days, $ePEP_{pow}$ stored at room temperature retained over 33% of its original viability, over 30% more than $ePEP_{aqu}$.

2.4 **Conclusion**

The straightforward methods of extract lyophilization and powdered energy systems presented here allow for >2x reduction in storage volume and >10x reduction in storage mass of eCFPS systems. These powdered systems are also more stable than their aqueous counterparts, permitting 1) more economic storage, 2) simplified transport conditions, and 3) a simplified "just-add-water" protein synthesis system. These benefits make powdered CFPS systems compelling

candidates for promising applications such as pharmacy-on-a-chip microfluidic devices for rapid "on-the-site" treatment and rapid large-scale vaccine or therapeutic protein production from stock-piled extract. Indeed, the development of lyophilized extract and powdered energy systems for CFPS reduces the cost, simplifies the procedure, and expands the viable applications of CFPS technology.

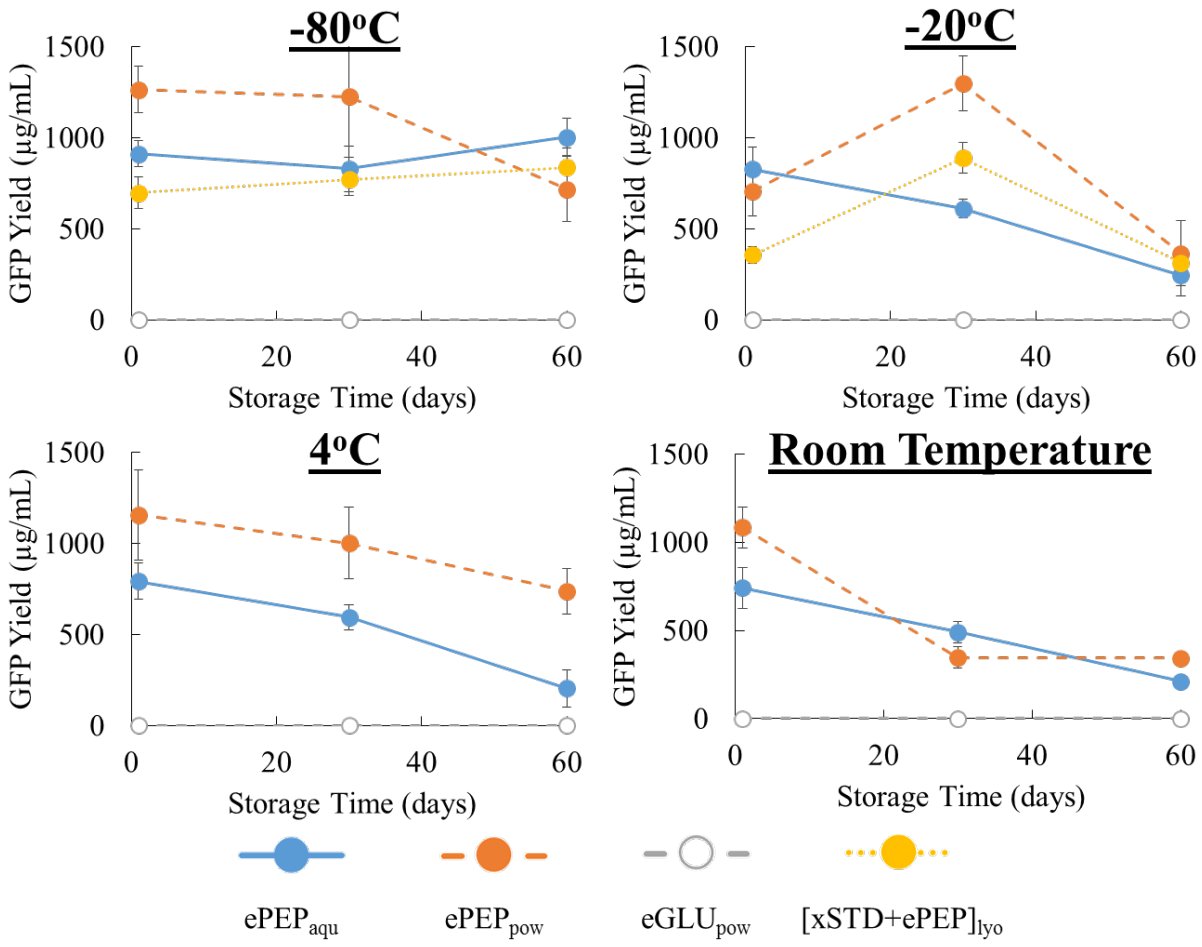

Figure 2-3 – CFPS Yields from Aqueous and Powdered Energy Systems Stored at Various Temperatures. Standard storage for CFPS energy sources is in an ultralow freezer at -80°C. Here, systems were stored at -80°C, -20 °C, 4 °C, and room temperature (27 °C±3 °C). The first data point (day 1) corresponds to one day after lyophilization or mixing of the powder. Error bars represent one standard deviation of protein yields and error contributed to hydrating the powders. n=3.

3 ALTERNATIVE FERMENTATION CONDITIONS FOR EXTRACT PREPARATION

This chapter is an adaptation from the article entitled "Alternative Fermentation Conditions for Improved *Escherichia coli*-based Cell-free Protein Synthesis for Proteins Requiring Supplemental Components for Proper Synthesis" published in *Process Biochemistry* in February 2014. This work was developed and lead by myself with the help of Anna Hawes, Prashanta Shrestha, Jay Rainsdon and Jeffrey Wu.

3.1 Introduction

The *in vitro* protein production system known as Cell-free Protein Synthesis (CFPS) is a propitious system for protein production when direct access to the reaction environment is desired (6,35). Compared to *in vivo* expression, CFPS maintains many advantages such as improved monitoring and control, reduced reaction volumes, virtually silenced background expression, simplified purification, and removed effect of many toxins (33,35,54,55). These traits make it quite versatile for applications in protein engineering such as the development of pharmaceutical proteins (18), toxic proteins (19,32), vaccines (56,57), bioimaging techniques (58), proteomic studies (59) and high-throughput protein engineering (6,12,60). In addition, cell-free systems are increasingly being exploited for the direct combination of biomachinery from different organisms to create synthetic pathways and products which has resulted in the emergence of cell-free synthetic biology (33,34,55,61-64).

One prevalent, straightforward, and enduring cell-free system is based on crude extracts prepared from *Escherichia coli* (*E. coli*) (35,65). Over the last 50 years, *E. coli*-based CFPS (eCFPS) methods have been modified to reduce cost and labor (10,21,66,67), decrease background gene expression (21,68), and increase protein production to levels to exceed 1 mg/mL (61,68,69). While these adjustments have made eCFPS more widely accessible, economic, high-yielding, and applicable than many other CFPS systems, the range of proteins that can be correctly produced is restricted by the inherent limitations of its prokaryotic-based biomachinery (35). For example, unmodified eCFPS cannot produce active [FeFe]-hydrogenases, cannot correctly fold some complex eukaryotic proteins, and cannot incorporate noncanonical amino acids site-specifically. However, the scenarios mentioned can be and have been accomplished in eCFPS through synthetic pathways by adding necessary purified exogenous components to the *in vitro* reaction and/or by heterologous expression of the necessary components during the *E. coli* fermentation used to prepare the extract eCFPS (2,8,60,70). Systems based on purified machinery become more labor intensive and monetarily expensive with each additional component, as epitomized by the P.U.R.E system where every component is purified and then reconstituted for eCFPS (43), making it greater than 100 times more expensive than crude extract systems (49). To counter the expense of such purification and increase the accessibility and efficacy of eCFPS systems requiring supplemental components, here we report the effects of plasmid-based heterologous gene expression on cell fermentation and cell extract viability, and demonstrate optimal conditions for such systems. Specifically, we optimized the fermentation conditions for cells heterologously expressing supplemental components in efforts to increase functional protein yields and broaden the potential of protein engineering and synthetic biology applications with eCFPS systems.

The gene expression profile of bacteria changes according to the growth rate and phase of the cell (71,72). Standard eCFPS traditionally harvests cells during the mid- to late-log phase to achieve maximum protein yields (25,68). The basis of this tenet is part empirical and part logical. Cells growing the most rapidly contain an efficient balance of transcription/translation machinery to maintain the steady pace of cellular division (71). In our experience, the heuristic of harvesting during mid- to late-log phase is highly accurate when standard, simple and stable proteins are being produced. To our knowledge, there have been no other reports exploring harvesting cells for eCFPS extracts outside of the mid- to late-log phase. However, Seo, Bailey and others demonstrated that maximum growth rates seen during log phase correspond to minimum plasmid copy number *in vivo (72,73).* Others have demonstrated the positive correlation between plasmid copy number and expression of plasmid-borne genes (74-76). Based on these findings, we hypothesized that a delayed harvest time following the log phase would yield higher levels of supplemental components and achieve more favorable ratios of endogenous to supplemental machinery. To test the effects of harvest time on extract viability of eCFPS, we explored three distinct cases: 1) the standard case of *E. coli* without plasmids as a control, 2) the modified case of *E. coli* containing a plasmid with genes for protein-folding chaperone complex GroEL/GroES (GroE), and 3) the modified case of *E. coli* containing plasmid with tRNA/tRNA-synthetase (RS) pair capable of incorporating a noncanonical amino acid at the amber codon (UAG) using a cell-free synthetic biological pathway (Figure 3-1).

The modifications described in this report are applied to two distinct eCFPS cases that demonstrate a conserved optimum harvest condition, suggesting that similar conditions could benefit other eCFPS systems using heterologous expression of essential supplemental components.

These techniques enhance the feasibility for using eCFPS as a high-throughput, economical, and efficient protein engineering and synthetic biology tool.

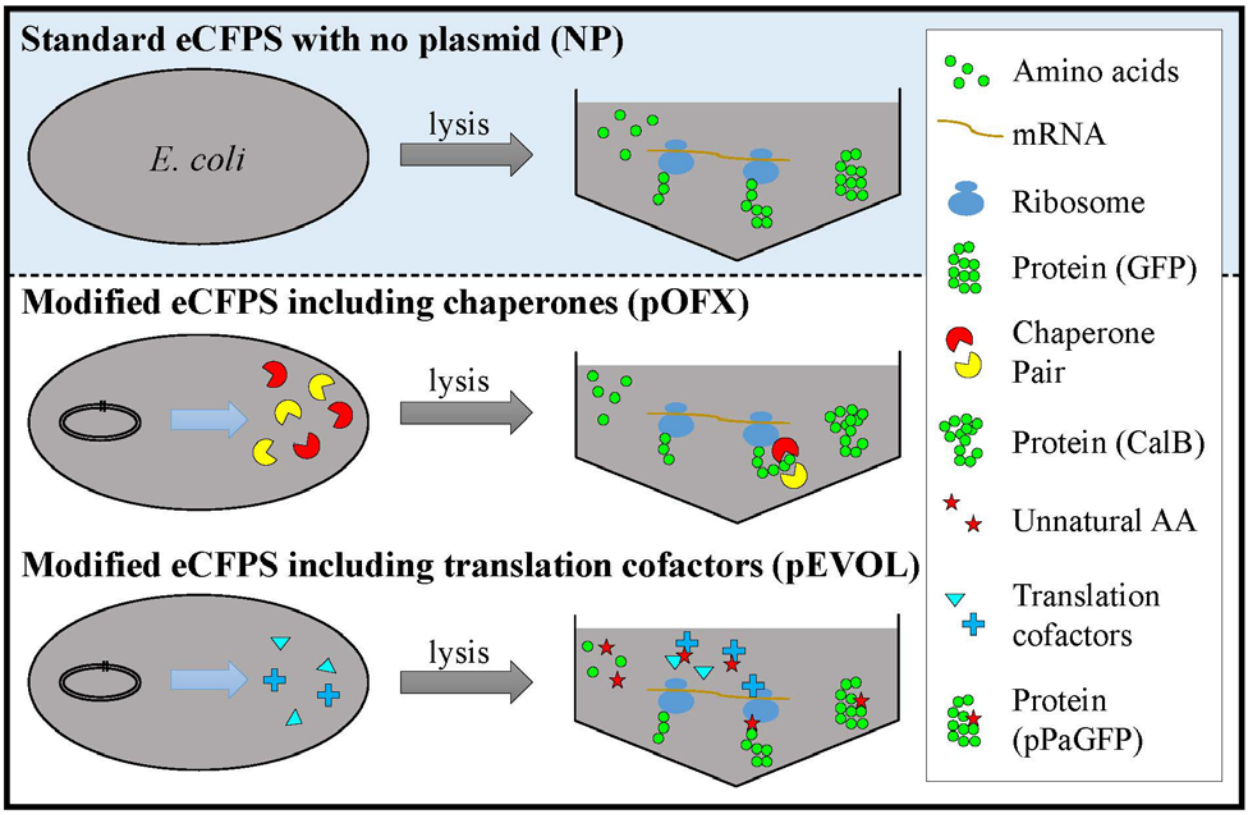

Figure 3-1 – Standard and Modified eCFPS Systems Employed for Exogenous Element Analysis

3.2 Materials and Methods

3.2.1 *E. coli* Cell Extract Growths

All extracts were prepared using the *Escherichia coli* strain BL21Star™ DE3 (Invitrogen, Carlsbad, CA) as follows: 1) containing no plasmid (NP), 2) containing pEVOL-*pPrF* plasmid (pEVOL), and 3) containing pOFX-GroEL/ES plasmid (pOFX). The pEVOL-*pPrF* plasmid, a kind gift from Dr. Peter Schultz (Scripps Research Institute), expresses chloramphenicol antibiotic resistance protein as well as a *Methanocaldococcus jannaschii* tyrosyl-aminoacyl-tRNA synthetase/tRNA pair (77). The pOFX-GroEL/ES plasmid, a kind gift from Dr. Dong-Myung Kim

(Chungnam National University), expresses spectinomycin antibiotic resistance protein as well as the chaperone proteins GroEL and GroES (2).

Each extract was grown with appropriate antibiotic and using sterile technique. All tubes and flasks were incubated at 37 ºC and 280 RPM. Overnight cultures in 5mL LB media were inoculated into 100mL 2xYT media in baffled intermediate flasks and grown until an OD_{600} of 2. Approximately 90 mL from the intermediate flasks were inoculated into 1L volumes of 2xYT media in 2.5L shake flasks. For cells grown with MOPS buffer, the 2.5L shake flasks contained 1L of 0.1 M MOPS in 2xYT media. At a cell density between OD_{600} 0.5 and 0.7 in the flasks, all fermentations were induced with 1mM isopropyl-β-d-thiogalactopyranoside and the pEVOL-harboring fermentations were additionally induced with 0.22g L-arabinose per liter fermentation. At 3, 4.5 and 6 hours after induction 300mL of extract were harvested. Two replicates were performed for each extract condition. Harvested cells were pelleted, homogenized using an Avestin Emulsiflex-B15 Homogenizer, and prepared as previously reported (49).

3.2.2 Cell-free Protein Synthesis Reactions

Cell-free protein synthesis reactions were performed with the following plasmids: 1) pY71-sfGFP 2) pY71-sfGFPT216Amber (8) and 3) pk7-CalB, a generous gift from Dong-Myung Kim (2). Reactions were run as previously described (20) with the following modifications. Reactions of 15 µL were conducted in flat bottom 96-well plates covered with plate sealing covers. Reactions were performed at 30 ºC and 37 ºC for 3 and 8 hours. Four replicates of each reaction were performed. As specified in the Results and Discussion, some reactions with the pY71-sfGFPT216Amber had purified *Methanocaldococcus jannaschii* aminoacyl-tRNA synthetase added at 12 µg per mL, as previously described (20). All reactions with the pk7-CalB plasmid

contained a 4:1 molar ratio of oxidized:reduced glutathione to stimulate disulfide bond formation (2,78).

3.2.3 Protein Yield Assays

GFP standard curve was assessed by comparing radioactivity and fluorescence yields, as previously described (49). Protein yields for CalB were measured by adding C^{14}-Leucine to the eCFPS reactions and scintillation counting the TCA-precipitated reaction product, as reported previously (79).

3.3 Results and Discussion

The traditional approach to eCFPS relies on using extract prepared from cells harvested at mid- to late-log phase (68). However, when extracts are prepared from cells grown with plasmids heterologously expressing supplemental components to aid in the synthesis of properly produced proteins, harvesting at mid- to late- log phase may not achieve an optimal balance of native and supplemental machinery to enable efficacious production of fully functional protein. To identify potentially more favorable conditions for cell fermentations used to produce extracts for eCFPS reactions, the following parameters were explored: **1)** delayed harvest times (3, 4.5, or 6 hours post induction) and **2)** buffered growth media with or without MOPS. MOPS was added to adjust against pH deviations typically observed during extended cell growth.

Under these growth parameters, we examined a standard eCFPS system with extract from cells containing no plasmid (NP) and two nonstandard plasmid-bearing systems: 1) extract from cells harboring the plasmid pOFX-GroEL/ES (pOFX), and 2) extract from cells harboring the plasmid pEVOL-*pPrF* (pEVOL). The NP system is defined as the standard eCFPS that uses extract from BL21Star™ DE3 *E. coli* cells without additional plasmids to and is commonly used to

produce proteins that do not require additional machinery or synthetic pathways. The pOFX system uses extracts from BL21Star™ DE3 *E. coli* cells harboring the pOFX plasmid and thus includes the folding chaperone proteins GroEL and GroES. The pEVOL system uses extracts from BL21Star™ DE3 *E. coli* cells harboring the pEVOL plasmid such that it includes an *E. coli*-orthogonal tRNA/tRNA synthetase (RS) pair. Thus the pEVOL system allows for the incorporation of a noncanonical amino acid when the amber stop codon is successfully suppressed. This tRNA/RS pair is essential for full length translation in proteins containing internal amber codons.

To test these cases, we expressed green fluorescent protein (GFP), *Candida antarctica* Lipase B (CalB), and a mutant GFP (pPaGFP). The protein GFP requires only native machinery for expression and therefore was chosen as a control across all cases. CalB is a large and complex eukaryotic protein that is only produced at low soluble yields without the aid of folding chaperones (2,12). Therefore, CalB was expressed in the pOFX system as well as the standard system. pPaGFP contains a T216 to amber codon mutation that requires the foreign transcription machinery found on pEVOL to produce full-length pPaGFP and therefore was only expressed with the pEVOL system (8).

3.3.1 Growth Conditions and Outcomes

Cells used to prepare eCFPS extract fermented in 1L cultures using the simple and inexpensive baffled shake flasks, as previously reported (10,49,67). This simple preparation technique allows for the eCFPS technology to be readily adapted by labs without specialized fermenters and may be combined with simple cost-effective lysis technologies, effectively lowering the entrance cost of the technology further (49).

As shown in Figure 3-2A, NP fermentations exhibited a definitive log phase with a transition near or shortly after 2 hours post induction to a clear stationary phase. Although MOPS clearly buffered the growth media, no apparent or statistical difference appeared between the growth profiles of buffered or unbuffered NP. Cells harboring plasmids displayed a similar log phase to the NP growths and began to transition out of log phase near or shortly after 2 hours post induction. However, the transitioning period between log and stationary phase took ~6 times longer for plasmid-harboring cells, resulting in higher overall OD_{600} and growth rate at harvest compared to the NP growths (Figure 3-2A). These results are consistent with previous reports that growth rates and maximum densities of cells harboring plasmids are altered by the presence of the plasmids (72,80).

The addition of the plasmid expressing heterologous elements during cell growth has the potential to increase the overall metabolic load and in turn change the proteomic profile of the cell (Appendix B Figure 10-4) (81). These effects could be exaggerated by factors such as plasmid copy number, gene expression level, and gene function (80,81). Both plasmids employed (pOFX and pEVOL) are high-copy number plasmids and should express the promoted genes at a high level The consistent deviation of the pOFX and pEVOL fermentation profiles from the plasmid-free cells suggests that similar fermentations will also likely result in altered growth profiles

As expected, the pH of media for cells grown with MOPS fluctuated less. Furthermore, all unbuffered growths exhibited a similar pH trend and all buffered growths exhibited a similar trend (Figure 3-2B). However, the pOFX growth trends were shifted approximately one half pH unit lower than the NP and pEVOL growths. The lower pH profile of pOFX growth is attributed to the mechanism of spectinomycin antibiotic resistance, which results in the release of pyrophosphoric acids (82).

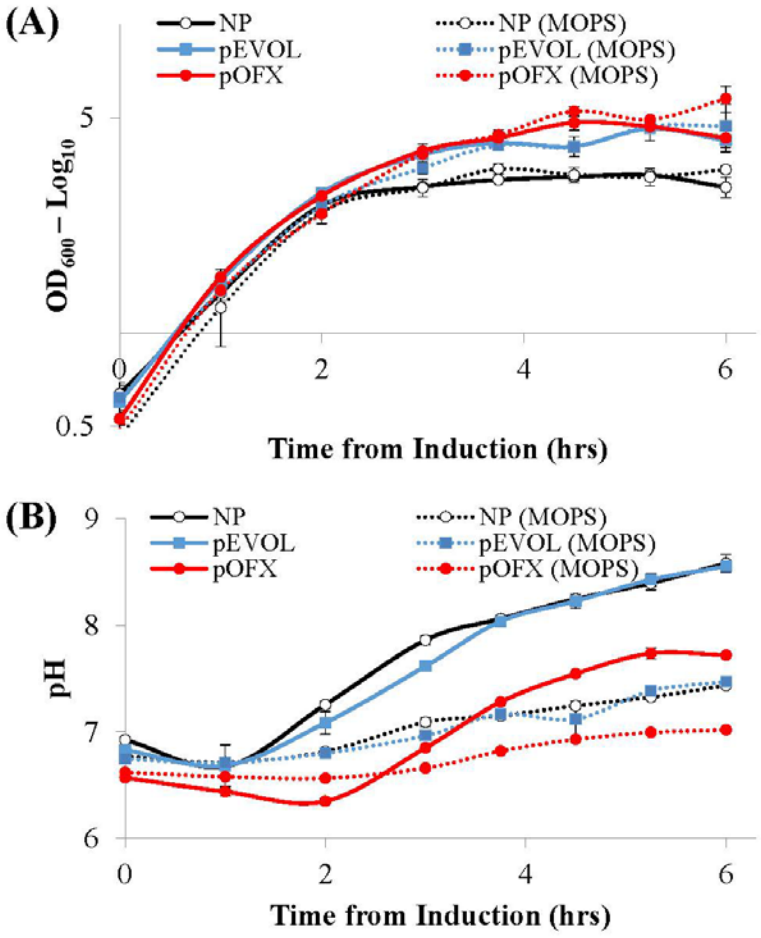

Figure 3-2 – Cell Growth and Media pH Curves for BL21Star™DE3 with and without Harboring Plasmids. Data was collected beginning at time of induction ($0.5<OD_{600}<0.7$). Growths were performed with and without 0.1M MOPS Buffer. (1A) OD_{600} profile of the fermentations. (1B) pH profile of the fermentations. The results from 2 separate fermentations (n=2) were averaged for each data point. Error bars represent one standard deviation.

To analyze the impact of growth conditions and harvest time on extract protein profiles, SDS PAGE and densitometry were performed on pEVOL and pOFX extracts (Appendix B Figure 10-4). The heterologous synthetase and GroEL/ES were overexpressed in pEVOL and pOFX, respectively. The amount of supplemental components as well as other extract proteins exhibited extract to extract variation and do not appear clearly correlated with harvest time. The changes throughout the extract profiles indicated that supplemental component concentration was not a singly important trait and the overall balance of the endogenous and supplemental components in

the extract likely plays a more significant role in extract viability. This is not entirely surprising, considering the many enzymes and small molecules involved in protein synthesis.

3.3.2 eCFPS Yields

After growth, cells were prepared for eCFPS reactions by harvesting, lysis, and clarification as reported previously (49). Cell extracts were then used with eCFPS to express the test proteins under the following traditionally optional conditions: **1)** eCFPS reaction time (3 or 8 hours) and **2)** eCFPS reaction temperature (30 or 37 ^{o}C) with n=4 replicates (n=2 extract preparations, n=2 eCFPS reactions per extract). To simplify the analysis of parameter impact on yields and cross-case comparisons, yields were fit to a simple linear regression, described in Figure 3-3. Individual reaction results can be found in Supplement Information (Figure 10-1).

3.3.3 Harvest Time

The NP system for eCFPS expressing GFP behaved consistent with the expectation that mid- to late-log phase harvesting produces highest yields, with highest yields occurring while using extract harvested nearest the log phase. For GFP, the average yield decreased by approximately 43%-45% for each 1.5 hours delay in harvest. The NP case expressing CalB also produced highest yields (total and soluble) when harvested at 3 hours and, as expected, the average solubility of CalB expressed with NP was low, at approximately 30%.

Although GFP does not require supplemental components, GFP expressed in pOFX and pEVOL extracts yielded 15-30% more protein than the standard NP case and appeared unaffected by harvest time (Figure 3-3). A possible explanation for the increase in yields is that cells harboring plasmids exhibited a delayed onset of stationary phase during cell growths, likely resulting in a distinct proteomic profile in comparison to the NP case. The lack of impact of harvest time on GFP

in pOFX and pEVOL extracts may be due to the similar growth rates observed across all harvest times.

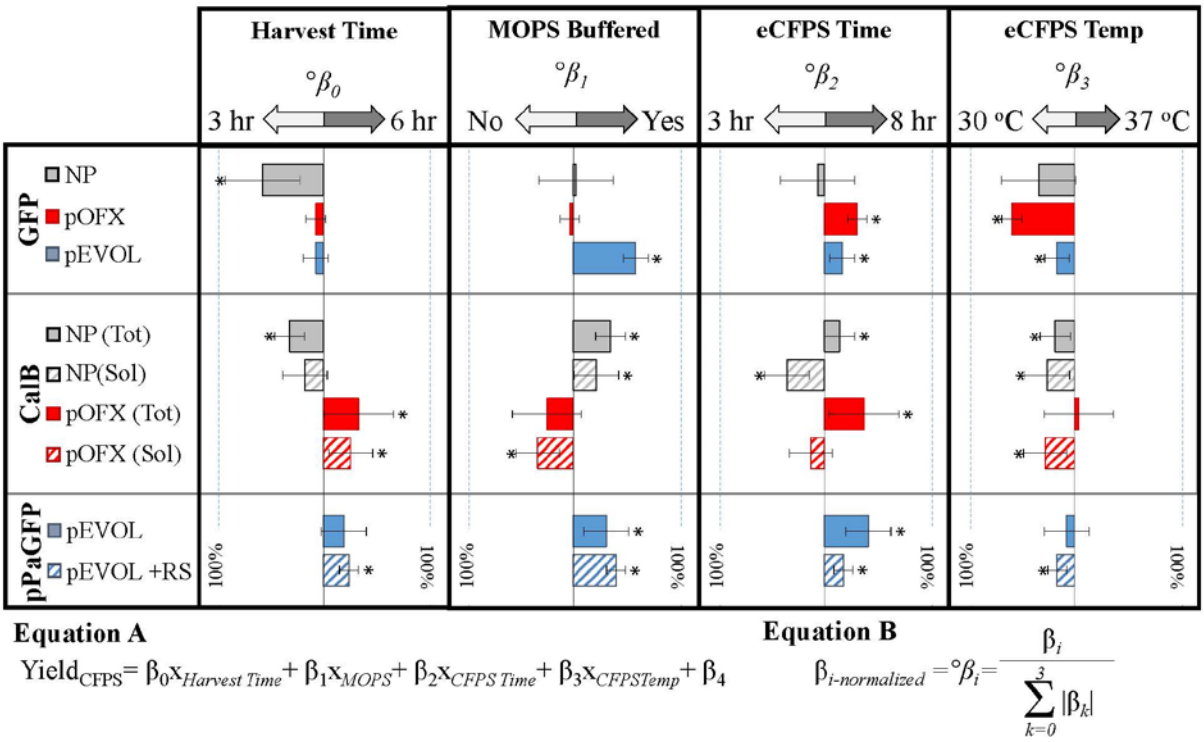

Figure 3-3 – Normalized Impact of Individual Parameter on CFPS Yield. A simple linear regression (Equation A) considering only parameter extremes allows for facile analysis of a given parameter's impact on specific extract/protein combinations. Parameter coefficients (β_i) were normalized within their regression, as described in Equation B. Normalized parameter coefficients ($^\circ\beta_i$) are plotted to readily compare relative impact within and between extract/protein conditions. For example, GFP yields expressed in NP extract are heavily affected by harvest time, with this statistically significant parameter coefficient accounting for roughly 55% of the regression weight and favoring a 3hr harvest time point. In contrast, the normalized harvest time parameter coefficients ($^\circ\beta_0$) for GFP yields produced in pEVOL or pOFX have no statistical significance to their respective linear regressions. The individual yields for each case are available in Figure 10-1 (Appendix B). Parameters were simplified to high/low as follows: $x_{HarvestTime}$ [3hr = -1; 6hr = 1], x_{MOPS} [No = -1; Yes = 1], $x_{CFPSTime}$ [3hr = -1; 8hr = 1], and $x_{CFPSTemp}$ [30 °C = -1; 37 °C = 1]. Error bars represent 95% confidence interval for the regression coefficient. *Designates the null hypothesis p-value of regression coefficient is <0.05. The individual yields for each case are available in Figure 10-1 (Appendix B).

For pOFX extract expressing CalB, longer harvest times results in higher total and soluble CalB yields (Figure 3-3). These yields were upwards of 3 times higher than previously reported CalB yields with similar CFPS systems (2,12). CalB expressed in pOFX extract was more than twice as soluble as CalB in NP (Appendix B Figure 10-2). The increase of CalB solubility was expected, as the addition of the GroE chaperone complex should aid in the proper folding of the

protein after translation (2,12). Curiously, CalB total yield was also more than twice as large in pOFX as NP. The increase in total yields is likely due to the overall increase of yields in pOFX compared to NP. This could also be attributed in part to a reduction of insoluble CalB, since aggregation of CalB may lead to coprecipitation of essential transcription and translation machinery. For reference, a selection of CFPS-produced CalB samples were assayed for lipase activity and achieved an average activity of 70% of a commercially acquired CalB standard (Appendix B Figure 10-3).

The pEVOL case expressing pPaGFP (GFP modified for noncanonical amino acid pPa incorporation) performed consistently better with delayed harvest time (Figure 3-3). The full-length pPaGFP production yields with the PEVOL extract were originally very low (less than 4% of the standard GFP yields), causing us to hypothesize there may not be sufficient foreign tRNA-synthetase or tRNA. Indeed while we performed this work, Albayrak and Swartz reported that the synthetase is likely the primary limiting factor in this relationship (52). We therefore performed reactions with exogenously purified tRNA-synthetase supplementing the pEVOL extract (pEVOL+RS, Figure 3-3). The ensuing yields increased by over 300%, confirming that the synthetase had been limiting (Appendix B Figure 10-1). Despite the limitation of plasmid-expressed synthetase, there remained a significant positive trend in yields with regards to delayed harvest times, suggesting that more plasmid-expressed tRNA may be available at later harvest times, resulting in an overall average increase in yields of greater than 150% by harvesting the pEVOL extract well after log phase (Appendix B Figure 10-1).

Delaying harvest was universally beneficial for pEVOL extracts and improved the efficacy of pOFX extracts, as well. The strong benefit in pEVOL is likely due to the essential nature of the transcription machinery expressed in that system. In essence, the pEVOL machinery must compete

with endogenous release factor 1 for the amber stop codon and is therefore more heavily affected by concentration. Thus, a delayed harvest is particularly important when there is competition between the exogenous and endogenous machinery.

3.3.4 pH Buffer

Extracts from cells fermented in MOPS-buffered media typically performed equally as well or better than their unbuffered counterparts. Buffering the media during growth likely decreases the burden on cellular mechanisms that adjust against suboptimal pH environments and thus may protect against shifts in the proteome that could be deleterious to extract viability (83). An exception from this general trend was the expression of soluble CalB in pOFX extracts where MOPS buffering was generally detrimental to yields. The exception is not all together surprising due to the pH-reducing effect of the antibiotic resistance mechanism used by the pOFX plasmid. Indeed, this effect can be observed in Figure 3-2B, where at harvest times of 3, 4.5, and 6hrs the pH of the unbuffered pOFX fermentation was closer to the MOPS-buffered NP and pEVOL fermentations than the unbuffered NP and pEVOL fermentations.

Closer inspection of the pH profiles and the respective yields suggests that maintaining the extracellular pH in the range 7.2-7.5 is preferred for viability of supplemented extracts. High or low deviations from this range appear to be deleterious to extract viability. This relationship is expected, as previous reports show that *E. coli* is sensitive to pH, particularly during active cellular reproduction (83,84).

Augmenting the growth media with MOPs adds a further cost to the extract preparation and raises the concern that addition of this chemical reduces the economy of the eCFPS. Yield improvements due to buffering more than offset the cost of the buffering agent in half of the reactions, with an average decrease in cost of 52% (data not shown) (49). The reactions costs not

offset by yield improvements increased the average cost of reaction by 14%. The cases with decreased reaction costs generally corresponded to the cases benefitting from MOPs buffering, as seen in Figure 3-3.

3.3.5 eCFPS Time and Temperature

Universally, all proteins expressed in eCFPS reactions for 8 hours outperformed 3 hour reactions, with the exception of GFP in NP and soluble CalB yields. Generally, longer reaction time should allow for higher overall conversion. The inconsequential effect of reaction time on GFP in NP may imply that the majority of the protein is synthesized within the first three hours and that most of the energy is exhausted, as has been previously reported (66). Previous works have also reported similar asymptotic maximums in protein yield between 3-8 hours (8).

The reduced solubility of CalB in 8 hour reactions compared to 3 hour reactions indicates increased aggregation of CalB. The complexity, disulfide bonds, and overall bulk of CalB likely contribute to higher aggregation rates than production rate. As expected, the presence of GroE chaperones reduces the negative impact of longer reaction time on solubility.

Universally, all extracts performed equally well or better at 30 ^{o}C than 37 ^{o}C. Although 37 ^{o}C is a traditional eCFPS reaction temperature, our results are consistent with multiple previous reports that advise performing reactions at 30 ^{o}C to achieve higher yields, particularly when nonstandard components are employed (8,9).

3.4 Conclusion

Here we have considered alternative fermentation conditions for three fundamentally different cases of eCFPS: 1) a standard extract - NP, 2) an extract supplemented with nonessential components - pOFX, and 3) an extract supplement with essential components for successful

translation – pEVOL. The traditional method of harvesting during or toward the end of log phase was shown to be best for the NP case compared to harvesting at later time points. However, a clear benefit to delayed harvesting of cells for extract preparation was observed when supplemental components were plasmid-expressed during fermentation. In addition, buffering the fermentation with MOPS was shown to be typically cost-reducing when beneficial to yields, although this effect can be complicated by factors such as antibiotic resistance mechanisms that affect the pH. To further reduce cost, other buffering agents might serve as possible inexpensive alternatives. Overall, the conservation of positive benefit at delayed harvest time and the positive effects of MOPS buffering intimates that the principles discussed here would apply to eCFPS systems requiring other supplemental components and the emerging field of cell-free synthetic biology (33,34,61). This potentially expands the range of proteins that could be produced in eCFPS and enhances the potency of protein engineering and synthetic biology applications with eCFPS.

4 RAPID VACCINE DEVELOPMENT AND PRODUCTION

4.1 Introduction

Vaccines have had a potent impact on the world. Due to vaccines, diseases such as smallpox and polio have nearly been eradicated (85,86). Despite promising results, hundreds of viral pathogens continue to persist throughout the world, having devastating impacts on the social, political, and economical status of those affected. Foot-and-mouth disease (FMD) is one such virus that persists throughout large swathes of the globe (87). There have been multiple vaccines developed against FMD; however the genetic diversity of the virus serotypes and subtypes prevents a single vaccine from being universally effective (88). In efforts to eradicate FMD, a rapid, versatile, and economically feasible system must be developed. Using CFPS technologies, we work towards a system that can rapidly produce diverse recombinant proteins for safe and economical vaccine production.

4.1.1 FMD Virus and Related Challenges

Foot-and-mouth disease virus belongs to the family picornaviridae – small, non-enveloped viruses with a single positive-sense RNA molecule. The viral genome encodes for 4 structural proteins (VP1, VP2, VP3, and VP4) and several non-structural proteins that promote infection, replication, and proper assembly of the virus particle (87). These proteins are encoded as a single polyprotein, then cleaved by a protease (protein 3C) located towards the C-terminus

of the polyprotein. FMD is genetically diverse, with seven distinct serotypes: type O, A, C, SAT 1, SAT 2, SAT 3, and Asia 1 (89). Furthermore, subtypes within each serotype contain a large spectrum of genetic diversity due to high mutation rates within the virus (90). The broad genetic diversity between and within serotypes complicates identifying and protecting against disease (91). Specifically, the variability in the epitope regions can reduce or effectively eliminate cross-subtype or -serotype protection from previous infection or vaccination as occurred in Iran in 2005 (88).

4.1.2 Disease Traits and Related Challenges

In addition to the significant genetic diversity of the virus, FMDV infects diverse hosts, affecting over 70 species of wild and domestic cloven-hoofed species such as cattle, sheep and swine (87). The variety of hosts and diversity of serotypes synergistically complicates disease prevention. Furthermore, signs and disease severity may significantly differ from species to species. Generally, cattle have obvious oral and pedal lesions, while swine primarily have pedal lesions (92). Sheep show milder signs - 25% of infected sheep develop no lesions and a further 25% develop only one lesion - making visible diagnosis difficult or impossible (93). In addition a number of other viral diseases including vesicular stomatitis, swine vesicular disease, and vesicular exanthema of swine cause disease signs similar to FMD [2]. Incubation periods from exposure to first signs vary by initial infection and route of transmission, ranging from as little as 1 day to up to 14 days (94). Therefore, some animals may remain asymptomatic and act as carriers while others are misdiagnosed. Such cases increase the possibility of accidental transmission from primary or secondary contact between herds.

The ability of the virus to infect cross-species through sundry routes increases transmission opportunities, particularly where livestock agriculture is densely populated (95).

Cattle and sheep are primarily infected through respiration of the virus in aerosol form, while swine are more likely to be infected through ingestion or subcutaneous wounds (94). Shedding of the virus may occur through multiple routes including in aerosol form, urine, feces, and bodily fluids (96). Excreted virus can retain virulence for significant durations in aerosol form, with examples of some strains naturally traveling as far as 300 km (94). The extent of FMD transmission can be further amplified by incidental transport on vehicles, humans, water, and animal products (94,97). The diverse routes of shedding and transmission coupled with the diversity of host species provide myriad opportunities for spread of the disease.

In certain hosts, including cattle and buffalo, the virus can persist and these asymptomatic, persistently infected animals can remain potentially contagious for up to 5 years (91,98). Infected animals are thought to reach a maximum transmission potential within 12 days of infection (99). In a dead host, the virus may remain stable, and persist in an infectious form for as long as 11 days in muscle tissue, and 4 months in the liver (97). Also, many other animal products such as milk and cheese can act as incubators of the virus (97). Some experts suspect that the longevity of the virus in animal products is what led to the 2001 outbreak in the UK. The outbreak is thought to have started when a farmer purportedly fed his animals FMD-contaminated imported food scraps, which were insufficiently heat treated to remove the possibility of infection (100).

The complexities of this highly infectious and persistent disease complicate strategies of eradication. Although an inactivated FMD-vaccine was developed and successfully used on large numbers of animals in the 1950's, FMD is still prolifically spread through the world (101,102).

4.1.3 Predominant Vaccine Technology

The predominately utilized FMD vaccine is based on inactivated FMDV (103). This vaccine is typically produced from live FMDV amplified in baby hamster kidney-21 cells, chemically inactivated, partially purified by some manufacturer's, and subsequently formulated with an adjuvant (104). Throughout the process, a sterile environment and meticulous management of temperature and pH is essential to ensure production of an effective, noninfectious vaccine (105). This vaccine technology comes with the inherent risk of live virus release from production facilities or insufficient inactivation of the virus during vaccine preparation (104). Indeed, it is thought that the 2005 FMD outbreak in China initiated when insufficiently inactivated virus was used to vaccinate, resulting in an outbreak that spread throughout China and into Russia and Mongolia (88). In addition, the 2007 outbreak in the UK was caused by inadvertent release of virus from the Pirbright vaccine and research institute (96).

The risk of virulent virus contamination or insufficient inactivation during vaccine production requires that production facilities maintain rigorous biosafety standards. This restricts the locations where production facilities can be successfully constructed, maintained, and operated. Furthermore, these facilities must operate at a high level of containment. The distance between production facilities and regions of FMD infections presents a logistical challenge of distribution, particularly where international borders are concerned. To help alleviate this challenge, in some parts of the world FMD vaccine banks have been established to increase vaccine accessibility (106,107).

FMD vaccine banks decide how much vaccine they will store for any given serotype, and regularly test these stored vaccines for efficacy (108,109). These tests are essential as a concern with the current technology for inactivated virus vaccine production is the possible selection of

antigenic variants during virus replication (110,111). It has been found that the selected variants may not always be protective against the circulating parental virus strain. In addition, the choice of which vaccines to store is complicated by limited cross-subtype and cross-serotype protection, requiring individual vaccines against each subtype that is currently circulating for effective protection (108,112). Vaccines must also be periodically replaced due to a shelf life of 1-2 years for conventional FMD vaccines (91). Storage of vaccines as concentrated antigens in liquid nitrogen improves shelf life (113). However, these concentrated antigens must be shipped to manufacturers for formulation with an adjuvant when needed, thus delaying their use in the field.

Administration of the vaccine also presents its own set of complexities, such as proper handling, correct dosage, and optimal time of vaccination. All of these variables can significantly impact the efficacy of the vaccine (104,114). For example, higher doses of vaccines generally result in better protection and reduce the time from administration to protection (104). As a consequence, during outbreaks in previously disease-free countries, emergency vaccination of animals with 6 protective dose 50 (PD50) is recommended by the OIE. Complexities of administration make it desirable for trained persons to administer the vaccine. However, persons administering vaccines to multiple herds may inadvertently act as disease carriers (115). Furthermore, regions with inadequate veterinary services face the added challenge of increasing competency among those administering vaccination (116).

Other vaccine technologies are becoming available that are attempting to address the shortcomings of inactivated virus vaccines. These include empty capsid vaccines, DNA vaccines, recombinant protein vaccines and peptide vaccines, among others (103,114,117-119). An example of a novel vaccine technology is the recent development of a replication-defective human adenovirus vector containing the FMDV capsid protein coding region for serotype A24

Cruzeiro (120). This vaccine has been granted a conditional license by the Center for Veterinary Biologics, Animal Plant and Health Inspection Service, USDA. This license allows the vaccine to be included in the U.S. National Veterinary Vaccine Stockpile to be used in cattle in the event of an emergency situation (121). Recent reviews have described the benefits and limitations of this and other novel vaccine technologies (103,119,122).

Vaccine production technologies must also become more efficient and economical, as is being pursued with emerging technologies involving production of virus-like particle FMD vaccines produced in *E. coli*, in insect cells infected with recombinant baculoviruses, and in cell-free systems (1,19,87,104). To be successful for eradication, vaccine technologies and systems must avoid the pitfalls of inactivated viruses and be sufficiently inexpensive as to be economically viable for developing countries. Using CFPS technologies, we work towards a rapid expression platform capable of production of diverse FMD proteins for safe and economical vaccine production.

4.2 Materials and Methods

4.2.1 Gene Design

Genes were designed using Gene Designer (DNA2.0, Menlo Park, CA) based on the GenBank Accession number AY593768.1. After selective removal of portions of the full protein (described in Results and Discussion), the codons were optimized for expression in *Escherichia coli* based on Class II Codon Usage. The resulting gene was cloned into the T7-expression vector pJ411 and called pJ411-P1-3C. To express the 3C protein exclusively, the Lpro-P1-2A section of the gene was excised and the vector was re-ligated, resulting in pJ411-3C.

4.2.2 CFPS Expression and Coexpression

CFPS reactions were performed as described previously with the following modifications (19). Coexpression from pJ411-P1-3C and pJ411-3C was performed at a consistent vector concentration (12 nmol per L) with the following ratios of pJ411-P1-3C to pJ411-3C: 1:0, 5:1, 2:1, 1:1, 1:2, 1:5, and 0:1. Reaction volumes were scaled from 20 μL to 1 mL without significant change in reaction performance.

4.2.3 Scintillation, SDS-PAGE and Autoradiography

Radiolabeled amino acids (Leu ^{14}C) were included into the CFPS reactions for incorporation into the proteins. Protein expression levels were calculated by TCA precipitation and liquid scintillation counting, as previously described (19). In cases of co-expression, protein yields were calculated based on the most prevalent gene vector in the reaction or pJ411-P1-3C in cases of equal vector concentrations.

To assess proper protein cleavage, the reactions were subjected to denaturing 10% Bis-Tris SDS-PAGE with MOPS running buffer according to the manufacturer's specifications (Novex Life Technologies, Grand Island, NY). Gels were dried and exposed to autoradiographic film for 1 week. Films were subsequently developed and analyzed.

4.3 Results and Discussion

4.3.1 Innocuous Gene Design

One of the primary drawbacks to predominant FMD vaccine technology is the necessity to have fully active and infectious particles at some given stage of vaccine development. The presence of complete viruses carries with it the inherent risk of accidental release and outbreak.

Recombinant expression technology (CFPS) allows us to circumvent the issue entirely by designing a gene unable to self-replicate and lacking the elements for production in the host. The steps to designing an effective yet innocuous gene are:

1. Exclude elements that aide in host expression
2. Exclude elements that aide in genome replication
3. Exclude elements that aide in host infection cycle

The first step in innocuous gene design is to identify the elements that promote protein expression in the host. In this case, the 5`and 3` untranslated regions (UTRs) both play a role in expression including an internal ribosome entry site (IRES) and a poly-A tail, respectively (87). As depicted in Figure 4-1, we exclude these elements and replace them with the specific T7 promoter (5` UTR) and a non-poly-A region (3` UTR).

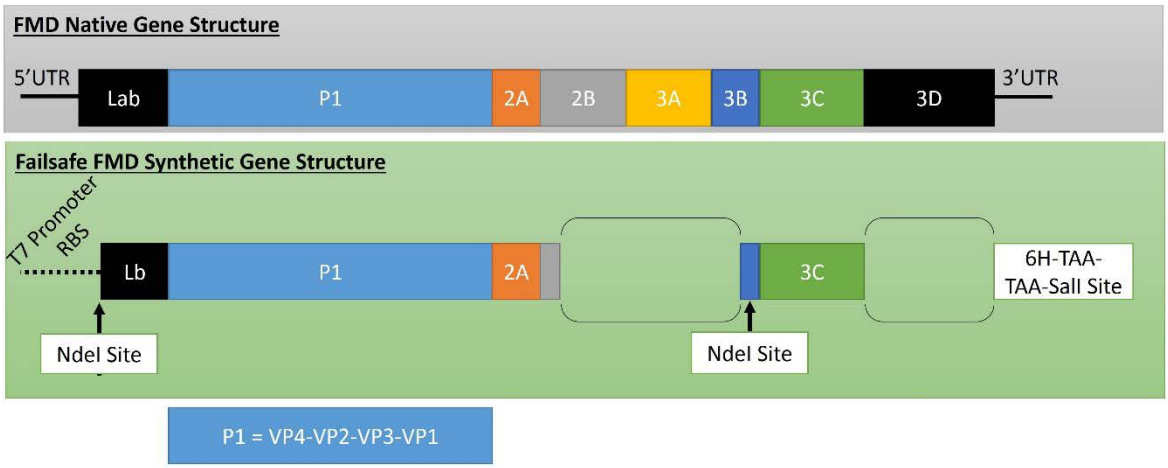

Figure 4-1 – Design of Innocuous FMD Gene

The second step in innocuous gene design is to remove the possibility of undesired genome replication. In this case, the protein 3D is known to be a RNA-replicase for genome replication during the infection cycle (87). We exclude the portion of the gene that encodes for 3D.

The third step is to identify and exclude elements that aide in the host infection cycle and are unnecessary for vaccine activity. In this case, the proteins 2B, 3A, and 3B aide in the infection cycle but are unnecessary for the vaccine (87). We exclude these elements as depicted in Figure 4-1.

To ensure useful, controlled, and high level of protein expression, we included a T7 promoter region 5` of the gene. This allows for expression only in systems that contain the T7 RNA polymerase. Finally, a 6xHis sequence was placed at the C-terminus of the 3C protein to enable purification and concentrating of the 3C protein, if necessary. The final innocuous gene design is depicted in Figure 4-1. The NdeI restriction sites were included for facile conversion of the vector pJ411-P1-3C to be made into pJ411-3C.

4.3.2 Coexpression and Protein Cleavage

In a natural infection cycle, the polyprotein is expressed by the host and then cleaved by the 3C protein (87). The cleaved structural proteins begin the formation of virus capsids containing copies of the RNA genome. This process leads to a buildup in the concentration of 3C as more polyprotein is expressed. Thus, catalytic activity of 3C-mediated cleavage likely increases over the duration of infection, making it unclear what ratio of 3C to polyprotein is ideal for full cleavage into the desired products. We therefore designed the system to be capable of coexpressing the polyprotein and 3C. Controlling the amount of the respective vectors has a direct effect on protein expression levels.

To analyze the effect of varying protein ratios, we performed CFPS using varying vector ratios. Figure 4-2 is an example autoradiogram of reactions containing differing vector ratios that have subsequently been run through SDS-PAGE. The extremes (1:0 and 0:1) demonstrate the individual expression level from pJ411-P1-3C and pJ411-3C, respectively. The cleavage of the

polyprotein is apparent, even at the ratio 1:0, suggesting the 3C protein contained in the polyprotein is sufficient for some extent of protein cleavage. However, noticeable new protein cleavage products appear when 3C is present at higher concentrations. These cleavage products suggest that the 3C found in the polyprotein is insufficient for full cleavage of the polyprotein and that some elevated concentration of 3C protein will aid the full cleavage of the polyprotein.

Figure 4-2 – Autoradiogram of FMD CFPS reactions. To achieve varying protein expression levels, the plasmids were added in ratios (pJ411-P1-3C to pJ411-3C). The increased level of 3C at 1:1 ratio exhibited a previously unseen cleavage product, suggesting that the ratio of plasmids could be optimized for maximum protein yield and cleavage.

4.4 Conclusions and Future Directions

The initial framework has been laid for the rapid production of FMD vaccines. The benefits of CFPS systems, such as speed to production and controllable gene content, make it a compelling candidate for rapid vaccine production. The ability to design safe and innocuous genes of virus-oriented vaccines is a further benefit that reduces safety hazards and in turn safety costs. This research could potentially be broadly applicable to FMD and many other virus pathogens that continue to plague the globe.

This work is being furthered pursued in the Brady Bundy Biotechnology Lab, spearheaded by Anthony Bennett. The next hurdles for effective FMD vaccine development are 1) proper assembly of the empty virus capsids, 2) purification of these assembled capsids, and 3) test

application of these empty virus capsids as a vaccine. This work was funded by the National Pork Board.

5 NOVEL VIRUS-BASED NANOPARTICLES

This chapter is an adaptation from the article entitled "The Incorporation of the A2 Protein to Produce Novel Q[beta] Virus-like Particles Using Cell-free Protein Synthesis" published in *Biotechnology Progress* in March 2012. This work was developed and lead by myself and Chad Varner with the help of Derek Bush.

5.1 Introduction

The development of techniques for protein characterization and production has led to significant biotechnological advancements in many major industries, including chemicals, pharmaceuticals, nanotechnologies, agriculture, energy and textiles (123). Commercial proteins represent a multibillion dollar annual U.S. market and methods to optimize protein production are continually being investigated (124). In this work, we demonstrate the value of an *Escherichia coli* based cell-free protein synthesis (CFPS) system to concurrently 1) directly control the ratio of co-expressed proteins, 2) directly probe the interactions between co-expressed proteins, and 3) produce cytotoxic proteins to develop novel viral-protein based nanoparticles.

Proteins are traditionally produced *in vivo* using a wide range of hosts, which enables the production of myriad proteins (123,125). However, *in vivo* systems are inherently constrained by 1) the cell wall and 2) susceptibility to cytotoxic proteins. The cell wall prevents direct access to the cytoplasm, limiting control over the protein synthesis environment. Cytotoxic protein

production can cause poor cell fermentation growth rates and cell death, lowering overall production yields (123).

CFPS overcomes these limitations by removing the cell wall, enabling direct control of the expression plasmid concentration. In addition, the concentrations of chaperones and reagents are directly controlled, enabling regulation and optimization of synthesis conditions (ionic strength, pH, temperature, redox potential, etc.) (1,126,127). In some cases, such an open system has demonstrated higher protein production yields than *in vivo* systems (32,128). Protein production is readily scalable and linear DNA expression templates generated by PCR can be used to greatly reduce the time required for plasmid construction and transformation or genome modification (1,5,12,129). The native genomic DNA and mRNA are removed from the CFPS environment prior to protein synthesis, which prevents expression of undesired proteins. This facilitates rapid and accurate determination of expression yields using small reaction volumes by adding radio-labeled amino acids to the reaction mixture. As will be demonstrated, relative production yields of multiple proteins can be assessed at high sensitivity with autoradiography following SDS-PAGE, eliminating the need for western blotting.

In this work, we demonstrate the use of CFPS to produce viral and cytotoxic proteins simultaneously, which self-assemble into non-infectious nanoparticles known as virus-like particles (VLPs) or viral nanoparticles (VNPs). VLPs are engineered for many applications, including drug delivery (130), biological imaging (131), battery electrodes (132), vaccination (133,134), and scaffolds for tissue engineering and directed cell differentiation (135). In this rapidly growing area of research, these applications often necessitate biochemical linkages of small molecules, polymers, peptides or entire proteins to amino acids exposed on the VLP surface (136,137). VLPs are typically genome-free virus capsids (outer protein shell), which are composed

of many capsomers (one or few subunit proteins bound to create the fundamental subunit of the VLP) that come together to form highly symmetric icosahedral structures. Due to this repeating array of capsomers, no linkage site is unique to the entire capsid (Figure 5-1). By controlling reactant concentrations, a single molecule could be attached to a VLP using a number of bioconjugation techniques (138). However, by the Poisson probability distribution, the theoretical maximum of VLPs having a single molecule attached is 37%. The remaining VLP population will contain zero (37%) or multiple (26%) molecules attached to each VLP and are not easily separated from VLPs with one molecule.

The bacteriophage Qβ is one of the most stable viruses due to disulfide bond cross-linking (78,139,140). Disulfide bonding in Qβ increases its thermal stability by more than 50 ^{o}C compared to the non-crosslinked capsid (140). This makes it an attractive candidate for VLP-based applications. Only the coat protein (CP) is required to form the VLP, where 180 CP self-assemble into the T=3 icosahedral VLP (78). However, the Qβ virion also naturally contains one unique protein, the A2 protein (141,142). The A2 protein is incorporated into the virus capsid in a surface-exposed manner and has two main functions (143). One is to facilitate infection by binding to the *E. coli* F-pili (144). The other is to competitively inhibit MurA (an essential enzyme for cell wall synthesis), which causes the lysis of infected *E. coli* and the escape of progeny virions (145). In addition to CP and 1 A2 protein, 3 to 5 A1 proteins are also inserted in the Qβ virus capsid. However, the mechanism of A2 incorporation and its interactions with the CP, A1, and the encapsidated genome are not well understood (144,146,147). Also, the tertiary structure of the A2 protein has yet to be determined. Expression and purification of soluble A2 have been problematic due to its low solubility and cytotoxic function (144,145). In this work, we employ the CFPS system to control relative expression of the A2 and CP, enabling the optimization of A2

incorporation into Qβ VLPs. In addition, the A2-CP interaction is probed. This is the first time to our knowledge that a Qβ VLP has been synthesized *de novo*, which contains the CP and incorporates the A2 protein.

5.2 Materials and Methods

5.2.1 Cell-free Protein Synthesis Reactions

Cell free reactions were performed using the PANOxSP system, as described previously (15). Reaction volumes were either 15 µL in 1.5 mL Eppendorf tubes, or 500 µL in 12-well plates (Corning, Corning, NY), and all reactions were incubated at 37ºC for 3 hrs. Reagents were obtained from Sigma-Aldrich (St. Louis, MO) and Roche Molecular Biochemicals (Indianapolis, IN) with the exception of the L-[U-14C] Leucine which was obtained from PerkinElmer (Waltham, MA). The total plasmid concentration was kept constant at 12 nM using expression plasmids pY71-Qβcp and pET11a-QβA2 (a kind gift from Catrina Reed and Dr. Ryland Young) (78,145). Each plasmid has the T7-RNAP promoter directly before the desired genes of the coat protein and the A2 protein, respectively. No other viral genes were included in the reaction mixture. *E. coli* strain KC6 was used to prepare the *E. coli* cell extract as previously described (15).

5.2.2 Protein Production Yield Calculations

Total protein production was determined by TCA protein precipitation and radioactivity measurements on a LS6500 Multipurpose Scintillation Counter (Beckman Coulter, Brea, CA). Soluble protein yields were found by TCA precipitation and radioactivity measurements of the supernatant after the reaction was centrifuged for 15 min at 4ºC and 17,000 x g. The detailed

procedure has been described previously (1). The A2 and CP protein production yields from co-expression reactions were determined by TCA protein precipitation and radioactivity measurements as described above and by analyzing the relative expression with SDS-PAGE, autoradiography and densitometry. Specifically, the cell-free reaction product was subjected to SDS-PAGE with NuPAGE 10% bis-tris gels (Invitrogen, Carlsbad, CA) while in the presence of 0.1 M dithiothreitol (DTT) and stained with SimplyBlue SafeStain (Invitrogen), all following manufacturer specifications. The gels were exposed to Kodak BioMax MR Autoradiography film (Rochester, NY) for 4-7 days. ImageJ software (National Institutes of Health, USA) was used to perform densitometry measurements on resulting autoradiograms (148). The A2 and CP are different sizes (molecular weights of 48.5 kD and 14.1 kD respectively) and migrate to different locations on the SDS-PAGE gel. Both A2 and CP incorporate C^{14}-leucine and the relative intensities of the bands on the autoradiogram were used to determine relative co-expression yields. The co-expression yields of soluble protein was determined following the same procedure with the inclusion of a 15 min centrifugal spin at 17,000 x g and 4°C to remove insoluble protein.

5.2.3 Purification of Virus-Like Particles

Purification of assembled Virus-Like Particles was performed as outlined previously (1). To remove all unincorporated ^{14}C-Leucine, the supernatant of 500 µL CFPS reaction product was immediately dialyzed against 300 mL NET buffer (150 mM NaCl, 5 mM EDTA, and 20 mM Tris-HCl, pH 7.8) per mL of reaction in 6-8 kDa MWCO Spectra/Por membrane tubing (Spectrum Labs, Rancho Dominguez, CA) at 4°C for 24 hrs with 2 buffer exchanges. Dialyzed reactions were loaded on a continuous 10-40% w/v sucrose gradient prepared using NET buffer in Polyallose 25x89 mm Beckman centrifuge tubes in a manner described previously (149). The formation of

linear gradients was verified by refractometry using an Atago RX-5000 alpha-BEV refractometer (Atago, Belleview, WA).

Gradients loaded with CFPS product were centrifuged in a swing-bucket SW-32 Rotor with a Beckman Coulter Optima L-100 XP ultracentrifuge at 105,000 x g for 3.5 hrs at 4°C. 1 mL fractions were collected with a Foxy Jr. fraction collector (Teledyne Isco, Lincoln, NE). The radiation in each fraction was measured with the LS6500 Multipurpose Scintillation Counter to determine CFPS-produced protein concentration. VLP assembly efficiency was quantified by comparing CFPS-produced protein in fractions 11-19 to the amount of CFPS-produced protein added to the gradient (78). Fractions 11-19 were combined and buffer exchanged with NET buffer by 3 washes of excess NET buffer using Amicon Ultra-4 30,000 MWCO Centrifugal Filter Devices (78). A final centrifugation at 5,000 x g at 4°C for 25 min was performed to concentrate the product with the Amicon Filters.

5.2.4 Characterization of Purified Virus-Like Particles

Sucrose gradient fractions 11-19 were collected and concentrated as described above for individual- and co-expression CFPS reactions. The concentrate was subjected to SDS-PAGE and autoradiography as specified above. Due to the disparity in A2 and CP concentrations expected in the VLP (A2:CP ratio of 1:180), 1x, 4x, and 16x serial dilutions were run in parallel on all gels to ensure proper densitometry measurements were made. Based on these measurements, A2 incorporation efficiency was calculated. A2 is assumed to be incorporated at a maximum of 1 A2 per 1 VLP based on the composition of Qβ virus (141,142,146).

VLPs (purified and concentrated as described above) were analyzed by dynamic light scattering (DLS) using a 90Plus Particle Size Analyzer (Brookhaven Instruments, Holtsville, NY).

Raw correlation data was analyzed with Brookhaven Particle Size Analyzing software to give the mean diameter of the VLPs.

VLPs (purified and concentrated as described above) were also analyzed by transmission electron microscopy (TEM). The concentrated VLPs were applied to plasma-treated, formvar-coated copper grids and negatively stained with 1% uranyl acetate. Images were digitally captured using a Tecnai T-12 TEM (FEI, Hillsboro, OR; Gatan, Pleasanton, CA) at 120kV acceleration voltage. The resulting images and scale bars were sized with ImageJ software (148).

VLP adsorption via A2 was tested as previously demonstrated by Tsukada, et al (150). The *E. coli* strain CHS 124, a generous gift from William McCleary (Brigham Young University), was used in place of the A/λ *E. coli* strain. VLPs were produced, assembled, purified, and concentrated from cell-free reactions containing plasmid ratios 0:1 and 1:5 (A2:CP plasmid), as described above. Adsorption was quantified using radioactivity measurements.

The stability of VLPs produced with and without A2 incorporated (plasmid ratios 0:1 and 1:5) was tested under both oxidizing (7 mM H_2O_2) and reducing (50 mM DTT) conditions as previously described(78). Incubation tempertures were 46, 56.8, and 70 ^oC.

5.3 Results and Discussion

5.3.1 Co-expression of the A2 Protein and the Coat Protein from the Qβ Bacteriophage

To facilitate the assembly of Qβ VLP containing both the coat protein (CP) and the A2 protein (A2), we first sought to assess the impact on protein solubility of the A2 when co-expressed with the CP. The A2 has been reported to be predominantly insoluble when expressed *in vivo* (144,145). The CP is the major component of the Qβ capsid and forms VLPs when expressed either *in vivo* or *in vitro*. The CP is also thought to interact with the A2 to stabilize its incorporation

into the VLP, although the insertion mechanism and the impact of other interactions are largely unknown (145,146). Taking advantage of our cell-free protein synthesis (CFPS) system's ability to express cytotoxic proteins (such as the A2) and directly control expression plasmid concentrations, the Qβ CP and the A2 were co-expressed as illustrated in Figure 5-1.

The total plasmid concentration was maintained at 12 nM, while the molar ratios of plasmids expressing A2 and CP were varied (A2:CP of 1:0, 1:1, 1:2, 1:5, 1:10, 1:20, 1:50, 0:1). The plasmids for A2 (pET11a-QβA2) and CP (py71-Qβcp) expression were both transcribed by T7 RNA polymerase during the CFPS reaction (8,78). The relative concentrations selected for this study of the A2 plasmid compared to the CP plasmid are high compared to the theoretical ideal of a 1 A2 per 180 CP in the assembled VLP (based on Qβ virus composition). This excess A2 is likely necessary as 1) not all A2 that is synthesized during viral infection is incorporated into the virus and 2) previous attempts at producing A2 reported low solubility (144-146).

Figure 5-1 illustrates total and soluble production yields from individual- and co-expression of A2 and CP in the CFPS system as determined by SDS-PAGE, autoradiography, and densitometry. The cytotoxicity of A2 did not appear to inhibit A2 production since A2 was produced at a significant yield of 410 ± 50 μg/mL (n=3, ± 1 standard error) when expressed individually (plasmid A2:CP of 1:0). In comparison, *in vivo* expression of A2 has been reported as 0.2 to 0.3 μg/mL (145). Interestingly, the mass yield of CP at 213 ± 29 μg/mL (n=3, ± 1 standard error) was lower than A2 when CP was expressed individually (plasmid A2:CP of 0:1). However, the short CP (133 amino acids) is produced at a higher molar yield than the longer A2 (420 amino acids) (Figure 5-1). The expression difference could be attributed to the disparity in the consumption of energy required to transcribe the short CP compared to longer A2. It has also been shown that even small changes in the initial coding sequence of a protein can drastically change

the production efficiency in a currently unpredictable manner (2). This further warrants the use of the open environment and high-throughput capabilities of the cell-free system to directly measure and optimize protein co-expression.

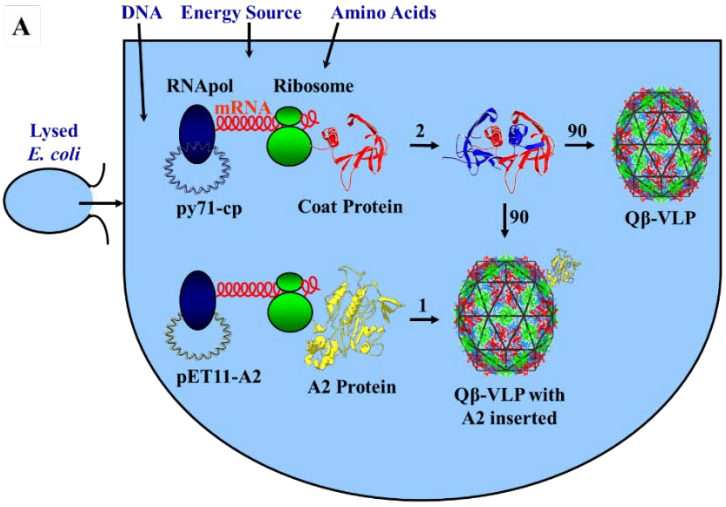

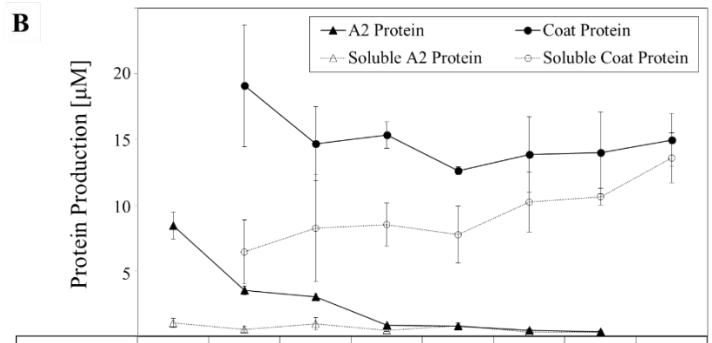

A2:CP	1:0	1:1	1:2	1:5	1:10	1:20	1:50	0:1
A2 Plasmid	12	6	4	2	1.1	0.6	0.2	0
CP Plasmid	0	6	8	10	10.9	11.4	11.8	12
Total Plasmid	12	12	12	12	12	12	12	12

Figure 5-1 – Co-expression of A2 and CP with the CFPS system. (A) Schematic of CFPS reaction. The predicted A2 structure shown was generated with I-TASSER prediction software. (B) Co-expression results with total (closed markers) and soluble (open markers) protein production shown for both A2 (triangles) and CP (circles). Error bares are one standard error with n=3 for all data points.

As shown in Figure 5-1, the CP concentration did not significantly increase with increasing CP plasmid concentration, suggesting plasmid concentration did not limit CP expression. However, A2 production varied linearly with A2 plasmid concentration (Appendix C) and A2 solubility was consistently 37 ± 6 μg/mL (n=15, ± 1 standard error) until total A2 expression

dropped below this value. Co-expression of the CP did not significantly impact A2 solubility, while the inverse was observed. Co-expression of A2 dropped CP soluble yields by up to 50% suggesting some interaction between A2 and CP.

5.3.2 Assembly of A2-incorporated Qβ VLPs

Encouraged by an observed A2-CP interaction, the incorporation of A2 into Qβ VLPs was probed. Separation of unincorporated proteins from the fully assembled capsids was accomplished by velocity sedimentation of the reaction products through continuous 10-40% sucrose gradients. The sedimentation profiles of CFPS reactions, determined by measuring the amount of radio-labeled protein in each collected fraction, are shown in Figure 5-2.

The presence of protein between fractions 11-19 with a peak at fractions 15-16 suggests the formation of assembled VLPs, as Qβ VLPs have been previously shown to sediment to a similar location under similar conditions (78). The positive control reaction with CP individually expressed (plasmid A2:CP of 0:1) has a similar protein profile as the CP-A2 co-expression reactions, further suggesting the presence of VLPs in these reactions. VLP assembly appears present in all CFPS reactions with the following exceptions: 1) the co-expression reaction where CP had the lowest solubility (plasmid A2:CP of 1:1) and 2) the individual A2 reaction (plasmid A2:CP of 1:0), which served as a negative control. Although CP expression levels remained relatively constant whether individually- or co-expressed, VLP assembly efficiency was lower in co-expression reactions. This is likely due to the lower CP solubility observed in the co-expression reactions (Figure 5-1, Figure 5-2; Table 5-1).

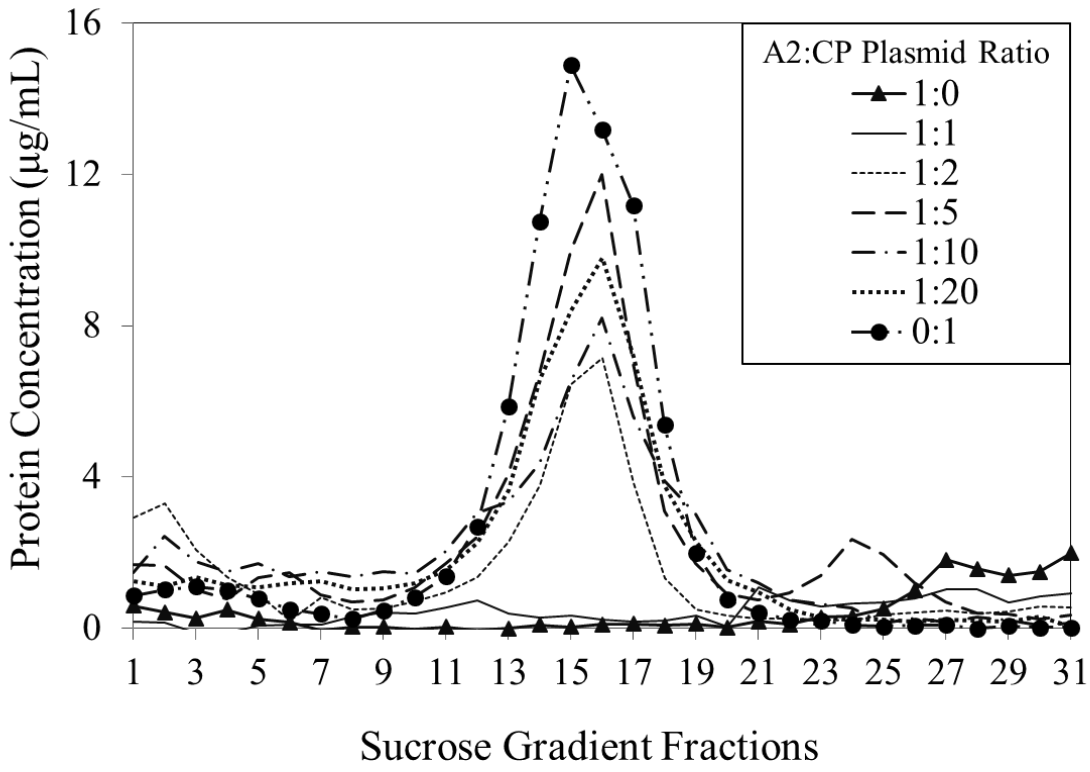

Figure 5-2 – Velocity Sedimentation Profiles of Product Proteins from CFPS Co-expression Reactions. Completed CFPS reactions were loaded onto a continuous 10-40% sucrose gradient and centrifuged to separate assembled VLPs. The radiation in collected fractions was measured to determine the protein concentration shown.

Table 5-1 – VLP Production Yields and Corresponding Efficiencies of A2 Incorporation

Assembled Capsid		
Plasmid Ratio A2:CP	Capsid Concentration (ug/mL CFPS reaction)	A2 Protein Incorporation Ratio A2:VLP
1:0	0.1 ± 0.1	1:0
1:1	3.2 ± 0.2	1:0
1:2	51.7 ± 7.8	1:2.42
1:5	97.2 ± 2.8	1:1.03
1:10	82.4 ± 1.1	1:2.98
1:20	107.6 ± 1.2	1:2.12
0:1	134 ± 0.7	0:1

5.3.3 Characterization of A2-incorporated Qβ VLP

The intrinsic nature of many VLPs is to self-assemble into a monodispersed population of nanoparticles with a high degree of symmetry. Previously, Qβ VLPs composed of only the CP and produced and purified using a similar *in vitro* system were shown to have a similar size and morphology to those produced *in vivo* (1,78,151). We thus used Qβ VLPs assembled *in vitro* from the CP only (plasmid A2:CP of 0:1) as a standard for VLP size and morphology.

VLPs were purified by collecting Fractions 11-19, shown in Figure 5-2, and concentrated by membrane filtration. The VLPs purified from a co-expression reaction (plasmid A2:CP of 1:10) were further characterized using dynamic light scanning (DLS). The presence of nanoparticles was detected at 29.8 nm ± 6.6 nm (n=10, ± 1 standard deviation, Appendix C) and is consistent with the published 27 nm diameter of the Qβ VLP (146). The VLPs purified from a separate co-expression reaction (plasmid A2:CP of 1:5) were analyzed by transmission electron microscopy (TEM) and compared to the VLPs purified from the individual CP reaction (plasmid A2:CP of 0:1) (Figure 5-3). Images of both VLPs reveal particles slightly less than 30 nm, exhibiting a structure similar to the icosahedral Qβ capsid.

With confirmation of VLP assembly by velocity sedemntation, DLS, and TEM, the incorporation of A2 was next studied. The purified VLPs from A2-CP co-expression reactions (plasmid A2:CP of 1:2, 1:5, 1:10, 1:20) and the purified VLPs from the individual CP reaction (plasmid A2:CP of 0:1) were subjected to SDS-PAGE and autoradiography as shown in Figure 5-4. In addition, fractions 11-19 for the A2-only CFPS sample (plasmid A2:CP of 0:1) were also collected, concentrated, and subjected to electrophoresis and autoradiography in an identical fashion as the other samples to serve as a negative control (Figure 5-4). The presence of a protein band at the expected molecular weight of A2 (48.5 kD) was observed in VLPs produced in co-

expression reactions but not in VLPs from CP-only reactions. In addition, no such band was observed in the negative control despite A2 being expressed at yields over twice as high as the co-expression reactions. From these results it appears that A2 is incorporated on the Qβ VLP.

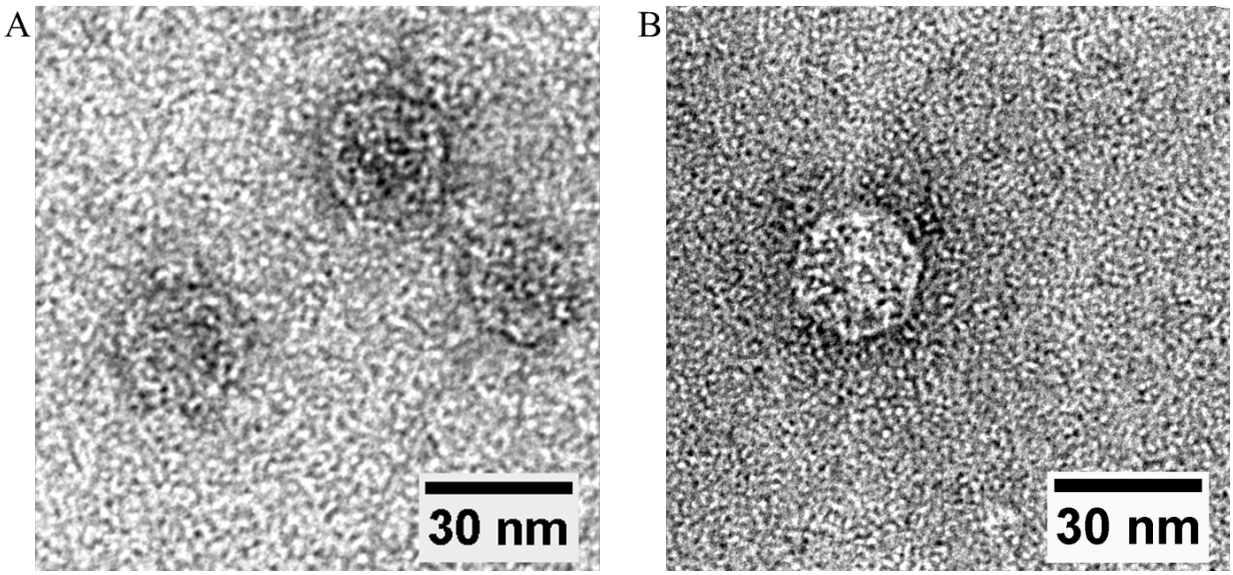

Figure 5-3 – Transmission Electron Microscopy Images of Assembled Qβ VLP. (A) Image of purified Qβ VLPs from the CP individual-expression CFPS reaction. (B) Image of purified Qβ VLP from the plasmid A2:CP of 1:5 co-expression CFPS reaction. Samples were negatively stained with 1% uranyl acetate.

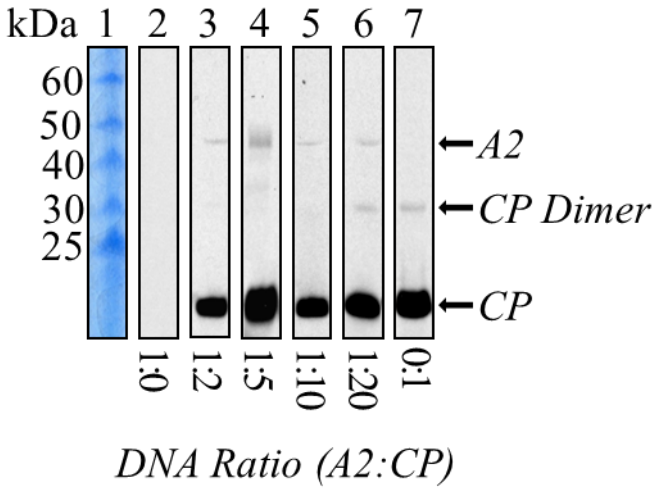

Figure 5-4 – A2 Incorporation into Assembled Qβ VLP. Lane 1) SDS-PAGE gel protein ladder aligned to the autoradiograms. Lanes 2-7) autoradiogram of the SDS-PAGE gel containing purified VLP from CFPS reactions. The presence of the CP dimer was observed in more concentrated 1:20 and 0:1 A2:CP samples due to insufficient denaturing.

The incorporation efficiency of A2 into the Qβ VLP was determined by subjecting serial dilutions of the purified VLPs to SDS-PAGE, autoradiography, and densitometry. The results are shown in Table 5-1, with the plasmid A2:CP of 1:5 reaction exhibiting the highest incorporation efficiency of 1 A2 to 1.03 VLPs, which is similar to the predicted theoretical maximum of 1 A2 to 1 VLP (based on Qβ virus composition) (141,146). Although it cannot be precluded that some VLP might incorporate more than one A2, it is likely that the VLP capsid behaves like the viral capsid. Previous works support a strong similarity between the Qβ virus and the Qβ VLP (1,78,151). In addition, the data support the hypothesis of a limited number of A2 per molecule. Despite the presence of excess soluble A2 (1 soluble A2 per ~9 soluble CP produced compared to the 1 A2 per 180 CP in the Qβ virus), incorporation efficiencies never exceeded 1 A2 per 1.03 VLP.

From these results, it appears that the A1 protein and the genome are not essential for efficient A2 incorporation. Also, as shown in Table 5-1, the incorporation of A2 was not nearly as efficient at higher and lower ratios of A2:CP. This suggests a careful balance between the expression of A2 and CP is necessary for efficient A2 incorporation. The observation is not entirely surprising, considering only ~2% of the A2 produced during infection is incorporated into infectious virions (145).

In the naturally occurring virus, the incorporated A2 protein is surface exposed, enabling it to bind with the F pilus of *E. coli* (143,150). We hypothesized that the A2 incorporated into the VLP would exhibit the same adsorption if it is also surface exposed. Using methods previously demonstrated by Tsukada, et al., adsorption of VLP with A2 was found to be significantly higher than VLP without A2 (Appendix C). This suggests that the A2 in many if not all the VLPs is surface exposed and maintains its functionality of binding the F Pilus.

Finally, we explored the effect of A2 incorporation on the thermal stability of the VLP. It has been demonstrated that the formation of disulfide bonds amongst the 180 CP of the Qβ VLP significantly increase its stability (78,140). However, the effect of A2 on VLP stability has not been explored. VLPs were produced, assembled, purified and concentrated from cell-free reactions containing plasmid ratios 0:1 and 1:5 (A2:CP plasmid). The VLPs were incubated with 7 mM H_2O_2 or 50 mM DTT to stimulate the formation or dissolution of disulfide bonds as previously reported (78). The incorporation of A2 did not seem to significantly alter the thermal stability of the oxidized (H_2O_2-treated) or reduced (DTT-treated) VLP (Appendix C).

5.4 **Conclusion**

We have demonstrated the utility of CFPS for directly tuning the relative expression levels of multiple proteins for the optimal production of self-assembling multi-protein macromolecular complexes. Additionally, the cytotoxic A2 protein was produced at significantly higher yields than previously reported for *in vivo* production, demonstrating the efficacy of CFPS for cytotoxic protein production. Co-production of A2 and CP resulted in the incorporation of A2 into the self-assembling Qβ VLPs without the presence of A1 protein and genomic RNA. By varying the A2-CP plasmid ratio, the relative expression levels of A2 and CP were optimized to produce A2-incorporated Qβ VLPs, approaching the theoretical maximum efficiency of 1 A2 per VLP. This is the first time to our knowledge that the CP-based Qβ VLP has been produced *de novo* to incorporate A2. The production of novel VLPs with unique surface accessible proteins, such as the one produced in this work, could enable more controlled engineering of VLPs for a growing assortment of applications.

6 STABILIZED PROTEIN THROUGH SITE-SPECIFIC IMMOBILIZATION

This chapter is an adaptation from the article entitled "Enhanced Protein Stability Through Minimally Invasive, Direct, Covalent, and Site-specific Immobilization" published in *Biotechnology Progress* in January 2013. This work was developed and lead by myself and Jeffrey Wu with the help of Chad Varner.

6.1 Introduction

Proteins represent a $100+ billion USD industry with rapid annual growth (152,153). The utilization of proteins for bioprocessing, sensing, and medical treatment is widespread over a number of industries including agricultural, textile, pharmaceutical, energy, and chemical processing (154-156). Proteins have a number of advantages over non-biological chemicals and chemical processes due to: **1** superior chemo-, regio-, and stereospecificity of enzymes (154,157-159); **2** green sustainability (renewable, biodegradable, non-toxic, milder reaction conditions, less energy consumption) (154,156,160-162); and **3** optimization through protein engineering (163,164). However, difficulties in recovery, reuse, and long-term stability limit the far-reaching industrial potential of proteins (165). Protein immobilization is a potential solution as it simplifies protein recovery and reuse, and reportedly increases protein stability in many cases (155,159,165). This work is focused on improving protein immobilization and we introduce the Protein Residue-

Explicit Covalent Immobilization for Stability Enhancement or PRECISE system that enables the targeted immobilization of proteins to enhance protein stability and durability.

The most robust immobilization techniques for protein-surface bioconjugations are covalent (166,167). However, precisely controlling which location on the protein covalently binds to a surface is complicated by the naturally limited pool of only 20 amino acid building blocks. Covalently targeting a given amino acid which appears in multiple locations in a protein commonly results in undesirable attachment orientations and loss of activity and stability (168-170).

A number of site-specific yet non-covalent approaches have demonstrated superior activity using recognition pairs such as 6His/Ni (171), biotin/streptavidin (172), more generally oligonucleotide/protein (173). However, long-term stability and reusability are compromised due to protein leaching that is further exacerbated under industrially relevant conditions (169). In addition, such systems commonly require the fusion of large tags which can negatively affect protein structure and function especially if inserted at locations other than the terminus (169,174).

Increasingly, research efforts have focused on developing both a covalent and site-specific immobilization technique. Specific targeting of the C and N termini for conjugation to peptide tags has been successfully reported with tags such as transglutaminase (175) and phosphatase (176), yet remains insufficient in cases where the termini are critical to protein folding and/or function. To target residues within the protein, complete elimination of all similar residues and chemical moieties except at the desired conjugation site can enable site-specific covalent linkage (168). However, mutagenesis of this magnitude is typically destabilizing. Alternatively, unnatural amino acids (uAAs) provide unique functional groups which can react with a number of bioorthogonal and highly efficient reaction chemistries such as click chemistry, the Staudinger reduction, and Diels-Alder reaction-like cycloadditions (169,170,177). Global replacement of a natural amino

acid with an uAA analogue achieved by omission of the natural amino acid during protein synthesis is commonly performed, although, site-specific immobilization is still complicated by the incorporation of the unnatural amino acid at many locations (178,179).

The PRECISE system overcomes the reported issues of non-specific and non-covalent immobilization by building upon a developed technology that site-specifically incorporates a single uAA at a single explicitly predetermined residue (77,180). This technology was initially developed as an *in vivo Escherichia coli*-based system that uses orthogonal tRNA and aminoacyl-tRNA synthetase from *Methanocaldococcus jannaschii* to incorporate the uAA only in the location encoded by the amber stop codon (UAG) on the mRNA (180,181). Using this method, over 70 uAA have been incorporated with generally high selectivity (182,183). Two particularly attractive unnatural amino acids are *p*-propargyloxyphenylalanine (pPa) and *p*-azidophenylalanine (pAz) which can be used with the highly selective, efficient, and biocompatible copper(I)-catalyzed azide-alkyne [3 + 2] cycloaddition click reaction. Due to the photoinstability of pAz, this work focuses on the incorporate pPa to enable direct click chemistry to the surface.

Using the *in vivo* site-specific insertion technique, Kim et al. targeted a predetermined residue location in the protein DrrA and clicked an alkyne-biotin with site-specifically incorporated pAz (184). The biotin-linked protein was them surface-immobilized by the non-covalent neutravidin-biotin interaction. Compared to randomly-oriented immobilized DrrA, the orientation-specifically immobilized DrrA exhibited higher activity of DrrA (184). Although Kim et al. demonstrated the capability of residue-explicit targeting, the non-covalent link limits the immobilization's robustness.

The PRECISE system uses site-specific uAA and direct covalent immobilization, eliminating the need for a non-covalent linker. In addition, the photostable pPa is incorporated

using an *E. coli*-based cell-free protein synthesis (CFPS) approach that eliminates membrane-transport limitations and has resulted in up to a 27 fold increase in protein production yields for proteins containing pPa (8). Other advantages of CFPS include direct access and optimization of the synthesis environment, simplified purification, and high-throughput automation potential (49,78,185).

The site-specific covalent surface immobilization of proteins presented herein provides a unique balance of stable protein binding and orientation control without the need of non-covalent linkers. While the technology for the site-specific incorporation of pPa using cell-free protein synthesis has been previously reported (8), here we report the application of this technology for site-specific immobilization of proteins onto non-protein surfaces such as superparamagnetic beads. Our results also indicate extended longevity and stability of active bound proteins under biologically-unfavorable conditions with potential implications for industrial biocatalysis, protein microarrays technologies and other protein based diagnostic applications.

6.2 Materials and Methods

6.2.1 Extract Preparation

E. coli extract was prepared using a BL21 Star™ (DE3) *E. coli* strain purchased from Invitrogen (Carlsbad, CA) harboring the pEVOL-*pPr*F plasmid, a kind gift from Peter Schulz, (Scripps Research Institute). The resulting *E. coli* strain produces the *Methanocaldococcus jannaschii* aminoacyl-tRNA synthetase/tRNA pair capable of recognizing and inserting pPa at the amber stop codon AUG (77). Cell extract was prepared as previously reported (8,78) with the following modifications. The strain was fermented in 1 L batches of 2xYT media buffered with 100 mM MOPS at 37° C and shaken in a 2.5 L Tunair baffled shake flask (IBI Scientific, Peosta,

IA) at 280 rpm. Cells were lysed through triple pass homogenization using an Avestin Emulsiflex B-15 cell disruptor (Ottawa, Canada) at 21,000 psi. Subsequently, the remaining cell extract was flash-frozen and stored at -80° C until used.

6.2.2 Cell-Free Protein Synthesis

Protein synthesis of T216pPa sfGFP (pPaGFP) was carried out *in vitro* using the PANOx-SP system as previously described (8) with the following minor modifications. Plasmids used were either pY71-sfGFP-Strep or pY71-T216Amb-sfGFP-Strep (8). Unless specified, all reactions contained 2 mM pPa. BL21 Star™ (DE3) *E. coli* extract was added at 25% v/v, without additional T7 RNA polymerase. Reactions contained 7 µg/mL *Methanocaldococcus jannaschii* aminoacyl-tRNA synthetase affinity purified according to a previously reported procedure (9). Reactions were performed at 30 ºC for 8 hours or overnight.

6.2.3 Protein Yield Assays

Total and soluble protein yield calculations were performed using liquid scintillation counting as discussed previously (1,19,186). An analysis of full-length protein yields was performed by first running sodium dodecylsulfate polyacrylamide gel electrophoresis on the supernatant of the CFPS reaction mixtures after centrifugation at 13,000 xg for 15 min, and on strep-column purified protein as per the manufacturer's specifications (Life Technologies, Carlsbad, CA). Autoradiograms were prepared on Kodak MR Autoradiography Films (Rochester, NY) and densitometry calculations were performed using ImageJ software (148).

6.2.4 Fluorescence Activity Assay

Fluorescence assays were performed using a Synergy MX (Biotek Instruments, Winooski, VT) at 485/510 nm excitation/emission and sensitivity of 100 in 60 or 125 μL of PBS buffer per well of a black-bottom 96-well plate.

6.2.5 Dynabead Preparation

The superparamagnetic M-270 Dynabeads decorated with terminal amines were reacted with azide-containing ligands, using a procedure adapted from Punna et al. (187). First, 4-nitrophenyl 5-azidopentanoate was synthesized through the addition of 5-azidopentanoic acid (3.5 mmol) and p-nitrophenol (3.7 mmol) to a solution with 1-(3-dimethylaminopropyl)-3-ethylcarbodiimide hydrochloride (3.7 mmol) in CH_2Cl_2 at room temperature overnight. The 4-nitrophenyl 5-azidopentanoate was then concentrated and purified using silica gel column chromatography.

After purification, the 4-nitrophenyl 5-azidopentanoate was dissolved in DMF and added to a tube containing 2 ml of Dynabeads ($2x10^9$ beads per ml) in 5% MES buffer and stirred gently at room temperature for two days. Measurement of the released p-nitrophenol absorbance at 412 nm was then performed and compared to a p-nitrophenol standard curve. A negative control reaction containing no beads (no amines) was performed and no change in 412 nm absorbance was observed suggesting no autohydrolysis of the 4-nitrophenyl 5-azidopentanoate. Beads were vigorously washed 10 times with PBS buffer to remove excess and non-specifically adsorbed azide ligand.

6.2.6 Click Reaction (Copper-catalyzed Azide-Alkyne Cycloaddition)

The aqueous click reaction conditions were performed with either 1 mM $CuSO_4$ and 5 mM sodium ascorbate or 1 mM tetrakis(acetonitrile)copper(I) hexafluorophosphate (Cu(I)Tet) for

$CuSO_4$ or Cu(I)Tet catalyzed reactions, respectively. Click reactions with Alexa Fluor® 555 alkyne (AF555) (Invitrogen, Carlsbad, CA) were performed exclusively with Cu(I)Tet with 0.2 to 20 nmol of AF555 in 30-50 µL reaction volumes. The reaction volume for click reactions with pPaGFP was 100 µL with 0.5 nmol pPaGFP and 5 nmol azide-functional groups in the reaction.

Reagents were prepared aerobically in microcentrifuge tubes with all components save the catalyst and sodium ascorbate. Tubes were then transferred to an anaerobic glove box atmosphere containing less than 0.0 ppm oxygen and allowed to degas for a minimum of 45 minutes. After degassing, catalyst and, if required, sodium ascorbate was added. The closed tubes were then rotated end-over-end for 8 to 14 hrs in darkness. Reactions were terminated by removal of the tubes from the anaerobic glove box and exposure to atmospheric oxygen.

6.2.7 Purification of Click-immobilized pPaGFP

To purify the superparamagnetic beads from the click reaction solution, a DynaMag Spin Magnet (Invitrogen, Carlsbad, CA) was used as follows. The microcentrifuge tubes containing the click reaction were placed on the DynaMag Spin Magnet for 8 mins, after which the supernatant was removed. The tubes were then removed from the magnet, 100 µL PBS-Tween buffer (137 mM NaCl, 2.7 mM KCl, 10 mM Na_2HPO_4, 2 mM KH_2PO_4, 0.05% v/v Tween20) was added to the samples, the samples were thoroughly vortexed, and the new suspensions were incubated for 8 mins at room temperature. Samples were returned to the DynaMag Spin Magnet and the cycle was repeated 2 times. After the final removal of the supernatant, the sample was re-suspended in 100 µL PBS.

6.2.8 Freeze Thaw

pPaGFP was immobilized on azide-functional Dynabeads using both $CuSO_4$ and Cu(I)Tet and purified as described above. In a single black 96-well plate (Plate A), both pPaGFP immobilized on beads and free pPaGFP was aliquoted into different wells to a final volume of 60 µL in PBS buffer. In a separate black 96-well plate (Plate B), free pPaGFP was aliquoted into different wells to a final volume of 60 µL in PBS buffer. Plate A was subjected to four freeze-thaw cycles by incubating it at -80°C for 20 min and then incubating it at room temperature for 20 min. Between each freeze-thaw cycle fluorescence measurements of the pPaGFP were taken with the Synergy MX microplate reader as described above. Concurrently, Plate B was incubated at 4°C and fluorescence measurements of the pPaGFP were also taken every 40 min.

6.2.9 Urea/Heat Incubation

pPaGFP were immobilized on azide-functional Dynabeads using both $CuSO_4$ and Cu(I)Tet and purified as described above. In a single black 96-well plate (Plate C), both pPaGFP immobilized on beads and free pPaGFP were aliquoted into different wells to a final volume of 50 µL in PBS buffer. To all wells containing pPaGFP immobilized on beads and to half of the wells containing free pPaGFP was added 75 µL of 10 M urea, bringing the final urea concentration to 6 M. To the remaining wells of free pPaGFP was added 75 µL of deionized sterile water in place of urea. In a separate black 96-well plate (Plate D), free pPaGFP was aliquoted into different wells to a final volume of 50 µL with PBS buffer following which 75 µL of deionized sterile H_2O was added.

Immediately after adding urea or water, Plate C was placed in the Synergy MS microplate reader with the sample chamber temperature maintained at 50°C and assayed for fluorescence activity every minute for 30 mins. The plate was removed from the plate reader and cooled to 4°C

and assayed for fluorescence activity after 1.5 and 12 hrs. Place D was treated in a similar manner with the exception of the microplate reader's sample chamber temperature being maintained at room temperature.

6.3 Results and Discussion

The Protein Residue-Explicit Covalent Immobilization for Stability Enhancement or PRECISE system introduced herein allowed for retention of protein activity and increased the stability and durability of the proteins. Azide-functional superparamagnetic beads were prepared as the attachment surface and tested using small alkyne-functional fluorophores. Then, GFP containing an unnatural amino acid (uAA) was synthesized, purified, and successfully immobilized to the beads with the PRECISE system as illustrated in Figure 6-1. Immobilized GFP maintained a significant fluorescence activity and exhibited increased stability against freeze-thaw cycles, urea and elevated temperature compared to unbound GFP, as will be described in detail below.

6.3.1 Preparation of Azide-Functional Surface

Superparamagnetic beads were selected as the immobilization surface for simplicity in purification, recovery, and reuse. Furthermore, they provide a macro, inorganic surface for conjugation. Amine-decorated superparamagnetic beads (Dynabeads® M-270, Invitrogen) were modified with terminal azide groups as shown in Figure 6-2. To make the beads viable reagents in the click reaction, the amine-coated beads were reacted with 4-nitrophenyl 5-azidopentanoate and the release of p-nitrophenol was measured by absorbance to determine extent of reaction, which resulted in azide-functionalization of 95% of the amine groups available as per the manufacturer's specifications (Invitrogen).

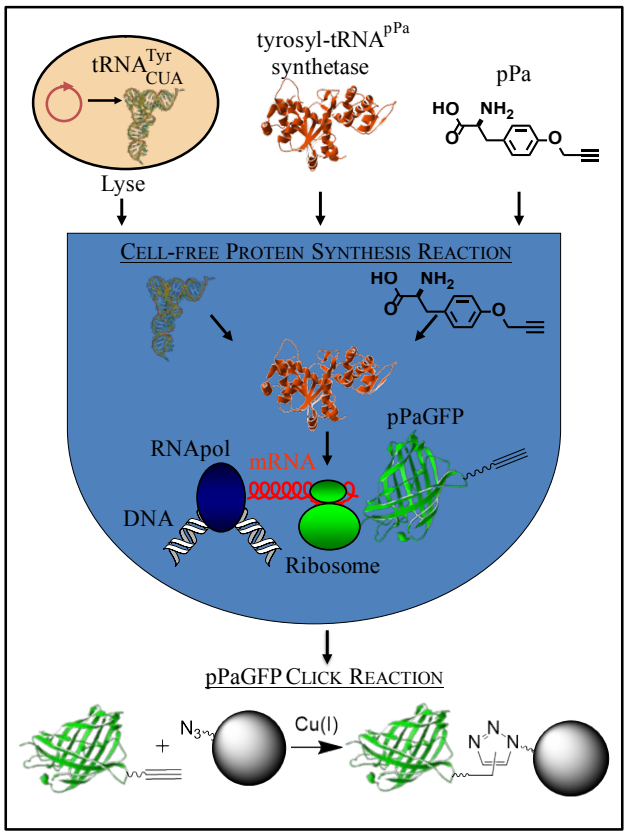

Figure 6-1 – Scheme of the PRECISE System

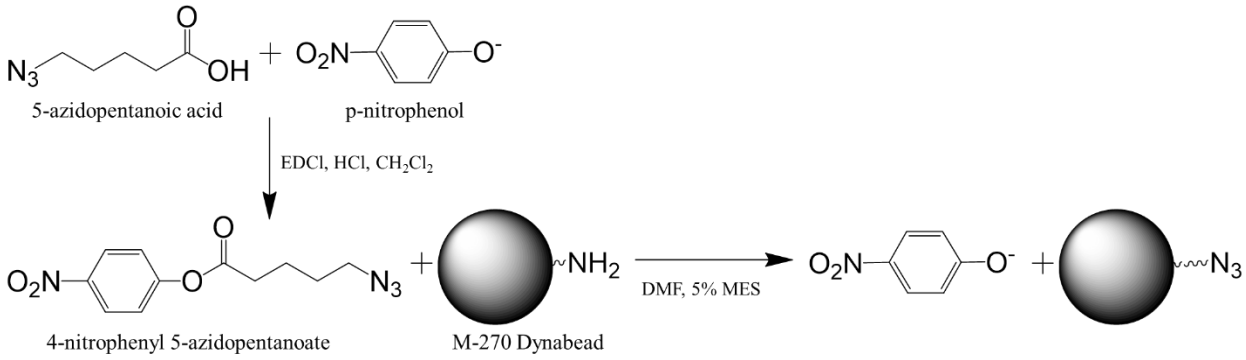

Figure 6-2 – Scheme of Azide Decoration of the Superparamagnetic Beads.

6.3.2 Cell-free Protein Synthesis

Superfolder Green Fluorescent Protein (sfGFP) was rationally engineered to incorporate an uAA at T216 and to contain a C-terminal purification tag (8). The site T216 was chosen for substitution by identifying a surface-accessible protruding loop near an end of the cylindrical

protein's crystal structure (Figure 12-1). The C-terminal Strep-tag provided means of purifying full-length protein from truncated product, which occurs when the uAA is not incorporated and results in early termination of the protein (Figure 6-3). By carefully choosing the location of mutagenesis and avoiding alterations to the main structural or active portions of the protein, the potential for improper folding or activity loss is minimized. Indeed, the activity of purified uAA-containing sfGFP did not drop compared to the activity of unmodified sfGFP (8).

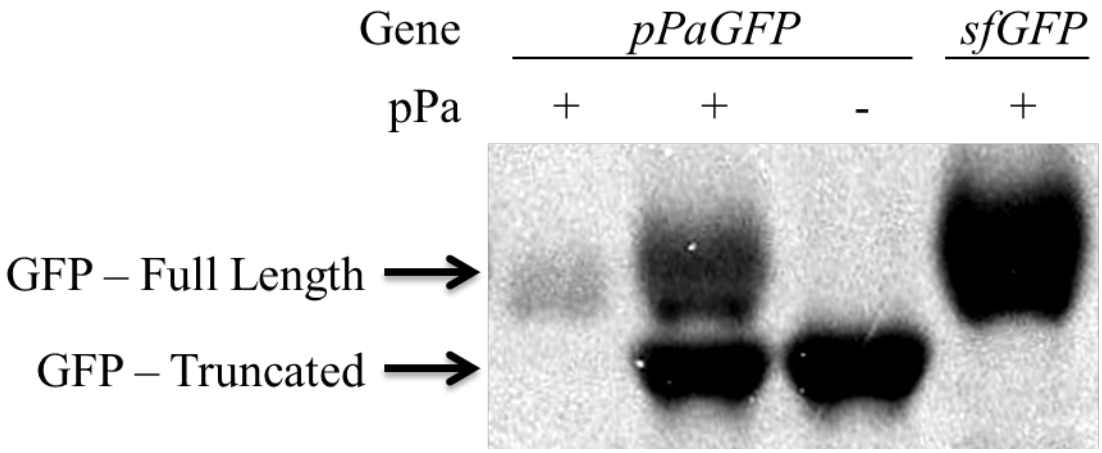

Figure 6-3 – SDS-PAGE and Autoradiogram of pPaGFP. The lanes are laid out from left to right as follows: 1) pPaGFP post-Strep-tag purification; 2) synthesized pPaGFP prior to purification; 3) pPaGFP synthesized without the presence of pPa; and 4) unmodified sfGFP synthesized under otherwise identical conditions to other products.

The PRECISE system utilizes the open access afforded by CFPS to optimize concentrations of the *Methanocaldococcus jannaschii* aminoacyl-tRNA synthetase (Figure 12-2), which works together with its tRNA pair to incorporate the uAA pPa at the Amber stop codon. As displayed in Figure 6-3, pPa was successfully incorporated approximately 40% of the time when pPa was present in the CFPS reaction. When pPa was absent, the protein was truncated at the amber stop codon with no detectable incorporation of pPa (Figure 6-3, Lane 3), which is consistent with previously reported works (8,188,189).

The CFPS production approach has specific advantages over *in vivo* protein production such energy focused toward expression of the product protein(s), simplified product purification, and elimination of transport-limiting cell-walls (8,19,78). In addition, CFPS enables direct access to the open synthesis environment and enables facile optimization and maximization in the concentration of synthetase, uAAs, and other cofactors essential for protein synthesis.

6.3.3 Click Immobilization

Preliminary click immobilizations to the beads exploring click conjugation efficiency were performed using a small fluorescent ligand, Alexa Fluor® 555 alkyne (AF555). Click conjugation was successful under multiple reagent concentrations as seen in Figure 6-4. Reactions containing 1 nmol or more AF555 resulted in the highest amount of immobilization. At 5 and 20 nmol AF555, the resulting attachment was not statistically higher than at 1 nmol (p-value = 0.78). This apparent maximum results in an average of 12 million AF555 per bead. The number of AF555 attached and the percentage attached in Figure 6-4 are conservatively reported and do not account for signal lost due to light diffraction and shadowing caused by the beads.

Reaction conditions for pPaGFP immobilization were selected based on AF555 results. pPaGFP were immobilized onto the azide-functional magnetic beads by anaerobic incubation using reduced copper from either $CuSO_4$ or tetrakis(acetonitrile)copper(I) hexafluorophosphate (Cu(I)Tet) as a catalyst. The results are reported in Table 6-1. The Cu(I)Tet-catalyzed reactions resulted in a higher click attachment percentage at 11% (9.6 million pPaGFP per bead), compared to the $CuSO_4$-catalyzed reactions at 4.5% (3.9 million pPaGFP per bead). The two catalyst systems provide the essential catalyst (Cu(I)) with differing mechanisms. Cu(I)Tet provides Cu(I) directly while the $CuSO_4$ system relies on the redox potential of sodium ascorbate to reduce Cu(II) to Cu(I). The divergence in catalyst-recovery mechanisms is a likely cause for the mild divergence in overall

reaction efficiency. While high reaction efficiencies are reported in literature for similar click reactions using protein reagents (178,190,191), the reagent concentrations used in this work are at least an order of magnitude lower. Excellent work by M.G. Finn's lab (Scripps Research Institute) has demonstrated that the optimal copper catalyst concentration is dependent upon the reagent concentration (190,192). In addition, Finn and others have reported a variety of ligands which improve the kinetics and reaction efficiency and the optimal concentration of such ligands can depend on the reagent types and concentrations (190,192). Further work to optimize the click reaction at the lower concentrations used in this work, could substantially increase the reaction efficiency. However, we do observed significant pPaGFP attachment with the reported reaction conditions.

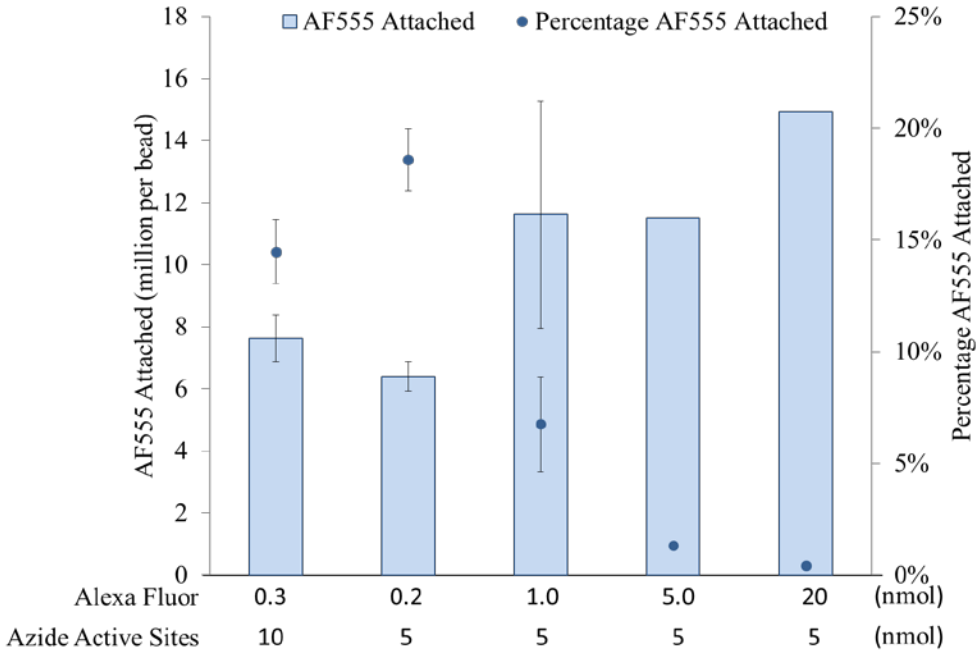

Figure 6-4 – Alexa Fluor® 555 and Bead Click-Conjugation Profile. The number of AF555 attached and the percentage attached are conservatively reported above and do not account for signal lost due to light diffraction and shadowing caused by the beads. "Percentage AF555 Attached" refers to the percentage of AF555 attached compared to the amount input into the reaction solution. No Background attachment of AF555 to beads was evident under any of the conditions considered. Error bars = standard deviation (n=2) or none (n=1).

After washing the beads with PBS-Tween buffer three times, non-specific adsorption was insignificant. However, washing with PBS only resulted in some non-specific adsorption (0.5 million pPaGFP per bead as compared to 3.9 and 9.6 million pPaGFP per bead attached via click conjugation) (Figure 12-3).

Table 6-1 – pPaGFP Attachment and Observed Activity Values

Unbound[a]	**$CuSO_4$**	**Cu(I)Tet**	**PBS Buffer**
Incubated Activity [RFU/mol pPaGFP]	37.0 ± 0.01	8.4 ± 3.0	109.7 ± 11.7
Bead-Conjugated	**$CuSO_4$**	**Cu(I)Tet**	**Adsorbed**[b]
Percent pPaGFP Attached	4.5% ± 1.2%	**11.3%** ± 3.5%	0.6%
Overall Attached [million per bead]	3.9 ± 1.0	**9.6** ± 3.0	0.5
Observed Activity Attached [RFU/mol pPaGFP]	**15.6** ± 4.4	4.2 ± 1.9	12.0

For all data n=2 with ± standard deviation unless specified.
a. Unbound protein were incubated in the respective reaction solutions and then assayed for activity without beads present.
b. Adsorbed proteins were incubated with azide-decorated beads in the absence of copper and then washed with PBS buffer in lieu of PBS-tween buffer (n=1). Similar trials washed in PBS-tween resulted in no detectable adsorption (n=2).

The cyclo-addition of azides to non-activated alkynes is Cu(I)-catalyzed to avoid high pressures and temperatures that would be incompatible with biological systems (193). However, copper ions can quench GFP fluorescence by direct, non-denaturing interaction with the chromophore (194,195). In addition, it is difficult to accurately assess the specific activity of the immobilized protein due to the complicating factors of bead-induced light diffraction and shadowing, which may cause up to 50% signal reduction. However, based on the very conservative assumption that all active pPaGFP on the bead were observed (i.e. no loss due to the bead-induced light diffraction and shadowing), immobilized pPaGFP retained at least 40% of the activity of the free pPaGFP incubated in the click reaction environment. For clarity, when reporting the stability of immobilized pPaGFP and free pPaGFP under the harsh conditions below, changes in activity per mol pPaGFP are reported to eliminate the impact of bead-induced signal loss factors.

6.3.4 Freeze Thawing

To evaluate if the immobilized pPaGFP exhibited improved stability, free pPaGFP and bead-immobilized pPaGFP were subjected to multiple cycles of freezing and thawing. Changes in pPaGFP activity were normalized per mol pPaGFP and are reported in Figure 6-5. The bead-immobilized pPaGFP activity increased slightly over the 4 freeze-thaw cycles. In contrast, freeze-thawed free protein lost an average 17% of the initial activity after each cycle, resulting in a 68% loss in activity after 4 freeze-thaw cycles. Free protein kept at 4 ºC over the entire experiment also resulted in a drop in activity after 4 cycles. Free proteins subjected to freeze-thaw or maintained at 4 ºC in the presence of the copper-catalyst of the click reaction exhibited very similar trends as their copper-free counterparts (Figure 12-4).

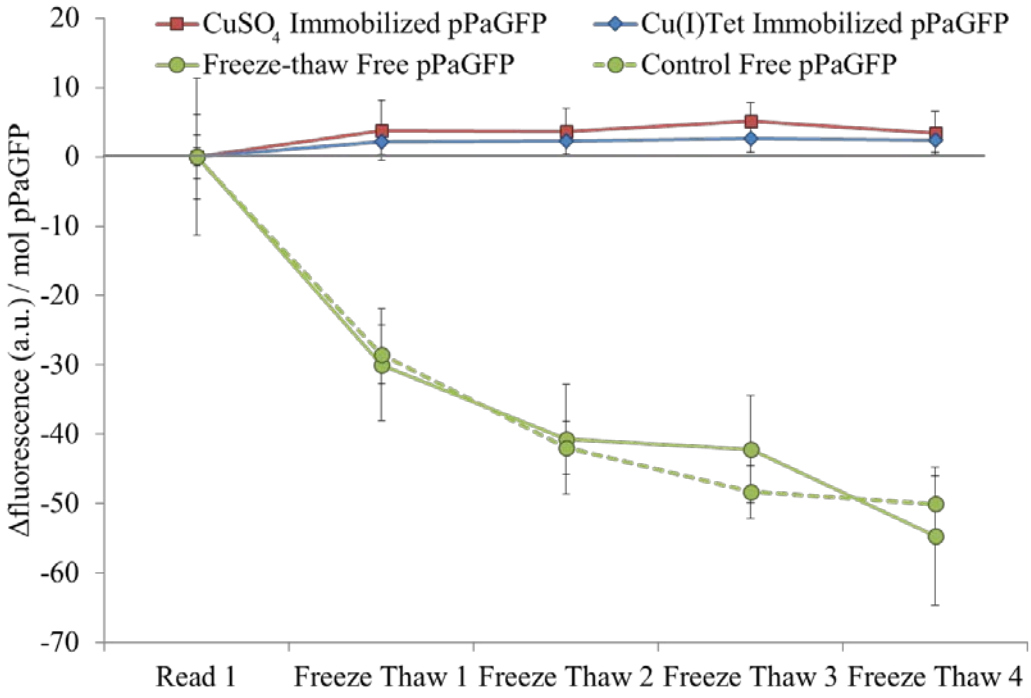

Figure 6-5 – Freeze Thaw Effects on Stability. Bead-conjugated pPaGFP were run in parallel through freeze thaw cycles (20 min at -80ºC, 20 mins at 25ºC, assay, repeat) following which the fluorescence activity was assayed. In addition, a control for the behavior of free pPaGFP consisted of free pPaGFP either freeze-thawed (solid-line, circles) or maintained at 4ºC (dashed line, circles). Error bars = standard error (n=2 for beads, 26 for freeze-thawed, 50 for control).

6.3.5 Urea/Heat Incubation

Bead-immobilized pPaGFP and free pPaGFP were incubated under the harsh conditions of urea (6 M) and elevated temperature (50 ºC). Resulting changes in activity were normalized per mol pPaGFP and are reported in Figure 6-6. Bead-immobilized proteins retained 57% or more of their initial activity throughout the duration of the incubation in urea at 50 ºC. After the samples were cooled to 4 ºC, the activity of immobilized pPaGFP recovered 83% or more of the initial value, despite continued incubation in urea. In contrast, free pPaGFP retained less than 10% of their initial activity during heating and after 12 hours of cooling exhibited less than 3% of the initial activity, regardless of urea's presence or absence.

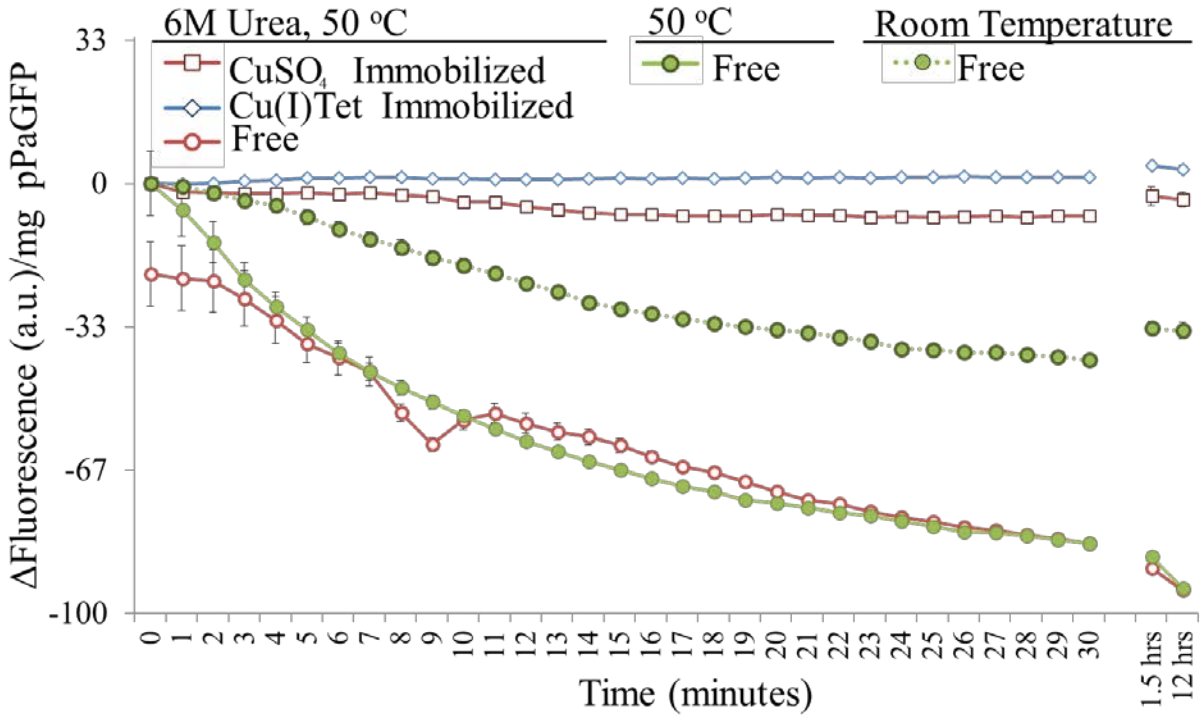

Figure 6-6 – Urea and Heat Effects on Stability. Bead-conjugated pPaGFP were run against multiple controls and assayed for fluorescence. The solutions, with the exception of the free pPaGFP at room temperature, began at room temperature and were incubated at 50ºC for the duration of the assay (30 min) directly after addition of room-temperature urea or water. After the initial 30 minute assay, samples were placed at 4ºC until the next data point was read. The addition of urea caused the free pPaGFP to drop in activity prior to any heating (empty circles). The bead-immobilized pPaGFP did not exhibit any immediate loss in activity due to the addition of urea (empty squares/diamonds). Error bars = standard error (n=2 for bead-conjugated pPaGFP, n=3 for free pPa GFP, and n=4 for free room temperature pPaGFP).

6.4 **Conclusion**

We have introduced an example of Protein Residue-Explicit Click Immobilization for Stability Enhancement or the PRECISE system. Click chemistry teamed with minimally invasive site-specific uAA-incorporation using cell-free protein synthesis allowed for the rationally engineered protein to be directly and site-specifically immobilized onto an inorganic surface. In all cases explored here, the immobilized pPaGFP appeared to exhibit superior stability, durability and retained activity during multiple harsh scenarios as compared to free protein in solution.

The ability to site-specifically attach proteins to a surface using bio-orthogonal chemistry at any predetermined site has provided a basis for more stable and longer lasting protein activity. This technology has numerous implications in the industrial, scientific and medical communities and could be applied to enhance industrial enzyme recovery, simplify laboratory assays and machinery, and reduce medical diagnostic costs while increasing consistency, availability and transportability. Furthermore, this work solidifies the foundation for the PRECISE system for highly stable protein immobilization.

7 EXPANDING THE LANGUAGE OF BIOLOGY: SENSE CODON REASSIGNMENT

7.1 Introduction

The 23 proteomic amino acids have provided for rich biological diversity on earth (196). Yet the narrow range of chemistries provided by these residues can frequently pose a challenge to the biochemist's quest for site-specific modifications to protein. The site-specific incorporation of unnatural amino acids (uAAs) in proteins unlocks the potential for unique residues. This rapidly growing field provides a unique tool that has already been applied toward improving pharmacokinetics, cancer treatments, vaccine development, proteomics and protein engineering (20,183,197-204). In short, the ability to site-specifically incorporate uAAs is a strong platform to expand the chemistry of life (8,9,180,183). Although decades of work have been devoted to this area of research, major strides have recently been made toward simple, productive, and readily transferable methods of site-specific uAA-incorporation (10,21,49,66,205). Most notably, Shultz and coworkers have developed a number of evolved aminoacyl tRNA-synthetase/tRNA pairs that act orthogonally to native synthetase/tRNA pairs, allowing for high fidelity protein synthesis without interactions between native and evolved synthetase/tRNA pairs. These evolved synthetases incorporate the uAAs site-specifically at Amber codons (180,183,206). Over 70 uAAs have been incorporated with high specificity using this system (183).

One considerable challenge with current uAA incorporation techniques is the limited availability and efficiency of uAA-codons. Amber stop codons are predominantly targeted with

some examples of opal and frame-shift codons being successfully employed (77,183). However, these systems suffer from competition of endogenous systems (release factors or native tRNA) and therefore have only achieved low efficiencies compared to naturally occurring coding efficiency (207). Furthermore, the limited selection of codons restricts the number of different uAAs that can be incorporated simultaneously. To more richly expand the language of biology, new unique codons must be identified and made available.

This work proposes a CFPS system that would be capable of simultaneously recoding up to 43 uAAs as well as the 20 universal natural amino acids. To achieve this goal, the following criteria must be fulfilled:

1. Removal or degradation of endogenous tRNA from cell extract
2. Development and expression of synthetic minimal tRNA set for natural AAs
3. Harness orthogonal aminoacyl-tRNA synthetase/tRNA pairs for uAA incorporation

Removing the endogenous tRNA from the cell extract effectively removes the link between native tRNA aminoacylation and the genetic code, opening the possibility to completely recode the relationship between codons and amino acids.

Development of a synthetic minimal tRNA set restores a minimalistic relationship between codons and amino acids. The synthetic minimal set should be sufficient to encode for the 20 universal amino acids, leave one codon for peptide synthesis termination while leaving up to 43 of the 64 total codons available for reassignment to uAA incorporation.

The final step to develop the system is to harness the power of aminoacyl-tRNA synthetase/tRNA (aaRS/tRNA) pairs that are orthogonal to our bacterial system. Orthogonal aaRS/tRNA pairs do not interfere with the synthetic minimal set tRNA, native aaRSs, nor natural

amino acids. The successful execution of such a system has the potential to disrupt current uAA-incorporation technology and open a new field of protein research otherwise impossible.

7.2 Results and Discussion

7.2.1 Removal of Endogenous tRNA

This first step to reassign the codons of our system is to remove the endogenous tRNA, effectively removing the connection between codon and amino acid. A study by Kanda and coworkers reported that incubating cell-extract with RNAse A effectively removes tRNA and shuts off the extract's protein synthesis capabilities (208). Kanda further reported that protein synthesis capabilities could be restored upon addition of mixed endogenous tRNA to the extract. These promising results laid the foundation for our tRNA degradation protocol.

To simplify the tRNA degradation protocol, RNAse A protein was immobilized on superparamagnetic beads (Dynabead M270, Life Technologies, Grand Island, NY) using amine-targeting epoxy groups. The superparamagnetic beads provided an easy mechanism for removal of the RNAses prior to addition of nucleic acids required for protein synthesis. Treatment of the extract resulted in extract without protein synthesis capability (Figure 7-1A). Addition of mixed endogenous tRNA to the extract resulted in recovery of protein synthesis viability. The beads with RNAse A immobilized are reusable, decreasing the overall cost of the treatment system (Figure 7-1B). This system is an effective method for removing tRNA from cell-extracts.

7.2.2 Design and Production of Synthetic Minimal tRNA Set

The design of a synthetic minimal set of tRNA is the next step in developing a native codon reassignment system. Twenty-one codons must be reserved for the 20 universal natural amino

acids and a single stop codon. The 20 amino acids each require one unique tRNA. In addition, protein synthesis requires a specialized tRNA for initiation. The stop codon requires no tRNA. Therefore, a synthetic minimal set capable of encoding for the universal 20 amino acids must have at least 21 synthetic tRNA.

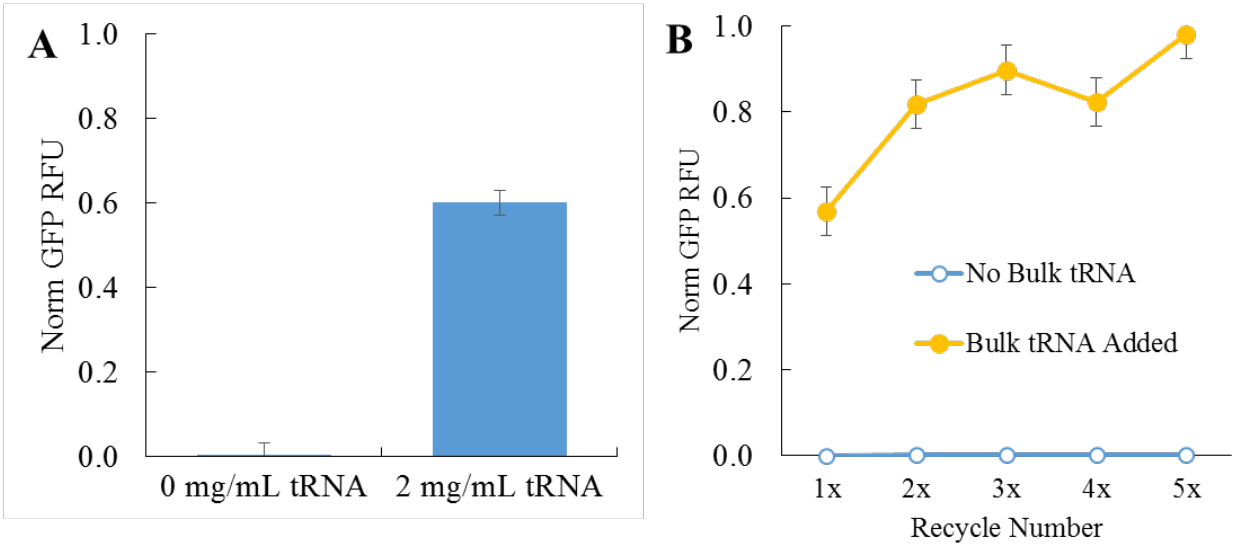

Figure 7-1 – Extract Performance after RNAse A Treatment. Extracts were incubated in the presence of beads with RNAse A covalently immobilized. (A) Comparing the performance of the treated extract with or without mixed *Escherichia coli* tRNA added. (B) Recycling the treatment beads for multiple treatments. All cycles were sufficient to prevent protein synthesis in the absence of mixed tRNA.

To avoid the necessity of engineering novel tRNA and their respective aaRS pairs, it is preferable to utilize the available endogenous aaRSs. Thus, the synthetic tRNA should be based primarily on known native tRNA sequences. One difficulty of directly copying the native genes is the question of sufficient expression levels. Native tRNA are promoted with a variety of promoters and terminators, and are often found in operons of other tRNA and mRNA for proteins. After transcription, many tRNAs are cleaved into their respective final formats. Employing native promoters would be troublesome in our CFPS system, as the endogenous RNA polymerases would likely be insufficient to obtain useable levels of tRNA.

To combat the problems of expression levels and post-transcriptional cleavage, we propose the use of a transfer RNA ribozyme construct, or "tranzyme." Fechter and coworkers demonstrated that synthetic tRNA could be promoted for transcription at high levels using a T7 promoter sequence in combination with a hammerhead ribozyme (HHR) (209). The HHR has autocatalytic activity that is capable of cleaving the transcribed product, resulting in proper tRNA products. Albayrak and coworkers demonstrated the versatility of this concept by developing further successful tranzyme products (38). Based on these reports, we designed a template for our tranzyme, depicted in Figure 7-2.

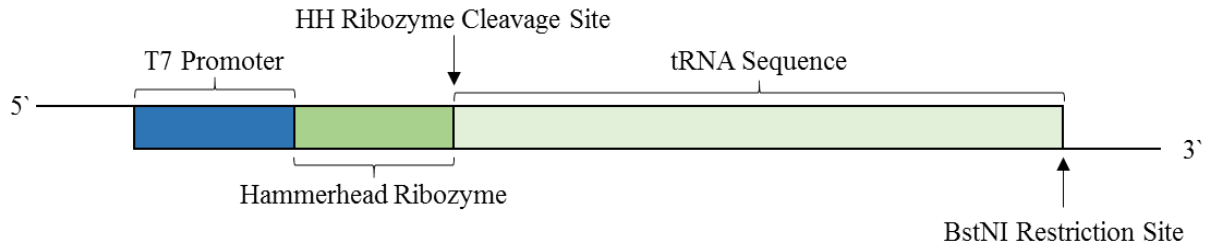

Figure 7-2 – tRNA "Tranzyme" Gene Designs. The design of the synthetic tRNA was produced such that the 5` and 3` ends of the final RNA product would have the appropriate termini for tRNA. The hammerhead ribozyme cleaves the 5` end appropriately, while the 3` end is digested prior to transcription to allow the T7 RNA polymerase to terminate transcription by releasing the DNA rather than using a T7 terminator sequence.

Selecting the tRNA sequences to include in our minimal set was based on iterative analysis of the following criteria:

1. Is the endogenous sequence known and available?
2. Does the tRNA anticodon experience promiscuous binding with multiple codons?
3. What is the *Escherichia coli* Class II codon bias for the pairing codon(s)?

The availability of the endogenous sequence is essential to take advantage of endogenous aaRSs. If the tRNA is promiscuous in its binding with codons, then a single tRNA could disallow multiple codons for uAA-incorporation. Therefore, preference is given to tRNA that are less promiscuous, thus leaving more available codons for reassignment.

Regarding codon bias, it has been established that tRNA content and codon bias are positively correlated (210). This would suggest that a codon with a high bias (i.e. one used more frequently in the genome of the expression host) would have more pairing tRNA available. Assuming our tRNA degradation method is not 100% efficient at removing all active tRNA, logic suggests that the remaining tRNA would be those found initially at high concentrations. Choosing these tRNA sequences and codons as part of our minimal set reduces the risk of interference from residual endogenous tRNA. Based on these criteria, we have selected a synthetic minimal set of tRNA for our codon reassignment system.

7.3 Conclusions and Future Directions

The initial framework has been cobbled for the development of a CFPS system capable of simultaneous incorporation of multiple unnatural amino acids using sense codon reassignment. The ability to directly access and manipulate the transcription/translation environment of CFPS has made it possible to degrade native tRNA and replace it with mixed endogenous tRNA. The design of a synthetic tRNA set lays the foundation for future work.

Continued pursuit on this research is being pursued by a team of researchers lead by Dr. Brady Bundy and myself, including Jeremy Hunt, Amin Saheli, Andrew Broadbent and Matthew Schinn. Jeremy and Amin are pursuing the next hurdle of the minimal tRNA set, specifically expression, purification, characterization and optimization. Andrew is pursuing the expression and characterization of orthogonal aaRS/tRNA pairs. Matthew Schinn is pursuing the expression of proteins using the synthetic minimal set and the orthogonal aaRS/tRNA pairs.

The potential ability to reassign native codons and expand the protein code by up to 43 uAAs has promising applications in effectively every space of protein biology, such as medical therapeutics, protein engineering, and microbiological diagnostics.

8 CONCLUSIONS AND FUTURE WORK

The results reported in this work demonstrate the utility and versatility of CFPS for protein and bioengineering. We have added to and improved the tool of CFPS by demonstrating a robust lyophilized system and improved fermentation conditions for systems requiring exogenous elements. We have laid clear foundations for multiple applications of CFPS, including the rapid production of recombinant vaccines, novel nanoparticles, site-specific protein immobilization techniques and an expanded protein code.

9 APPENDIX A. SUPPLEMENTARY MATERIAL FOR CHAPTER 2

9.1 Resuspension Volume Calculations – Cell Extracts

9.1.1 DC™ Assay Results

Prior to lyophilization, DC™ assays (Bio-Rad, Hercules, California) were employed to estimate the protein content of the cell extracts. Figure 9-1 depicts the results from an assay using bovine serum albumin (BSA) as a standard. Equation 9-1 was derived from a regression of the data in Figure 9-1. OD_{750} was measured for serial dilutions of extract and the approximate protein content was estimated using Equation 9-1. The untreated aqueous extract was estimated to contain 72 mg/mL protein.

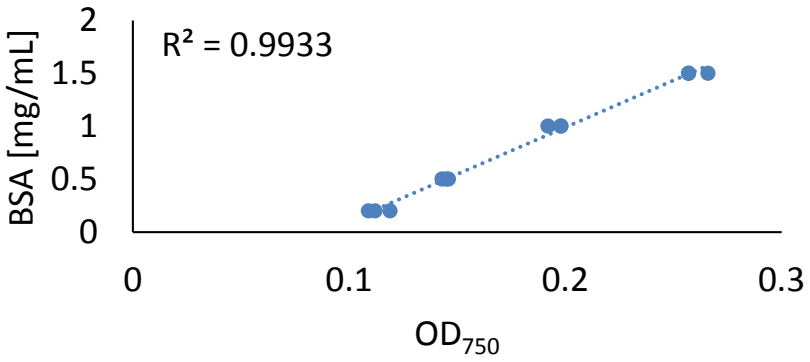

Figure 9-1 - DC™ Assay Employing BSA as a Standard. Example of DC™ assay analysis that provides a standard relationship between protein concentration and OD_{750}. This analysis was performed according to the manufacturer's specifications (Bio-Rad, Hercules, California) using bovine serum albumin (BSA) as the protein standard.

Equation 9-1 – Estimate Extract Protein Content

$$Extract\ Protein\ Content\left[\frac{mg}{mL}\right] = 8.8656\left[\frac{mg}{mL \times OD_{750}}\right] \times OD_{750} - 0.7825\left[\frac{mg}{mL}\right]$$

9.1.2 Water Loss during Lyophilization

Equation 9-2A was used to estimate the amount of water loss during lyophilization. The density of the water (ρ_{H2O}) was calculated as detailed in Equation 9-2C. The density of extract was calculated from direct extract volume and weight measurements. Protein density ($\rho_{protein}$) was estimated using the DC™ assay results (Equation 9-1). Sucrose and Energy mix densities ($\rho_{sucrose}$ and $\rho_{energy\ mix}$, respectively) were directly calculated based on their respective known constituents.

Equation 9-2 – Estimate Percentage Water Loss During Lyophilization

A $\%H_2O\ lost = \frac{\Delta m_{total}}{m_{H2O}}$

B $m_{H2O} = \rho_{H2O} \times vol_{ext}$

C $\rho_{H2O} = \rho_{Extract} - \rho_{protein} - \rho_{Sucrose} - \rho_{energy\ mix}$

9.1.3 Rehydration Ratios

Lyophilized extracts must be rehydrated prior to use in an aqueous reaction. To obtain a proper extract rehydration ration (mL water per gram lyophilized extract) for lyophilized extracts, standard lyophilized extract was rehydrated with the rehydration ratio ($Ratio_{rehydration}$) of 10.5 mL water per gram powder as an initial estimate. This solution was subsequently subjected to DC™ assay analysis and estimated to contain 62 mg/mL protein ($\rho_{rehydration}$). A simple calculation using Equation 9-3A indicated that an appropriate extract rehydration ratio of standard lyophilized extract was 9 mL water per gram powder.

Lyophilized extracts that were supplemented with sucrose or an energy mix required individual rehydration ratios. These ratios were calculated as specified in Equation 9-3B and C for extract supplemented with sucrose and energy mix, respectively. Sucrose was added to the extract

at 0.1 gram per 10 mL extract. The additional volume of sucrose was considered negligible. The energy mix was added as an aqueous solution at a 1-to-1 ratio to extract. The calculated rehydration ratios for sucrose and energy mix supplemented extracts was 6.21 and 6.51 mL water per gram powder, respectively.

Equation 9-3 – Rehydration Ratios (RR)

A $$Extract\ RR\ \left[\frac{mL}{g}\right] = \frac{\rho_{rehydration} \times Ratio_{rehydration}}{\rho_{extract}}$$

B $$Sucrose + Extract\ RR = \frac{1}{\frac{1}{RR_{Ext}} + \rho_{sucrose}}$$

C $$Energy\ Mix + Extract\ RR = \frac{1}{\frac{1}{2 \times RR_{Ext}} + \frac{\rho_{energy\ mix}}{2}}$$

9.2 CFPS Yield Error due to Rehydration

To estimate the error in the CFPS yields caused by inaccuracies in weighing and rehydrating the lyophilized extracts, 5x aliquots of $xSTD_{lyo}$ were rehydrated and used with the same cell-free reaction premix lacking extract. The standard deviation between these reactions was attributed to errors in weighing and rehydration and included as a portion of the error found in Figure 9-1.

9.3 Bacterial Contamination

Preparation of cell extracts for cell-free protein synthesis begins with bacterial fermentation and subsequent lysis. This lysis is thorough, at 99.9996% for the system employed in this work (49). However, the pre-lysis concentration of cells is near 600 billion cells per mL solution, leaving about 2 million cells per mL after lysis. Therefore, there is a risk of extracts being degraded by bacterial growth, particularly at temperatures conducive to bacterial replication. To examine this risk, the amount of contamination was measured based on colonies formed per µL extract plated on sterile LB Miller Agar plates. By 14 days, aqueous extract was too contaminated to be

quantified properly. In contrast, lyophilized extracts showed comparatively lowered contamination. This reduction in contamination is potentially caused by the lyophilization process. Another possible cause of reduced contamination is the hyper-salinity of the lyophilized extracts. As the extracts are dried, the salts from the buffers become exceedingly concentrated, reaching concentrations that cause cell death.

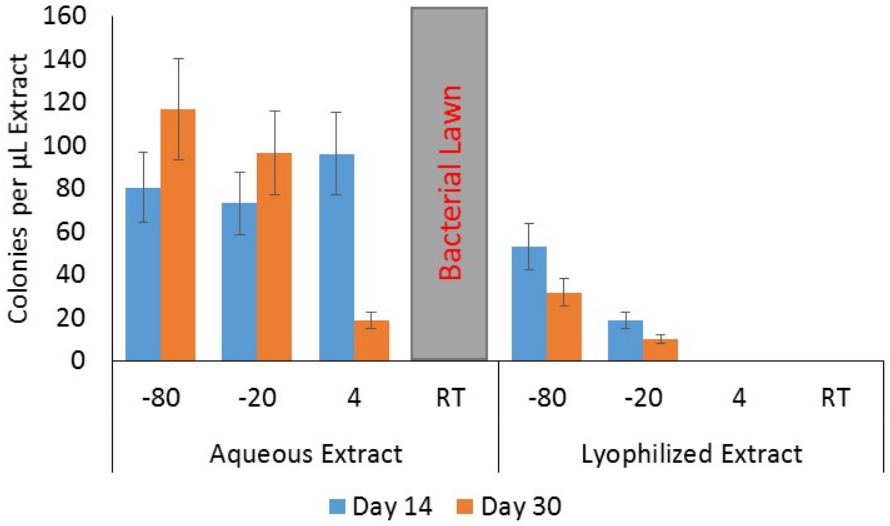

Figure 9-2 – Bacterial Contamination in Aqueous and Rehydrated Lyophilized Extract. Aqueous and rehydrated extracts were diluted into an appropriate amount of SOC media, of which 200 µL was plated on sterile LB Miller Agar plates. Plates were incubated at 37°C for 16-24 hours, at which time the colonies were counted using ImageJ software (148). Aqueous extract for day 14 and 30 produced a total bacterial lawn on the plate (>200-fold dilution). Error bars are 20% of the measured value, n=1.

9.4 Powdered Energy Systems

9.4.1 Energy System Selection

Five energy systems were considered for development as powdered energy systems: 1) phosphoenolpyruvate system (14), 2) creatine-phosphate/creatine-kinase system (211), 3) the "cytomim" system (15), 4) fructose-1,6-bisphosphate system (7), and 5) glucose system (13). A powdered PEP-based system ($ePEP_{pow}$) based upon the aqueous PEP-based system ($ePEP_{aqu}$) was developed to serve as a direct comparison. In efforts to establish a potentially more stable energy

system, the other systems were examined for the stability of their individual components. A glucose based system ($eGLU_{pow}$) was selected based upon the high stability of the main energy source, namely glucose.

9.4.2 Hydration Volumes for Energy Systems

The amount of water to be added to the powder energy systems (called here the "hydration volume") was estimated using Equation 9-4. Ideally, the final density of the solution of hydrated powder should be the same as the density of aqueous energy systems (ρ_{final}). The volume of the powder components in the final solution must be considered to prevent excessive dilution. Thus, the density of the dry powder was measured (ρ_{powder}) and void fraction (φ) of the powder was assumed to be 1/3.

Equation 9-4 – Hydration Volume

$$Hydration\ \boldsymbol{volume} = mass_{\boldsymbol{powder}}\left(\frac{1}{\rho_{final}} - \frac{1}{\rho_{powder}(1-\varphi)}\right)$$

9.4.3 pH Optimization of Phosphoenolpyruvate Energy Systems

The $ePEP_{pow}$ energy system is not readily brought to an optimal pH in its powdered format. Therefore, after dissolving the powder in water, it was necessary to adjust the pH. Due to the small volumes being optimized, this challenge was addressed through the addition of varying volumes of 5M NaOH. Figure 9-3 depicts the results of increasing levels of NaOH, with an optimum at approximately 192 mM NaOH in the final energy mix. Small volumes of these energy mixes were placed on litmus paper for rough comparisons of pH (acidic to basic corresponding to red to green, respectively). The optimum pH corresponded to neutral or slightly acidic. When no NaOH is added, the white coloring on the litmus paper is undissolved PEP.

The differences in pH and protein yield between optimized $ePEP_{pow}$ and $ePEP_{aqu}$ indicate that the aqueous system may not be pH optimized. To test this concept, HCl was added to $ePEP_{aqu}$ and examining the CFPS results, depicted in Figure 9-4. The apparent optimum for this work is near 10-15 mM HCl.

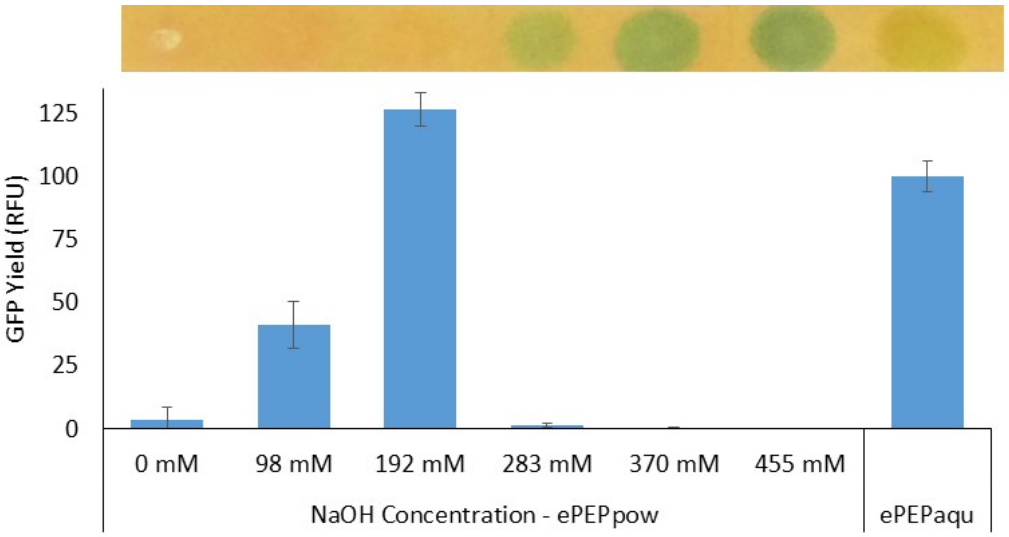

Figure 9-3 – pH Optimization of Powdered PEP-based Energy System. NaOH was added at increasing levels to the $ePEP_{pow}$ energy system, sampled on litmus paper and added to cell-free reactions. For the litmus paper, red is acidic, green is basic, and the mustard yellow is neutral pH. The white coloring on the litmus paper for 0 mM NaOH is undissolved PEP. Error bars represent one standard deviation and n=3.

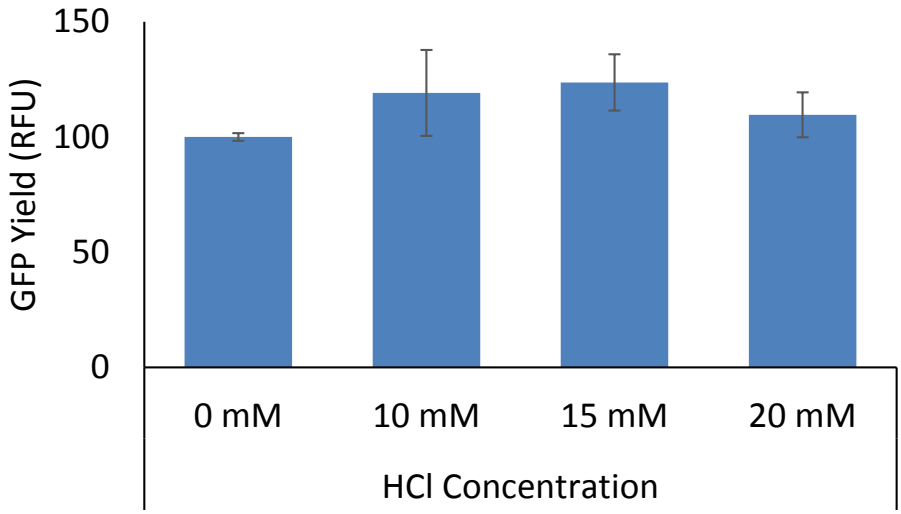

Figure 9-4 - pH Optimization of Aqueous PEP-based Energy System. HCl was added at increasing levels to $ePEP_{aqu}$ prior to its use in CFPS reactions. Reactions with HCl added outperformed the control reaction (0 mM HCl). GFP Yield was normalized to unaltered $ePEP_{aqu}$ yields. Error bars represent one standard deviation with n=3.

10 APPENDIX B – SUPPLEMENTARY MATERIAL FOR CHAPTER 3

Harvest Time (hr)		3	3	3	3	3	3	3	3	4.5	4.5	4.5	4.5	4.5	4.5	4.5	4.5	6	6	6	6	6	6	6	6
MOPs		N	N	N	N	Y	Y	Y	Y	N	N	N	N	Y	Y	Y	Y	N	N	N	N	Y	Y	Y	Y
eCFPS Temperature (°C)		30	30	37	37	30	30	37	37	30	30	37	37	30	30	37	37	30	30	37	37	30	30	37	37
eCFPS Time (hr)		3	8	3	8	3	8	3	8	3	8	3	8	3	8	3	8	3	8	3	8	3	8	3	8
PLASMID	PROTEIN																								
NP	GFP	428	254	338	97	610	912	651	200	444	316	370	175	349	657	223	348	307	479	118	260	7	13	3	3
		485	495	389	108	266	633	82	41	273	136	233	104	289	254	253	320	348	515	141	299	8	15	3	3
pEVOL	GFP	456	641	399	467	960	1050	775	935	607	685	592	486	585	912	744	585	535	551	393	484	732	1023	802	765
		234	363	178	71	101	340	250	99	285	192	117	323	461	357	274	284	88	140	150	97	244	155	163	68
pOFX	GFP	785	1186	552	665	815	989	432	594	705	1098	457	616	764	1158	642	766	770	952	456	562	757	983	569	653
		32	71	49	62	66	156	217	132	210	185	137	209	117	160	142	55	43	98	70	73	46	121	43	66
pEVOL+RS	pPaGFP	28	51	9	17	78	113	58	64	73	92	47	59	71	111	73	68	52	83	47	50	77	129	97	114
		15	25	13	21	23	28	21	34	27	19	16	26	24	19	50	29	28	57	52	43	20	44	34	33
pEVOL	pPaGFP	9	14	9	11	17	29	19	21	13	19	13	20	15	21	17	30	15	25	15	24	15	25	16	22
		6	7	9	6	5	12	8	11	4	6	6	13	5	3	4	11	7	13	8	16	4	11	8	13
NP	CalB Tot	101	135	48	136	395	626	345	360	89	148	30	21	141	228	49	66	145	182	91	101	123	197	71	102
		99	121	72	25	124	71	72	253	36	21	7	5	11	26	19	36	42	41	29	40	45	108	14	44
NP	CalB Sol	36	17	54	7	113	41	36	24	39	28	25	8	49	41	19	11	41	27	25	11	41	37	33	18
		40	17	89	5	45	8	13	12	14	2	4	2	2	5	2	3	5	3	4	3	2	4	2	7
pOFX	CalB Tot	373	455	353	434	170	237	195	312	139	227	181	193	380	478	394	429	328	405	315	383	338	485	421	451
		26	49	42	36	182	269	215	361	146	258	192	218	22	227	113	54	83	58	115	23	68	91	50	32
pOFX	CalB Sol	342	336	307	172	152	197	118	87	130	174	140	150	372	285	282	174	296	301	248	270	282	314	331	162
		42	62	33	8	160	225	123	95	137	197	150	177	55	78	29	41	59	34	47	55	43	48	39	26

Figure 10-1 - Cell-free Protein Synthesis Yields in µg Protein per mL Cell-free Reaction. Average yields (µg/mL) of n_{Total}=4 reactions ($n_{extracts}$=2, n_{eCFPS}=2) is given in large font with one standard deviation given in small font. Protein yields have been colorized as with higher yields corresponding to darker shades of color as follows: GFP=blue, pPaGFP=red, and CalB=Green.

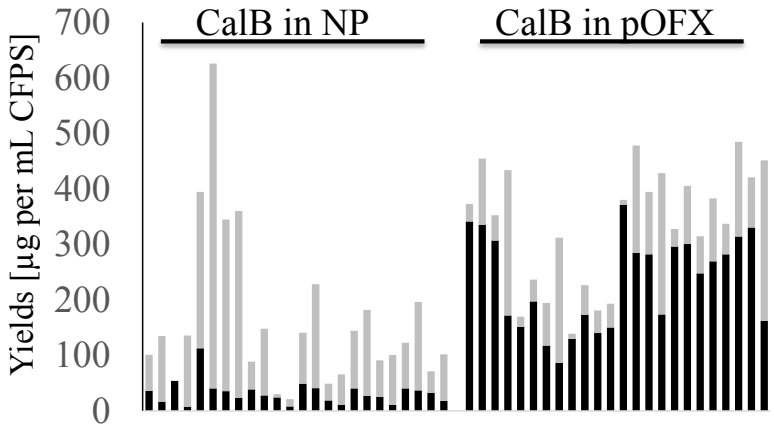

Figure 10-2 - Graphical Soluble and Total Yields for CalB. Average soluble [black] and total [grey] yields (µg/mL) of n_{Total}=4 reactions ($n_{extracts}$=2, n_{eCFPS}=2). Comparing pOFX to the NP [no plasmid] system, the average increase in soluble percentage of CalB is over 350%.

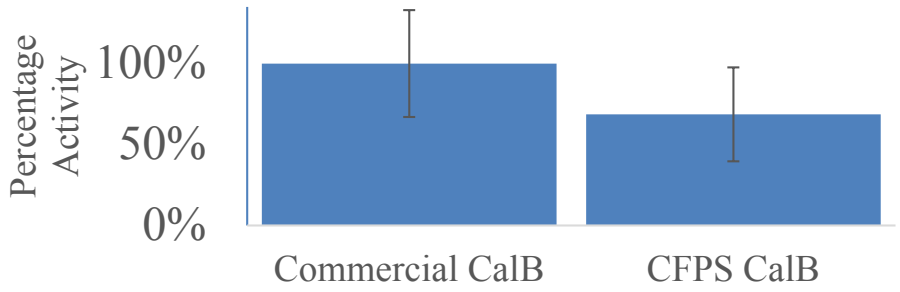

Figure 10-3 - Activity of Commercial and CFPS-produced CalB. The activity of CalB produced in a pOFX extract system was compared to the activity of a commercially available CalB (Sigma Aldrich). Activity was determined using methods previously described, with the following modifications (2). CFPS-produced enzyme was purified via strep-tag affinity, dialyzed against PBS buffer, concentrated in Amicon Ultra concentrators, and quantified using scintillation as described previously (79). Initial concentration of assays were 0.05 mM p-nitrophenol palmitate, 0.14 M Tris-HCl, 0.14 M NaCl, 4% vol/vol ethanol, and 2.4 ng per mL enzyme. The change in absorbance of 405 nm was monitored for 1 hour. n=7 for commercial CalB, n=6 for CFPS CalB. Error bars represent one standard deviation. The activity of the commercial CalB was normalized to 100%.

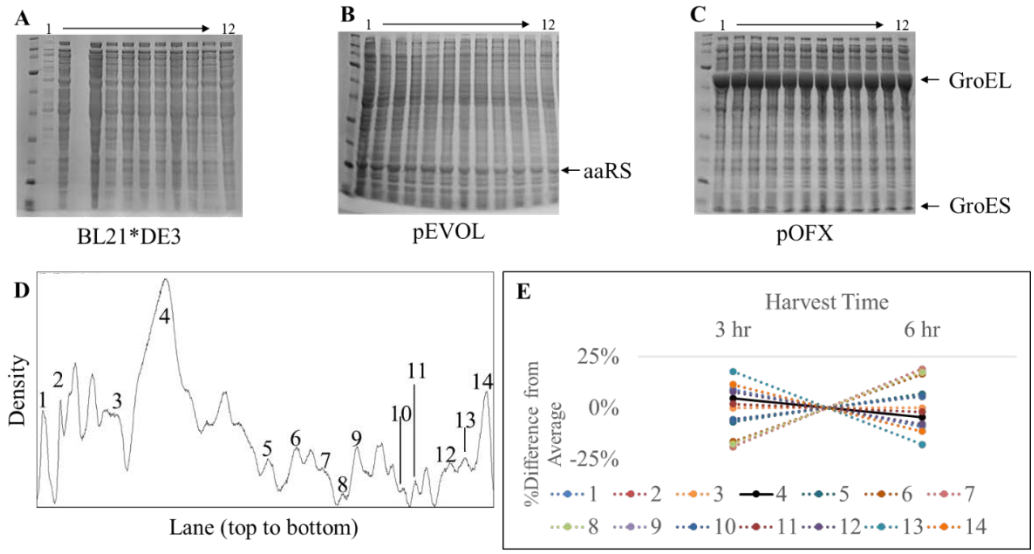

Figure 10-4 - SDS PAGE of Extracts and Example Densitometry. Uniform amounts (0.5 µL each) of the pEVOL and pOFX extracts were analyzed using SDS PAGE on 10% Bis-Tris gels in MOPs-SDS running buffer and ImageJ software (148). The gels of NP (A), pEVOL (B) and pOFX (C) stained with SimplyBlue™ SafeStain (Invitrogen) revealed overexpression of pEVOL and GroEL/ES, respectively. Gel lanes are laid out by harvest time and presence or absence of MOPs during fermentation as follows: Lanes 1-6 were growth without MOPs, lanes 7-12 were grown with MOPs. Lane 1, 2, and 3 are 3, 4.5 and 6 hour harvest, respectively, and this pattern is continued through lane 12. The initial unnumbered lane is the P7710S prestained protein ladder (New England Biolabs). To analyze the protein density at a given molecular weight in each extract, a densitometry map was made for each lane, as exemplified in (D), which represents lane 7 of pOFX. Peaks were selected for analysis across harvest times, such as the peak for GroEL (Peak 4), GroES (Peak 14), and peaks estimated to be associated with the ribosomal proteins (Peaks 10 and 11) (212). Peak intensities were measured and compared across extracts. (E) The graph displays example trends of protein peak intensities within a single fermentation processed at different harvest times, in this case lanes 7 and 9 of pOFX. There is no single or clear trend amongst the different proteins, rather some proteins increase, some decrease, and some remain at approximately the same densities. This lack of distinct trends complicates the identification of direct correlations between individual protein densities and overall extract viability. NOTE: Lane 3 of (A) had no sample loaded.

11 APPENDIX C – SUPPLEMENTARY MATERIAL FOR CHAPTER 5

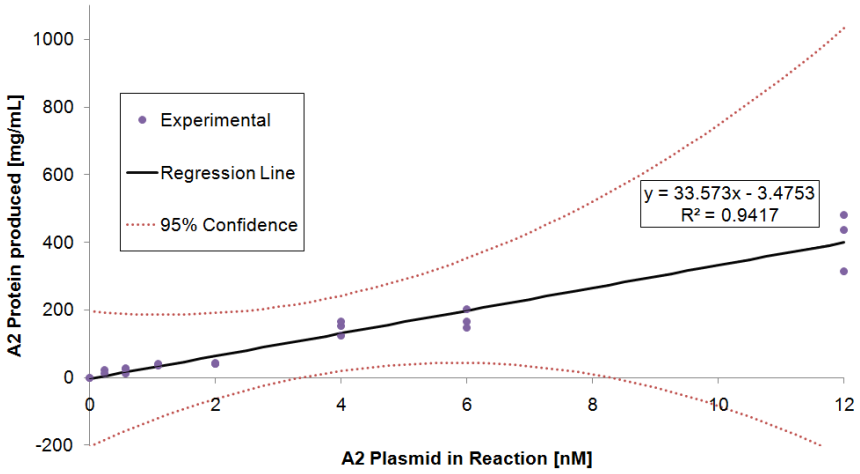

Figure 11-1 - Linear Regression of Total A2 Protein Production Against A2 Plasmid Concentration. The production data of A2 Protein being co-expressed with coat protein. A2 plasmid concentration was varied while the total plasmid concentration (A2 and CP) remained at 12 nM.

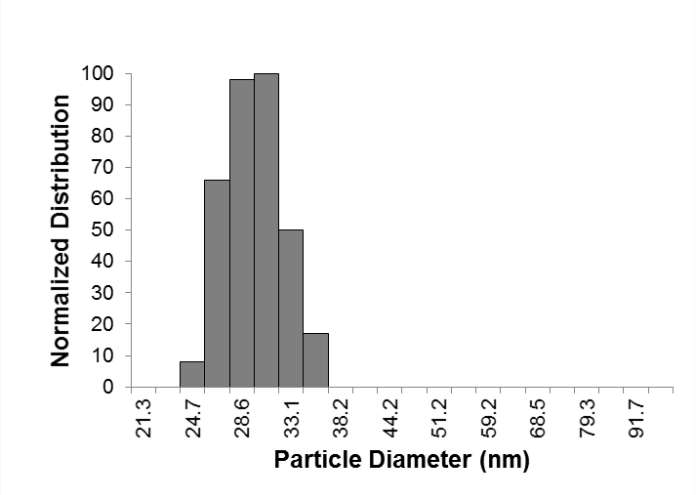

Figure 11-2 - Dynamic Light Scattering Data of the Qβ VLP with A2 incorporated. A 90Plus Particle Size Analyzer was used to measure the diameter of the VLP produced from the CFPS reaction with 1:10 molar ratio of A2:CP plasmids . As illustrated above, the mean diameter was measured as 29.8 nm ± 6.6 nm (n=10 – one minute runs, ± 1 standard deviation).

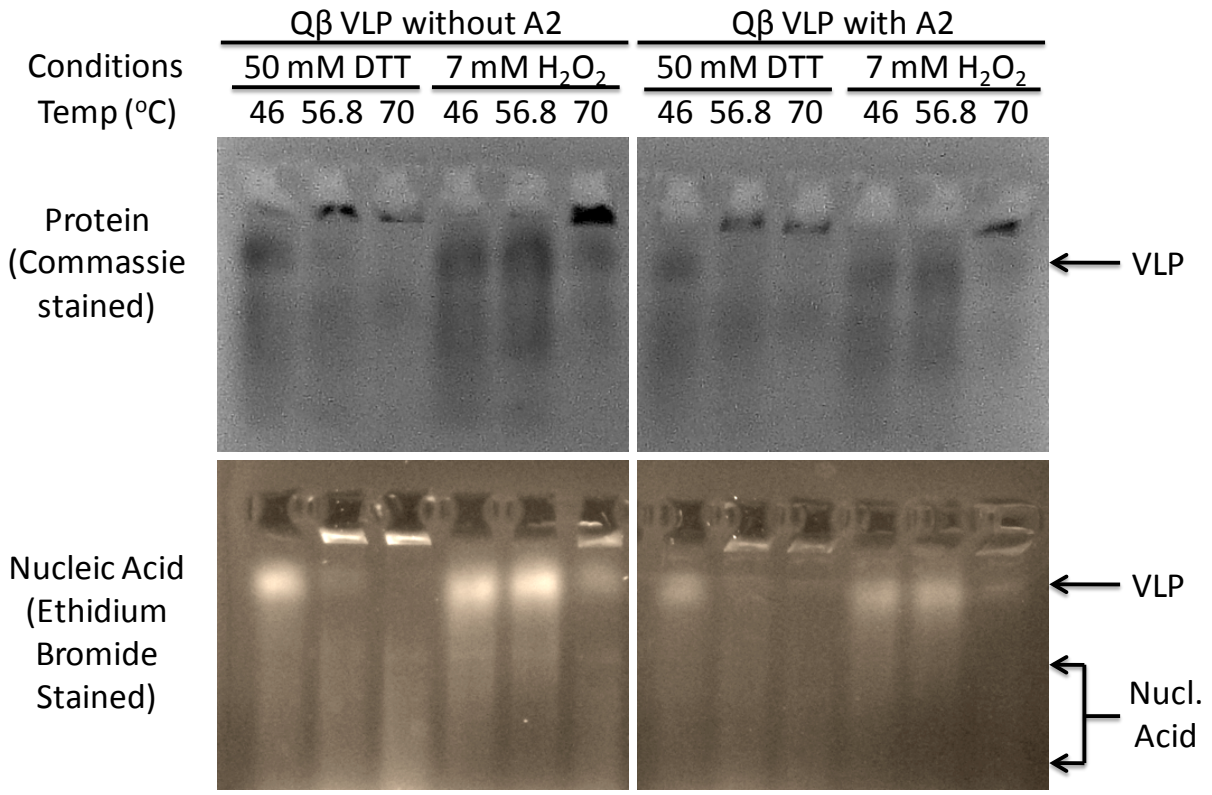

Figure 11-3 - Agarose Gel Electrophoresis of Qβ VLP Demonstrating Thermal Stability. The VLP were produced, assembled, purified and concentrated as described. The A2-protein:Coat-protein plasmid ratios were 0:1 (left) and 1:5 (right). VLP were incubated for 60 mins at room temperature in 50 mM DTT or 7 mM H_2O_2. Reactions were then heated with a thermocycler to 46, 56.8 or 70 °C for 5 mins before being cooled to 4 °C. The 1% agarose gel (0.001% ethidium bromide) was run at a constant 18 volts f7or 2.5 hours before staining with commassie stain.

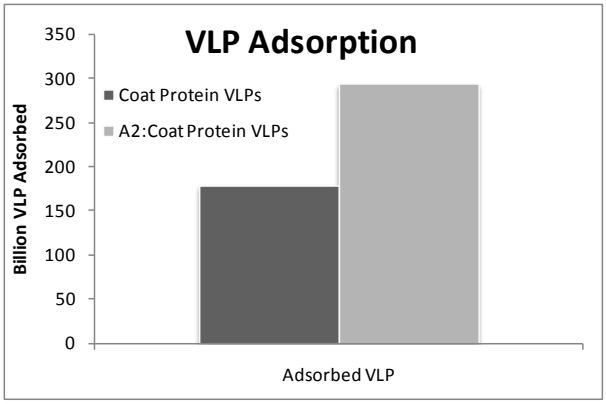

Figure 11-4 - Qβ VLP adsorption onto *E. coli* F pili. VLPs produced, purified, and concentrated as described in *Materials and Methods* at A2:CP plasmid ratios of 0:1 and 1:5. Following the methods for phage adsorption demonstrated previously (Tsukada, et al. *Biochem Biophy J*, 2009), VLP were incubated with excess cells of *E. coli* strain CHS 124 (an F` strain) for 60 mins at 37°C. Samples were then filtered through a syringe-driven 0.2 µm polyvinylidene difluoride membrane filter (ThermoFisher). VLP concentration was quantified using radioactivity measurements.

12 APPENDIX D – SUPPLEMENTARY MATERIAL FOR CHAPTER 6

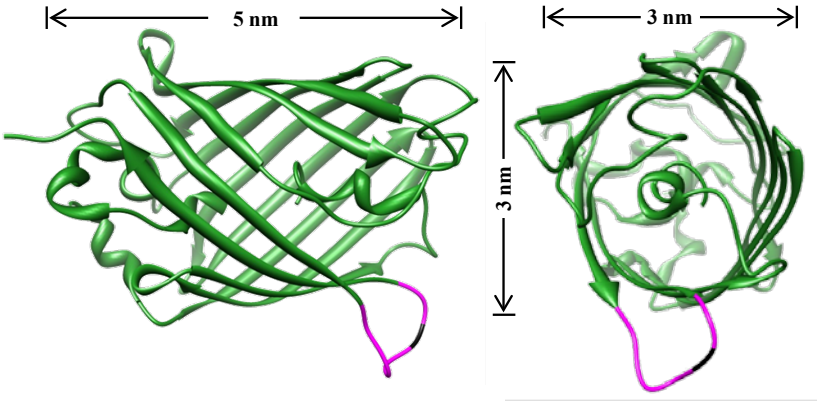

Figure 12-1 - Crystal Structure of sfGFP-related Protein. The potential implications of the residue location for unnatural amino acid incorporation were investigated using the known crystal structure of a superfolder green fluorescent protein variant closely related to the pPaGFP (pdbID 2B3P).(213) In the Fig. S1, the beta-barrel (dark green) is approximated as a cylinder with the loop of interest (pink) extending from the main body. The pink loop contains the location for the unnatural amino acid incorporation (black).

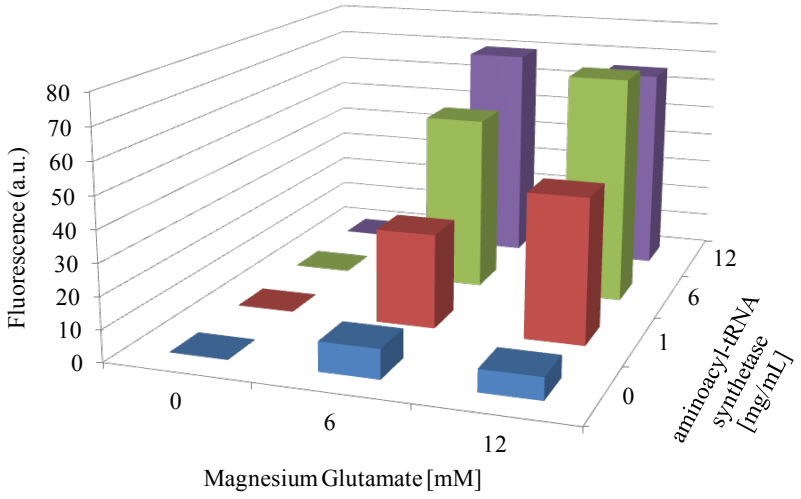

Figure 12-2 - Aminoacyl-tRNA Synthetase Optimization. Cell-free protein synthesis allows for direct access to the synthesis environment, enabling optimization and maximization of synthesis cofactors. To maximize the unnatural amino acid incorporation, the effect of different concentrations of aminoacyl-tRNA synthetase and magnesium glutamate on the production of active pPaGFP was assessed.

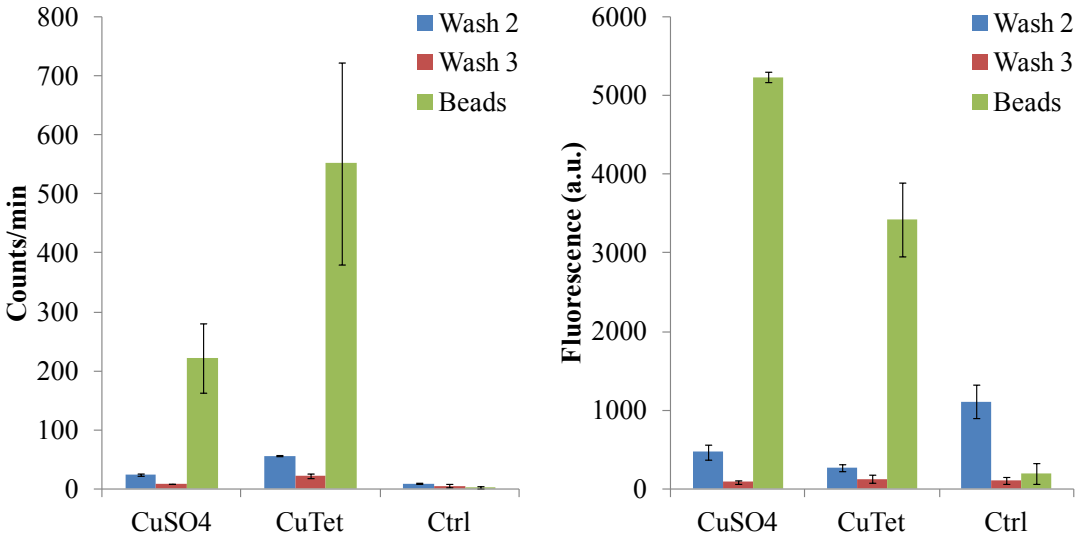

Figure 12-3 - Scintillation and Fluorescence for Washes after pPaGFP Immobilization. To ensure that the proteins were not remaining in solution or non-specifically binding to the magnetic beads, the beads were washed 3 times using a PBS-Tween buffer. Each wash consisted of isolating the magnetic beads, removing the supernatant, and resuspending the beads in 100 µL PBS-Tween buffer. The final suspension (labeled "Beads") was in 100 µL PBS and was vortexed directly prior to analysis for a uniform suspension of beads. Displayed above are the results from liquid scintillation and fluorescence analysis of supernatant from washes 2 and 3, along with the final suspension containing beads. During the washing process, the unclicked pPaGFP was removed to background or statistically insignificant levels. For the control reactions containing no copper, the resuspended beads contained no or insignificant levels of pPaGFP. The prewash and wash 1 results were removed to provide appropriate scaling. Error bars = standard deviation, n=2.

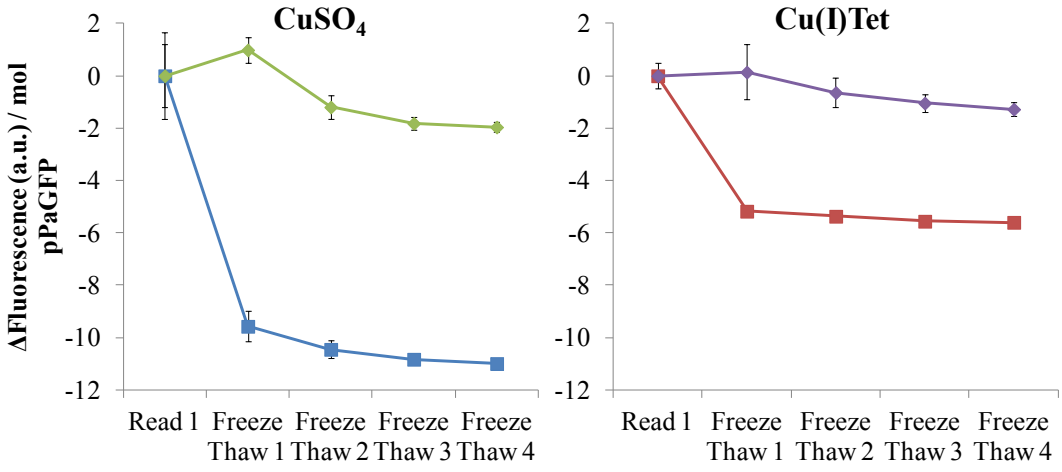

Figure 12-4 - Freeze-thaw Activity for Free pPaGFP in Copper-containing Solutions. Free pPaGFP was incubated under the same conditions as bead-immobilized pPaGFP and then was left in its respective reaction solution. The unbound pPaGFP was subjected to multiple freeze-thaw cycles (squares) or incubated at 4 ºC (diamonds) and assayed for activity. Each freeze-thaw cycle consisted of an incubation for 20 min at -80 ºC followed by a 20 min incubation at room temperature. Samples left unfrozen were maintained at 4 ºC for 40 min between assays. The results suggest that incubation with copper plays little role in terms of stability during freeze-thaw cycles. Error bars = standard deviation, n=2.

REFERENCES

1. **Bundy, B.C., M.J. Franciszkowicz, and J.R. Swartz.** 2008. Escherichia coli-based cell-free synthesis of virus-like particles. Biotechnol Bioeng *100*:28-37.

2. **Park, C.G., T.W. Kim, I.S. Oh, J.K. Song, and D.M. Kim.** 2009. Expression of functional Candida antarctica lipase B in a cell-free protein synthesis system derived from Escherichia coli. Biotechnol Prog *25*:589-593.

3. **Park, N., S.H. Um, H. Funabashi, J. Xu, and D. Luo.** 2009. A cell-free protein-producing gel. Nat Mater *8*:432-437.

4. **Purnick, P.E.M. and R. Weiss.** 2009. The second wave of synthetic biology: from modules to systems. Nat Rev Mol Cell Biol *10*:410-422.

5. **Ahn, J.H., T.J. Kang, and D.M. Kim.** 2008. Tuning the expression level of recombinant proteins by modulating mRNA stability in a cell-free protein synthesis system. Biotechnol Bioeng *101*:422-427.

6. **Sawasaki, T., T. Ogasawara, R. Morishita, and Y. Endo.** 2002. A cell-free protein synthesis system for high-throughput proteomics. Proc Natl Acad Sci U S A *99*:14652-14657.

7. **Shrestha, P., M.T. Smith, and B.C. Bundy.** 2014. Cell-free unnatural amino acid incorporation with alternative energy systems and linear expression templates. New Biotechnol *31*:28-34.

8. **Bundy, B.C. and J.R. Swartz.** 2010. Site-Specific Incorporation of p-Propargyloxyphenylalanine in a Cell-Free Environment for Direct Protein−Protein Click Conjugation. Bioconjug Chem *21*:255-263.

9. **Goerke, A.R. and J.R. Swartz.** 2009. High-level cell-free synthesis yields of proteins containing site-specific non-natural amino acids. Biotechnol Bioeng *102*:400-416.

10. **Liu, D.V., J.F. Zawada, and J.R. Swartz.** 2005. Streamlining Escherichia Coli S30 Extract Preparation for Economical Cell-Free Protein Synthesis. Biotechnol Prog *21*:460-465.

11. **Ozawa, K., K.V. Loscha, K.V. Kuppan, C.T. Loh, N.E. Dixon, and G. Otting.** 2012. High-yield cell-free protein synthesis for site-specific incorporation of unnatural amino acids at two sites. Biochem Biophys Res Commun *418*:652-656.

12.**Park, C.G., M.A. Kwon, J.K. Song, and D.M. Kim.** 2011. Cell-free synthesis and multifold screening of Candida antarctica lipase B (CalB) variants after combinatorial mutagenesis of hot spots. Biotechnol Prog *27*:47-53.

13.**Calhoun, K.A. and J.R. Swartz.** 2005. Energizing cell-free protein synthesis with glucose metabolism. Biotechnology and Bioengineering *90*:606-613.

14.**Calhoun, K.A. and J.R. Swartz.** 2007. Energy Systems for ATP Regeneration in Cell-Free Protein Synthesis Reactions, p. 3-17. *In* G. Grandi (Ed.), Methods in Molecular Biology. Humana Press, Totowa, NJ.

15.**Jewett, M.C. and J.R. Swartz.** 2004. Mimicking the Escherichia coli cytoplasmic environment activates long-lived and efficient cell-free protein synthesis. Biotechnol Bioeng *86*:19-26.

16.**Kim, H.-C., T.-W. Kim, and D.-M. Kim.** 2011. Prolonged production of proteins in a cell-free protein synthesis system using polymeric carbohydrates as an energy source. Process Biochem *46*:1366-1369.

17.**Swartz, J.R.** 2012. Transforming biochemical engineering with cell-free biology. AIChE J *58*:5-13.

18.**Zawada, J.F., G. Yin, A.R. Steiner, J. Yang, A. Naresh, S.M. Roy, D.S. Gold, H.G. Heinsohn, and C.J. Murray.** 2011. Microscale to manufacturing scale-up of cell-free cytokine production—a new approach for shortening protein production development timelines. Biotechnol Bioeng *108*:1570-1578.

19.**Smith, M.T., C.T. Varner, D.B. Bush, and B.C. Bundy.** 2012. The incorporation of the A2 protein to produce novel Qβ virus-like particles using cell-free protein synthesis. Biotechnol Prog *28*:549-555.

20.**Smith, M.T., J.C. Wu, C.T. Varner, and B.C. Bundy.** 2013. Enhanced protein stability through minimally invasive, direct, covalent, and site-specific immobilization. Biotechnol Prog *29*:247-254.

21.**Kim, T.W., J.W. Keum, I.S. Oh, C.Y. Choi, C.G. Park, and D.M. Kim.** 2006. Simple procedures for the construction of a robust and cost-effective cell-free protein synthesis system. J Biotechnol *126*:554-561.

22.**Ahn, J.-H., H.-S. Chu, T.-W. Kim, I.-S. Oh, C.-Y. Choi, G.-H. Hahn, C.-G. Park, and D.-M. Kim.** 2005. Cell-free synthesis of recombinant proteins from PCR-amplified genes at a comparable productivity to that of plasmid-based reactions. Biochem Biophy Res Commun *338*:1346-1352.

23.**Sun, Z.Z., E. Yeung, C.A. Hayes, V. Noireaux, and R.M. Murray.** 2013. Linear DNA for rapid prototyping of synthetic biological circuits in an Escherichia coli based TX-TL cell-free system. ACS synthetic biology **Article ASAP**.

24.**Fallah-Araghi, A., J.-C. Baret, M. Ryckelynck, and A.D. Griffiths.** 2012. A completely in vitro ultrahigh-throughput droplet-based microfluidic screening system for protein engineering and directed evolution. Lab Chip *12*:882-891.

25.**Klammt, C., D. Schwarz, V. Dötsch, and F. Bernhard.** 2007. Cell-Free Production of Integral Membrane Proteins on a Preparative Scale, p. 57-78. *In* G. Grandi (Ed.), In Vitro Transcription and Translation Protocols. Humana Press.

26.**Neuman, B.W., D.A. Stein, A.D. Kroeker, A.D. Paulino, H.M. Moulton, P.L. Iversen, and M.J. Buchmeier.** 2004. Antisense Morpholino-Oligomers Directed against the 5′ End of the Genome Inhibit Coronavirus Proliferation and Growth†. J Virol *78*:5891-5899.

27.**Oh, I.-S., J.-C. Lee, M.-s. Lee, J.-h. Chung, and D.-M. Kim.** 2010. Cell-free production of functional antibody fragments. Bioprocess Biosyst Eng *33*:127-132.

28.**Lee, S.H., Y.-C. Kwon, D.-M. Kim, and C.B. Park.** 2013. Cytochrome P450-catalyzed O-dealkylation coupled with photochemical NADPH regeneration. Biotechnol Bioeng *110*:383-390.

29.**Woodrow, K.A., I.O. Airen, and J.R. Swartz.** 2006. Rapid expression of functional genomic libraries. J Proteome Res *5*:3288-3300.

30.**Woodrow, K.A. and J.R. Swartz.** 2007. A sequential expression system for high-throughput functional genomic analysis. PROTEOMICS *7*:3870-3879.

31.**Klammt, C., F. Löhr, B. Schäfer, W. Haase, V. Dötsch, H. Rüterjans, C. Glaubitz, and F. Bernhard.** 2004. High level cell-free expression and specific labeling of integral membrane proteins. Eur J Biochem *271*:568-580.

32.**Avenaud, P., M. Castroviejo, S. Claret, J. Rosenbaum, F. Mégraud, and A. Ménard.** 2004. Expression and activity of the cytolethal distending toxin of Helicobacter hepaticus. Biochem Biophys Res Commun *318*:739-745.

33.**Hodgman, C.E. and M.C. Jewett.** 2012. Cell-free synthetic biology: Thinking outside the cell. Metab Eng *14*:261-269.

34.**Arnaz, K.R., J.C. Wu, B.C. Bundy, and M.C. Jewett.** 2013. Transforming Synthetic Biology with Cell-free Systems., p. 277-301. *In* H. Zhao (Ed.), Synthetic Biology: Tools and Applications. Academic Press, Waltham, MA.

35.**Carlson, E.D., R. Gan, C.E. Hodgman, and M.C. Jewett.** 2012. Cell-free protein synthesis: Applications come of age. Biotechnol Adv *30*:1185-1194.

36.**Smith, M.T., A.K. Hawes, P. Shrestha, J.M. Rainsdon, J.C. Wu, and B.C. Bundy.** 2013. Alternative fermentation conditions for improved Escherichia coli-based cell-free protein synthesis for proteins requiring supplemental components for proper synthesis. Process Biochem *49*:217-222.

37.**Mureev, S., O. Kovtun, U.T. Nguyen, and K. Alexandrov.** 2009. Species-independent translational leaders facilitate cell-free expression. Nat Biotechnol *27*:747-752.

38.**Albayrak, C. and J.R. Swartz.** 2013. Cell-free co-production of an orthogonal transfer RNA activates efficient site-specific non-natural amino acid incorporation. Nucleic Acids Res *41*:5949-5963.

39.**Boyer, M.E., J.A. Stapleton, J.M. Kuchenreuther, C.-w. Wang, and J.R. Swartz.** 2008. Cell-free synthesis and maturation of [FeFe] hydrogenases. Biotechnol Bioeng *99*:59-67.

40.**Kubick, S., J. Schacherl, H. Fleischer-Notter, E. Royall, L.O. Roberts, and W. Stiege.** 2003. In Vitro Translation in an Insect-Based Cell-Free System, p. 209-217. *In* J. Swartz (Ed.), Cell-Free Protein Expression. Springer Berlin Heidelberg.

41.**Kigawa, T., T. Yabuki, N. Matsuda, T. Matsuda, R. Nakajima, A. Tanaka, and S. Yokoyama.** 2004. Preparation of Escherichia coli cell extract for highly productive cell-free protein expression. J Struct Funct Genomics *5*:63-68.

42.**Ma, R., Z. Yang, L. Huang, X. Zhu, L. Kai, J. Cai, X. Wang, and Z. Xu.** 2010. Construction of an efficient Escherichia coli cell-free system for in vitro expression of several kinds of proteins. Eng Life Sci *10*:333-338.

43.**Shimizu, Y., A. Inoue, Y. Tomari, T. Suzuki, T. Yokogawa, K. Nishikawa, and T. Ueda.** 2001. Cell-free translation reconstituted with purified components. Nat Biotechnol *19*:751-755.

44.**Endo, Y. and T. Sawasaki.** 2006. Cell-free expression systems for eukaryotic protein production. Curr Opin Biotechnol *17*:373-380.

45.**Madono, M., T. Sawasaki, R. Morishita, and Y. Endo.** 2011. Wheat germ cell-free protein production system for post-genomic research. New Biotechnol *28*:211-217.

46.**Martin, G., R. Kawaguchi, Y. Lam, A. DeGiovanni, M. Fukushima, and W. Mutter.** 2001. High-yield, in vitro protein expression using a continuous-exchange, coupled transcription/translation system. Biotechniques *31*:948-953.

47.**Kaiser, L., J. Graveland-Bikker, D. Steuerwald, M. Vanberghem, K. Herlihy, and S. Zhang.** 2008. Efficient cell-free production of olfactory receptors: detergent optimization, structure, and ligand binding analyses. Proc Natl Acad Sci U S A *105*:15726-15731.

48.**Blesneac, I., S. Ravaud, C. Juillan-Binard, L.-A. Barret, M. Zoonens, A. Polidori, B. Miroux, B. Pucci, and E. Pebay-Peyroula.** 2012. Production of UCP1 a membrane protein from the inner mitochondrial membrane using the cell free expression system in the presence of a fluorinated surfactant. Biochim Biophys Acta -Biomembranes *1818*:798-805.

49.**Shrestha, P., T.M. Holland, and B.C. Bundy.** 2012. Streamlined extract preparation for Escherichia coli-based cell-free protein synthesis by sonication or bead vortex mixing. Biotechniques *53*:163-174.

50.**Kim, T.-W., H.-C. Kim, I.-S. Oh, and D.-M. Kim.** 2008. A highly efficient and economical cell-free protein synthesis system using the S12 extract of <i>Escherichia coli</i&gt. Biotechnol Bioprocess Eng *13*:464-469.

51.**Wang, W.** 2000. Lyophilization and development of solid protein pharmaceuticals. Int J Pharm *203*:1-60.

52.**Albayrak, C. and J.R. Swartz.** 2013. Using E. coli-based cell-free protein synthesis to evaluate the kinetic performance of an orthogonal tRNA and aminoacyl-tRNA synthetase pair. Biochem Biophys Res Commun *431*:291-295.

53.**Ahn, J.H., C.Y. Choi, and D.M. Kim.** 2005. Effect of energy source on the efficiency of translational termination during cell-free protein synthesis. Biochem Biophys Res Commun *337*:325-329.

54.**Harris, D.C. and M.C. Jewett.** 2012. Cell-free biology: exploiting the interface between synthetic biology and synthetic chemistry. Curr Opin Biotechnol *23*:672-678.

55.**Rollin, J.A., T.K. Tam, and Y.H.P. Zhang.** 2013. New biotechnology paradigm: cell-free biosystems for biomanufacturing. Green Chemistry *15*:1708-1719.

56.**Yang, J., G. Kanter, A. Voloshin, N. Michel-Reydellet, H. Velkeen, R. Levy, and J.R. Swartz.** 2005. Rapid expression of vaccine proteins for B-cell lymphoma in a cell-free system. Biotechnol Bioeng *89*:503-511.

57.**Patel, K.G., P.P. Ng, S. Levy, R. Levy, and J.R. Swartz.** 2011. Escherichia coli-based production of a tumor idiotype antibody fragment – tetanus toxin fragment C fusion protein vaccine for B cell lymphoma. Protein Expr Purif *75*:15-20.

58.**Matsuda, T., S. Furumoto, K. Higuchi, J. Yokoyama, M.-R. Zhang, K. Yanai, R. Iwata, and T. Kigawa.** 2012. Rapid biochemical synthesis of 11C-labeled single chain variable fragment antibody for immuno-PET by cell-free protein synthesis. Bioorgan Med Chem *20*:6579-6582.

59.**Chandra, H. and S. Srivastava.** 2010. Cell-free synthesis-based protein microarrays and their applications. PROTEOMICS *10*:717-730.

60.**Stapleton, J.A. and J.R. Swartz.** 2010. A Cell-Free Microtiter Plate Screen for Improved [FeFe] Hydrogenases. PLoS ONE *5*:e10554.

61.**Jewett, M.C., K.A. Calhoun, A. Voloshin, J.J. Wuu, and J.R. Swartz.** 2008. An integrated cell-free metabolic platform for protein production and synthetic biology. Mol Syst Biol *4*:220.

62.**Zhang, Y.H.P.** 2010. Production of biocommodities and bioelectricity by cell-free synthetic enzymatic pathway biotransformations: Challenges and opportunities. Biotechnol Bioeng *105*:663-677.

63.**Billerbeck, S., J. Härle, and S. Panke.** 2013. The good of two worlds: increasing complexity in cell-free systems. Curr Opin Biotechnol *24*:1037-1043.

64.**Meyer, A., R. Pellaux, and S. Panke.** 2007. Bioengineering novel in vitro metabolic pathways using synthetic biology. Curr Opin Microbiology *10*:246-253.

65.**Zubay, G.** 1973. In vitro synthesis of protein in microbial systems. Annu Rev Genet *7*:267-287.

66.**Calhoun, K.A. and J.R. Swartz.** 2005. An Economical Method for Cell-Free Protein Synthesis using Glucose and Nucleoside Monophosphates. Biotechnol Prog *21*:1146-1153.

67.**Yang, W.C., K.G. Patel, H.E. Wong, and J.R. Swartz.** 2012. Simplifying and streamlining Escherichia coli-based cell-free protein synthesis. Biotechnol Prog *28*:413-420.

68.**Schwarz, D., F. Junge, F. Durst, N. Frolich, B. Schneider, S. Reckel, S. Sobhanifar, V. Dotsch, and F. Bernhard.** 2007. Preparative scale expression of membrane proteins in Escherichia coli-based continuous exchange cell-free systems. Nat Protoc *2*:2945-2957.

69.**Kim, T.W., D.M. Kim, and C.Y. Choi.** 2006. Rapid production of milligram quantities of proteins in a batch cell-free protein synthesis system. J Biotechnol *124*:373-380.

70.**Zheng, Q., R. Shi, X. Zhu, L. Huang, J. Cai, W. Han, and Z. Xu.** 2012. Functional expression of Bacillus subtilis xylanase A in an Escherichia coli derived cell-free protein synthesis system and subsequent expression improvement via DNA gel technique. Process Biochem *47*:1186-1191.

71.**Chang, D.-E., D.J. Smalley, and T. Conway.** 2002. Gene expression profiling of Escherichia coli growth transitions: an expanded stringent response model. Mol Microbiol *45*:289-306.

72.**Seo, J.-H. and J.E. Bailey.** 1985. Effects of recombinant plasmid content on growth properties and cloned gene product formation in Escherichia coli. Biotechnol Bioeng *27*:1668-1674.

73.**Lee, C.L., D.S.W. Ow, and S.K.W. Oh.** 2006. Quantitative real-time polymerase chain reaction for determination of plasmid copy number in bacteria. J Microbiol Methods *65*:258-267.

74.**Grabherr, R., E. Nilsson, G. Striedner, and K. Bayer.** 2002. Stabilizing plasmid copy number to improve recombinant protein production. Biotechnol Bioeng *77*:142-147.

75.**Swartz, J.R.** 2001. Advances in Escherichia coli production of therapeutic proteins. Curr Opin Biotechnol *12*:195-201.

76.**Yamagishi, M., H. Matsushima, A. Wada, M. Sakagmi, N. Fujita, and A. Ishihama.** 1993. Regulation of the Esherichia coli rmf gene encoding the ribosome modulation factor: growth phase- and growth rate-dependent control. EMBO J *12*:625-630.

77.**Young, T.S., I. Ahmad, J.A. Yin, and P.G. Schultz.** 2010. An Enhanced System for Unnatural Amino Acid Mutagenesis in E. coli. J Mol Biol *395*:361-374.

78.**Bundy, B.C. and J.R. Swartz.** 2011. Efficient disulfide bond formation in virus-like particles. J Biotechnol *154*:230-239.

79.**Jewett, M.C. and J.R. Swartz.** 2004. Rapid expression and purification of 100 nmol quantities of active protein using cell-free protein synthesis. Biotechnol Prog *20*:102-109.

80.**Cheah, U.E., W.A. Weigand, and B.C. Stark.** 1987. Effects of recombinant plasmid size on cellular processes in Escherichia coli. Plasmid *18*:127-134.

81.**Glick, B.R.** 1995. Metabolic load and heterologous gene expression. Biotechnol Adv *13*:247-261.

82.**Benveniste, R. and J. Davies.** 1973. Mechanisms of Antibiotic Resistance in Bacteria. Annu Rev Biochem *42*:471-506.

83.**Hickey, E.W. and I.N. Hirshfield.** 1990. Low-pH-induced effects on patterns of protein synthesis and on internal pH in Escherichia coli and Salmonella typhimurium. Appl Environ Microbiol *56*:1038-1045.

84.**Small, P., D. Balnkenhorn, D. Welty, E. Zinser, and J.L. Slonczewski.** 1994. Acid and base resistance in Escherichia coli and Shingella flexneri: role of rpoS and growth pH. J Bacteriol *176*:1729-1737.

85.**de Quadros, C.A., J.K. Andrus, J.-M. Olive, C.G. de Macedo, and D.A. Henderson.** 1992. Polio Eradication From the Western Hemisphere. Annual Review of Public Health *13*:239-252.

86.**Henderson, D.A. and P. Klepac.** 2013. Lessons from the eradication of smallpox: an interview with D. A. Henderson. Philosophical Transactions of the Royal Society B: Biological Sciences *368*.

87.**Grubman, M.J. and B. Baxt.** 2004. Foot-and-Mouth Disease. Clin Microbiol Rev *17*:465-493.

88.**Keith Sumption, J.P., Juan Lubroth, Subhash Morzaria, Tom Murray, Stephane De La Rocque, Feliz Njeumi.** 2007. Foot-and-Mouth Disease Situation worldwide and major epidemiological events in 2005-2006, p. 11.

89.**Reid, S.M., N.P. Ferris, G.H. Hutchings, Z. Zhang, G.J. Belsham, and S. Alexandersen.** 2002. Detection of all seven serotypes of foot-and-mouth disease virus by real-time, fluorogenic reverse transcription polymerase chain reaction assay. J Virol Met *105*:67-80.

90.**Domingo, E., C. Escarmis, M. Martinez, E. Martinez-Salas, and M. Mateu.** 1992. Foot-and-mouth disease virus populations are quasispecies, p. 33-47. Genetic Diversity of RNA Viruses. Springer.

91.**Animals, M.o.D.T.a.V.f.T.** 2009. Foot and Mouth Disease.

92.**Yoon, H., S. Yoon, S. Wee, Y. Kim, and B. Kim.** 2012. Clinical Manifestations of Foot-and-Mouth Disease During the 2010/2011 Epidemic in the Republic of Korea. Transboundary and Emerging Diseases *59*:517-525.

93.**Kitching, R. and G. Hughes.** 2002. Clinical variation in foot and mouth disease: sheep and goats. Revue Scientifique Et Technique-Office International Des Epizooties *21*:505-510.

94.**Alexandersen, S., Z. Zhang, A.I. Donaldson, and A.J.M. Garland.** 2003. The Pathogenesis and Diagnosis of Foot-and-Mouth Disease. J Comp Pathology *129*:1-36.

95.**Morgan, E.R., M. Lundervold, G.F. Medley, B.S. Shaikenov, P.R. Torgerson, and E.J. Milner-Gulland.** 2006. Assessing risks of disease transmission between wildlife and livestock: The Saiga antelope as a case study. Biological Conservation *131*:244-254.

96.**Cottam, E.M., J. Wadsworth, A.E. Shaw, R.J. Rowlands, L. Goatley, S. Maan, N.S. Maan, P.P. Mertens, et al.** 2008. Transmission pathways of foot-and-mouth disease virus in the United Kingdom in 2007. PLoS Pathogens *4*:e1000050.

97.**Ryan, E., D. Mackay, and A. Donaldson.** 2008. Foot-and-Mouth Disease Virus Concentrations in Products of Animal Origin. Transboundary and emerging diseases *55*:89-98.

98.**Salt, J.** 1993. The carrier state in foot and mouth disease—an immunological review. British Veterinary Journal *149*:207-223.

99.**Charleston, B., B.M. Bankowski, S. Gubbins, M.E. Chase-Topping, D. Schley, R. Howey, P.V. Barnett, D. Gibson, et al.** 2011. Relationship between clinical signs and transmission of an infectious disease and the implications for control. Science *332*:726-729.

100.**Scudamore, J.** 2002. Origin of the UK foot and mouth disease epidemic in 2001. Department of Environment, Food and Rural Affairs, London, United Kingdom.

101.**Lombard, M., P. Pastoret, and A. Moulin.** 2007. A brief history of vaccines and vaccination. Revue Scientifique et Technique-Office International des Epizooties *26*:29.

102.**Mahy, B.W.** 2005. Introduction and history of foot-and-mouth disease virus, p. 1-8. Foot-and-Mouth Disease Virus. Springer.

103.**Rodriguez, L.L. and M.J. Grubman.** 2009. Foot and mouth disease virus vaccines. Vaccine *27, Supplement 4*:D90-D94.

104.**Parida, S.** 2009. Vaccination against foot-and-mouth disease virus: strategies and effectiveness. Expert Rev Vaccines *8*:347-365.

105.**Bank, I.W.o.F.V.** 2006. Requirements for Vaccines and Diagnostic Biologicals p. 51-57. FMD and CSF Coordination Action, Pirbright, United Kingdom.

106.**Barnett, P., J. Bashiruddin, J. Hammond, D. Geale, and D. Paton.** 2010. Toward a global foot and mouth disease vaccine bank network. Revue scientifique et technique (International Office of Epizootics) *29*:593-602.

107.**Lombard, M. and A. Füssel.** 2007. Antigen and vaccine banks: technical requirements and the role of the european antigen bank in emergency foot and mouth disease vaccination. Revue scientifique et technique (International Office of Epizootics) *26*:117-134.

108.2008. Guidelines for International Standars for Vaccine Banks, p. 115-119. OIE Terrestrial Manual 2008. Office International des Epizooties, Paris, France.

109.**Forman, A. and A. Garland.** 2002. Foot and mouth disease: the future of vaccine banks. Revue scientifique et technique-Office international des épizooties *21*:601-608.

110.**Rieder, E., T. Henry, H. Duque, and B. Baxt.** 2005. Analysis of a foot-and-mouth disease virus type A24 isolate containing an SGD receptor recognition site in vitro and its pathogenesis in cattle. J Virol *79*:12989-12998.

111.**Bolwell, C., A. Brown, P. Barnett, R. Campbell, B. Clarke, N. Parry, E. Ouldridge, F. Brown, and D. Rowlands.** 1989. Host cell selection of antigenic variants of foot-and-mouth disease virus. J General Virol *70*:45-57.

112.**Doel, T.** 2005. Natural and vaccine induced immunity to FMD, p. 103-131. Foot-and-mouth disease virus. Springer.

113.**Barnett, P. and R. Statham.** 1998. Long term stability and potency of antigen concentrates held by the International Vaccine Bank, European Commission for the Control of Foot-and-Mouth Disease. Research Group of the Standing Technical Committee, Aldershot (United Kingdom), 14-18 Sep 1998. FAO.

114.**Liu, F., S. Ge, L. Li, X. Wu, Z. Liu, and Z. Wang.** 2012. Virus-like particles: potential veterinary vaccine immunogens. Res Vet Sci *93*:553-559.

115.**Sáiz, M., J.I. Núñez, M.A. Jimenez-Clavero, E. Baranowski, and F. Sobrino.** 2002. Foot-and-mouth disease virus: biology and prospects for disease control. Microbes and Infection *4*:1183-1192.

116.**Kitching, R.P.** 1999. Foot-and-mouth disease: current world situation. Vaccine *17*:1772-1774.

117.**Zheng, H., J. Guo, Y. Jin, F. Yang, J. He, L. Lv, K. Zhang, Q. Wu, et al.** 2013. Engineering Foot-and-Mouth Disease Viruses with Improved Growth Properties for Vaccine Development. PLoS ONE *8*:e55228.

118.**Uddowla, S., J. Hollister, J.M. Pacheco, L.L. Rodriguez, and E. Rieder.** 2012. A safe foot-and-mouth disease vaccine platform with two negative markers for differentiating infected from vaccinated animals. J Virol *86*:11675-11685.

119.**Hua Tang, X.-S.L., Yu-Zhen Fang, Li Pan, Zhong-Wang Zhang, Peng Zhou, Jian-Liang LV, Shou-Tian Jiang, Wen-Fa Hu, Pan Zhang, Yong-Lu Wang, Yong-Guang Zhang.** 2012. Advances in Studies on Vaccines of Foot-and-mouth Disease. Asian Journal of Animal and Veterinary Advances:1245-1254.

120.**Grubman, M.J., M.P. Moraes, C. Schutta, J. Barrera, J. Neilan, D. Ettyreddy, B.T. Butman, D.E. Brough, and D.A. Brake.** 2010. Adenovirus serotype 5-vectored foot-and-mouth disease subunit vaccines: the first decade. Future Virology *5*:51-64.

121.**Grubman, M.J., F. Diaz-San Segundo, C.C. Dias, M.P. Moraes, E. Perez-Martin, and T. de los Santos.** 2012. Use of replication-defective adenoviruses to develop vaccines and biotherapeutics against foot-and-mouth disease. Future Virology *7*:767-778.

122.**Liang, Z., Z. Jie, C. Hao-tai, and Z. Jian-hua.** 2011. Research in advance for FMD Novel Vaccines. Virol J *8*:268-274.

123.2008. Protein production and purification. Nat Meth *5*:135-146.

124.**Demain, A.L. and P. Vaishnav.** 2009. Production of recombinant proteins by microbes and higher organisms. Biotechnol Adv *27*:297-306.

125.**Chu, L. and D.K. Robinson.** 2001. Industrial choices for protein production by large-scale cell culture. Curr Opin Biotechnol *12*:180-187.

126.**Genji, T., A. Nozawa, and Y. Tozawa.** 2010. Efficient production and purification of functional bacteriorhodopsin with a wheat-germ cell-free system and a combination of Fos-choline and CHAPS detergents. Biochem Biophys Res Commun *400*:638-642.

127.**Knapp, K.G., A.R. Goerke, and J.R. Swartz.** 2007. Cell-free synthesis of proteins that require disulfide bonds using glucose as an energy source. Biotechnol Bioeng *97*:901-908.

128.**Kigawa, T., E. Yamaguchi-Nunokawa, K. Kodama, T. Matsuda, T. Yabuki, N. Matsuda, R. Ishitani, O. Nureki, and S. Yokoyama.** 2002. Selenomethionine incorporation into a protein by cell-free synthesis. J Struct Funct Genomics *2*:29-35.

129.**Yabuki, T., Y. Motoda, K. Hanada, E. Nunokawa, M. Saito, E. Seki, M. Inoue, T. Kigawa, and S. Yokoyama.** 2007. A robust two-step PCR method of template DNA production for high-throughput cell-free protein synthesis. J Struct Funct Genomics *8*:173-191.

130.**Wu, M., W.L. Brown, and P.G. Stockley.** 1995. Cell-specific delivery of bacteriophage-encapsidated ricin A chain. Bioconjug Chem *6*:587-595.

131.**Ewers, H., A.E. Smith, I.F. Sbalzarini, H. Lilie, P. Koumoutsakos, and A. Helenius.** 2005. Single-particle tracking of murine polyoma virus-like particles on live cells and artificial membranes. Proc Natl Acad Sci U S A *102*:15110-15115.

132.**Nam, K.T., D.W. Kim, P.J. Yoo, C.Y. Chiang, N. Meethong, P.T. Hammond, Y.M. Chiang, and A.M. Belcher.** 2006. Virus-enabled synthesis and assembly of nanowires for lithium ion battery electrodes. Science *312*:885-888.

133.**Bachmann, M.F. and G.T. Jennings.** 2004. Virus-Like Particles: Combining Innate and Adaptive Immunity for Effective Vaccination. Wiley-VCH Verlag GmbH & Co. KGaA.

134.**Lechner, F., A. Jegerlehner, A.C. Tissot, P. Maurer, P. Sebbel, W.A. Renner, G.T. Jennings, and M.F. Bachmann.** 2002. Virus-like particles as a modular system for novel vaccines. Intervirology *45*:212-217.

135.**Kaur, G., M.T. Valarmathi, J.D. Potts, and Q. Wang.** 2008. The promotion of osteoblastic differentiation of rat bone marrow stromal cells by a polyvalent plant mosaic virus. Biomaterials *29*:4078-4081.

136.**Kovacs, E.W., J.M. Hooker, D.W. Romanini, P.G. Holder, K.E. Berry, and M.B. Francis.** 2007. Dual-Surface-Modified Bacteriophage MS2 as an Ideal Scaffold for a Viral Capsid-Based Drug Delivery System. Bioconjug Chem *18*:1140-1147.

137.**Peabody, D.S., B. Manifold-Wheeler, A. Medford, S.K. Jordan, J. do Carmo Caldeira, and B. Chackerian.** 2008. Immunogenic display of diverse peptides on virus-like particles of RNA phage MS2. J Mol Biol *380*:252-263.

138.**Pokorski, J.K. and N.F. Steinmetz.** 2010. The Art of Engineering Viral Nanoparticles. Mol Pharm *8*:29-43.

139.**Takamatsu, H. and K. Iso.** 1982. Chemical evidence for the capsomeric structure of phage q beta. Nature *298*:819-824.

140.**Ashcroft, A.E., H. Lago, J.M. Macedo, W.T. Horn, N.J. Stonehouse, and P.G. Stockley.** 2005. Engineering thermal stability in RNA phage capsids via disulphide bonds. J Nanosci Nanotechnol *5*:2034-2041.

141.**Weiner, A.M. and K. Weber.** 1971. Natural read-through at the UGA termination signal of Q-beta coat protein cistron. Nat New Biol *234*:206-209.

142.**Karnik, S. and M. Billeter.** 1983. The lysis function of RNA bacteriophage Qbeta is mediated by the maturation (A2) protein. EMBO J *2*:1521-1526.

143.**Toropova, K., P.G. Stockley, and N.A. Ranson.** 2011. Visualising a viral RNA genome poised for release from its receptor complex. J Mol Biol *408*:408-419.

144.**Bernhardt, T.G., I.N. Wang, D.K. Struck, and R. Young.** 2001. A protein antibiotic in the phage Qbeta virion: diversity in lysis targets. Science *292*:2326-2329.

145.**Langlais, C.L.** 2007. Understanding the Lytic Function of A2: The Maturation Protein of ssRNA Bacteriophage Qbeta, p. 118. PhD Thesis. Department of Biochemistry and Biophysics, Texas A&M University, College Station, TX.

146.**Golmohammadi, R., K. Fridborg, M. Bundule, K. Valegard, and L. Liljas.** 1996. The crystal structure of bacteriophage Q beta at 3.5 A resolution. Structure *4*:543-554.

147.**Kim, H. and J. Yin.** 2004. Energy-efficient growth of phage Q Beta in Escherichia coli. Biotechnol Bioeng *88*:148-156.

148.**Abramoff, M.D., Magelhaes, P.J. & Ram, S.J.** 2004. Image Processing with ImageJ. Biophotonics Int *11*:36-42.

149.**Stone, A.B.** 1974. A simplified method for preparing sucrose gradients (Short Communication). Biochemical J *137*:117-118.

150.**Tsukada, K., M. Okazaki, H. Kita, Y. Inokuchi, I. Urabe, and T. Yomo.** 2009. Quantitative analysis of the bacteriophage Qbeta infection cycle. Biochim Biophys Acta *1790*:65-70.

151.**Engelberg-Kulka, H., M. Israeli-Reches, L. Dekel, and A. Friedmann.** 1979. Q beta-defective particles produced in a streptomycin-resistant Escherichia coli mutant. J Virol *29*:1107-1117.

152.**Sarrouh, B., T.M. Santos, A. Miyoshi, R. Dias, and V. Azevedo.** 2012. Up-To-Date Insight on Industrial Enzyme Applications and Global Market. Bioprocessing & Biotechniques *2*.

153.**Carlson, B.** 2011. Pipeline Bodes Well for Biologics Growth: 2010 Estimated Market of $105B Expected to Swell to $149B by 2015, p. 2. Genetic Eng Biotechnol News.

154.**Schoemaker, H.E., D. Mink, and M.G. Wubbolts.** 2003. Dispelling the myths--biocatalysis in industrial synthesis. Science *299*:1694-1697.

155.**Adamczak, M. and S.H. Krishna.** 2004. Strategies for improving enzymes for efficient biocatalysis. Food Technol Biotechnol *42*:251-264.

156.**Ragauskas, A.J., C.K. Williams, B.H. Davison, G. Britovsek, J. Cairney, C.A. Eckert, W.J. Frederick, Jr., J.P. Hallett, et al.** 2006. The path forward for biofuels and biomaterials. Science *311*:484-489.

157.**Grunwald, P.** 2010. Biocatalysis: Biochemical Fundamentals and Applications. Imperial College Press, London.

158.**Patel, R.N.** 2001. Biocatalytic synthesis of intermediates for the synthesis of chiral drug substances. Curr Opin Biotechnol *12*:587-604.

159.**Bornscheuer, U.T.** 2003. Immobilizing Enzymes: How to Create More Suitable Biocatalysts. Angew Chem Int Ed *42*:3336-3337.

160.**Alcalde, M., M. Ferrer, F.J. Plou, and A. Ballesteros.** 2006. Environmental biocatalysis: from remediation with enzymes to novel green processes. Trends Biotechnol *24*:281-287.

161.**Fahrenkamp-Uppenbrink, J.** 2002. Chemistry Goes Green. Science *297*:798.

162.**Schmid, A., J.S. Dordick, B. Hauer, A. Kiener, M. Wubbolts, and B. Witholt.** 2001. Industrial biocatalysis today and tomorrow. Nature *409*:258-268.

163.**Vick, J. and C. Schmidt-Dannert.** 2010. Directed Enzyme and Pathway Evolution, p. 41-76. *In* Y.H. Yeh W, McCarthy J R (Ed.), Enzyme Technologies - Metagenoics, Evolution, Biocatalysis, and Biosynthesis. John Wiley & Sons, New Jersey.

164.**Fox, R.J. and L. Giver.** 2010. Principles of Enzyme Optimization for the Rapid Creation of Industrial Biocatalysts, p. 99-124. *In* Y.H. Yeh W, McCarthy J R (Ed.), Enzyme Technologies - Metagenoics, Evolution, Biocatalysis, and Biosynthesis. John Wiley & Sons, New Jersey.

165.**Sheldon, R.A.** 2007. Enzyme Immobilization: The Quest for Optimum Performance. Advanced Synthesis & Catalysis *349*:1289-1307.

166.**Dyal, A., K. Loos, M. Noto, S.W. Chang, C. Spagnoli, K.V.P.M. Shafi, A. Ulman, M. Cowman, and R.A. Gross.** 2003. Activity of Candida rugosa Lipase Immobilized on γ-Fe2O3 Magnetic Nanoparticles. J Am Chem Soc *125*:1684-1685.

167.**Wang, W., Y. Xu, D.I.C. Wang, and Z. Li.** 2009. Recyclable Nanobiocatalyst for Enantioselective Sulfoxidation: Facile Fabrication and High Performance of Chloroperoxidase-Coated Magnetic Nanoparticles with Iron Oxide Core and Polymer Shell. J Am Chem Soc *131*:12892-12893.

168.**Ladavière, C., T. Delair, A. Domard, A. Novelli-Rousseau, B. Mandrand, and F. Mallet.** 1998. Covalent Immobilization of Proteins onto (Maleic Anhydride-alt-methyl Vinyl Ether) Copolymers: Enhanced Immobilization of Recombinant Proteins. Bioconj Chem *9*:655-661.

169.**Rusmini, F., Z. Zhong, and J. Feijen.** 2007. Protein Immobilization Strategies for Protein Biochips. Biomacromolecules *8*:1775-1789.

170.**Stephanopoulos, N. and M.B. Francis.** 2011. Choosing an effective protein bioconjugation strategy. Nat Chem Biol *7*:876-884.

171.**Kuan, I., R. Liao, H. Hsieh, K. Chen, and C. Yu.** 2008. Properties of Rhodotorula gracilis d-Amino Acid Oxidase Immobilized on Magnetic Beads through His-Tag. J Biosci Bioeng *105*:110-115.

172.**Yu, C.-C., Y.-Y. Kuo, C.-F. Liang, W.-T. Chien, H.-T. Wu, T.-C. Chang, F.-D. Jan, and C.-C. Lin.** 2012. Site-Specific Immobilization of Enzymes on Magnetic Nanoparticles and Their Use in Organic Synthesis. Bioconj Chem *23*:714-724.

173.**Niemeyer, C.M.** 2002. The developments of semisynthetic DNA–protein conjugates. Trends Biotechnol *20*:395-401.

174.**Carson, M., D.H. Johnson, H. McDonald, C. Brouillette, and L.J. DeLucas.** 2007. His-tag impact on structure. Acta Crystallogr Sect D Biol Crystallogr *63*:295-301.

175.**Tanaka, Y., Y. Tsuruda, M. Nishi, N. Kamiya, and M. Goto.** 2007. Exploring enzymatic catalysis at a solid surface: a case study with transglutaminase-mediated protein immobilization. Org Biomol Chem *5*:1764-1770.

176.**Gauchet, C., G.R. Labadie, and C.D. Poulter.** 2006. Regio- and Chemoselective Covalent Immobilization of Proteins through Unnatural Amino Acids. J Am Chem Soc *128*:9274-9275.

177.**Boyce, M. and C. Bertozzi.** 2011. Bringing Chemistry to Life. Nat Meth *8*:638-642.

178.**Patel, K.G. and J.R. Swartz.** 2011. Surface functionalization of virus-like particles by direct conjugation using azide-alkyne click chemistry. Bioconjug Chem *22*:376-387.

179.**Strable, E., D.E. Prasuhn, A.K. Udit, S. Brown, A.J. Link, J.T. Ngo, G. Lander, J. Quispe, et al.** 2008. Unnatural Amino Acid Incorporation into Virus-Like Particles. Bioconjug Chem *19*:866-875.

180.**Wang, L., A. Brock, B. Herberich, and P.G. Schultz.** 2001. Expanding the Genetic Code of Escherichia coli. Science *292*:498-500.

181.**Xie, J. and P.G. Schultz.** 2006. A chemical toolkit for proteins--an expanded genetic code. Nat Rev Mol Cell Biol *7*:775-782.

182.**Wang, L., J. Xie, A.A. Deniz, and P.G. Schultz.** 2002. Unnatural Amino Acid Mutagenesis of Green Fluorescent Protein. J Org Chem *68*:174-176.

183.**Liu, C.C. and P.G. Schultz.** 2010. Adding New Chemistries to the Genetic Code. Annu Rev Biochem *79*:413-444.

184.**Seo, M.-H., J. Han, Z. Jin, D.-W. Lee, H.-S. Park, and H.-S. Kim.** 2011. Controlled and Oriented Immobilization of Protein by Site-Specific Incorporation of Unnatural Amino Acid. Anal Chem *83*:2841-2845.

185.**Kim, T.-W., H.A. Chokhawala, M. Hess, C.M. Dana, Z. Baer, A. Sczyrba, E.M. Rubin, H.W. Blanch, and D.S. Clark.** 2011. High-Throughput In Vitro Glycoside Hydrolase (HIGH) Screening for Enzyme Discovery. Angew Chem *123*:11411-11414.

186.**Swartz, J.R., M.C. Jewett, and K.A. Woodrow.** 2004. Cell-Free Protein Synthesis With Prokaryotic Combined Transcription-Translation. Recombinant Gene Expression, p. 169-182. *In* P. Balbás, and A. Lorence (Eds.). Humana Press.

187.**Punna, S., E. Kaltgrad, and M.G. Finn.** 2005. "Clickable" agarose for affinity chromatography. Bioconjug Chem *16*:1536-1541.

188.**Hohsaka, T., Y. Ashizuka, H. Taira, H. Murakami, and M. Sisido.** 2001. Incorporation of Nonnatural Amino Acids into Proteins by Using Various Four-Base Codons in an Escherichia coli in Vitro Translation System. Biochemistry *40*:11060-11064.

189.**Saraogi, I., D. Zhang, S. Chandrasekaran, and S.-o. Shan.** 2011. Site-Specific Fluorescent Labeling of Nascent Proteins on the Translating Ribosome. J Am Chem Soc *133*:14936-14939.

190.**Hong, V., S.I. Presolski, C. Ma, and M.G. Finn.** 2009. Analysis and Optimization of Copper-Catalyzed Azide–Alkyne Cycloaddition for Bioconjugation. Angew Chem Int Ed *48*:9879-9883.

191.**Li, X.Y., T.H. Li, J.S. Guo, Y. Wei, X.B. Jing, X.S. Chen, and Y.B. Huang.** 2012. PEGylation of bovine serum albumin using click chemistry for the application as drug carriers. Biotechnol Prog *28*:856-861.

192.**Presolski, S.I., V. Hong, S.H. Cho, and M.G. Finn.** 2010. Tailored ligand acceleration of the Cu-catalyzed azide-alkyne cycloaddition reaction: practical and mechanistic implications. J Am Chem Soc *132*:14570-14576.

193.**Prescher, J.A. and C.R. Bertozzi.** 2005. Chemistry in living systems. Nat Chem Biol *1*:13-21.

194.**Jung, K., J. Park, P. Maeng, and H. Kim.** 2005. Fluorescence Quenching of Green Fluorescent Protein during Denaturation by Guanidine. Bull Korean Chem Soc *26*:413-417.

195.**Barondeau, D.P., C.J. Kassmann, J.A. Tainer, and E.D. Getzoff.** 2002. Structural Chemistry of a Green Fluorescent Protein Zn Biosensor. J Am Chem Soc *124*:3522-3524.

196.**May, R.M.** 2011. Why Worry about How Many Species and Their Loss? PLoS Biol *9*:e1001130.

197.**Esser-Kahn, A.P. and M.B. Francis.** 2008. Protein-Cross-Linked Polymeric Materials through Site-Selective Bioconjugation. Angew Chem *120*:3811-3814.

198.**Hermanson, G.T.** 2008. Bioconjugate Applications, p. 743-1045. Bioconjugate Techniques (Second Edition). Academic Press, New York.

199.**Kohrer, C., J.H. Yoo, M. Bennett, J. Schaack, and U.L. RajBhandary.** 2003. A possible approach to site-specific insertion of two different unnatural amino acids into proteins in mammalian cells via nonsense suppression. Chemistry & Biology *10*:1095-1102.

200.**Dougherty, D.A.** 2000. Unnatural amino acids as probes of protein structure and function. Curr Opin Chem Biol *4*:645-652.

201.**Kearney, P.C., H. Zhang, W. Zhong, D.A. Dougherty, and H.A. Lester.** 1996. Determinants of Nicotinic Receptor Gating in Natural and Unnatural Side Chain Structures at the M2 9′ Position. Neuron *17*:1221-1229.

202.**Kiick, K.L., E. Saxon, D.A. Tirrell, and C.R. Bertozzi.** 2002. Incorporation of azides into recombinant proteins for chemoselective modification by the Staudinger ligation. Proc Natl Acad Sci U S A *99*:19-24.

203.**Taki, M., T. Hohsaka, H. Murakami, K. Taira, and M. Sisido.** 2001. A non-natural amino acid for efficient incorporation into proteins as a sensitive fluorescent probe. FEBS Letters *507*:35-38.

204.**Smith, M.T., A.K. Hawes, and B.C. Bundy.** 2013. Reengineering viruses and virus-like particles through chemical functionalization strategies. Curr Opin Biotechnol *24*:620-626.

205.**Kim, T.W., J.W. Keum, I.S. Oh, C.Y. Choi, H.C. Kim, and D.M. Kim.** 2007. An economical and highly productive cell-free protein synthesis system utilizing fructose-1,6-bisphosphate as an energy source. J Biotechnol *130*:389-393.

206.**Deiters, A. and P.G. Schultz.** 2005. In vivo incorporation of an alkyne into proteins in Escherichia coli. Bioorg Med Chem Lett *15*:1521-1524.

207.**Loscha, K.V., A.J. Herlt, R. Qi, T. Huber, K. Ozawa, and G. Otting.** 2012. Multiple-Site Labeling of Proteins with Unnatural Amino Acids. Angew Chem Int Ed *51*:2243-2246.

208.**Kanda, T., K. Takai, S. Yokoyama, and H. Takaku.** 1997. Removing tRNA from a cell-free protein synthesis system for use in protein production. Nucleic Acids Symposium Series *37*:319-320.

209.**Fechter, P., J. Rudinger, R. Giegé, and A. Théobald-Dietrich.** 1998. Ribozyme processed tRNA transcripts with unfriendly internal promoter for T7 RNA polymerase: production and activity. FEBS Letters *436*:99-103.

210.**Novoa, Eva M., M. Pavon-Eternod, T. Pan, and L. Ribas de Pouplana.** 2012. A Role for tRNA Modifications in Genome Structure and Codon Usage. Cell *149*:202-213.

211.**Kim, T.W., I.S. Oh, J.W. Keum, Y.C. Kwon, J.Y. Byun, K.H. Lee, C.Y. Choi, and D.M. Kim.** 2007. Prolonged cell-free protein synthesis using dual energy sources: Combined use of creatine phosphate and glucose for the efficient supply of ATP and retarded accumulation of phosphate. Biotechnol Bioeng *97*:1510-1515.

212.**Arnold, R.J. and J.P. Reilly.** 1999. Observation ofEscherichia coliRibosomal Proteins and Their Posttranslational Modifications by Mass Spectrometry. Anal Biochem *269*:105-112.

213.**Pedelacq, J.-D., S. Cabantous, T. Tran, T.C. Terwilliger, and G.S. Waldo.** 2006. Engineering and characterization of a superfolder green fluorescent protein. Nat Biotech *24*:79-88.